DFIG Based Wind Turbine Contribution to System Frequency Control

by

Mansour Jalali

A thesis
presented to the University of Waterloo
in fulfillment of the
thesis requirement for the degree of
Master of Applied Science
in
Electrical and Computer Engineering

Waterloo, Ontario, Canada, 2011

Author's Declaration

I hereby declare that I am the sole author of this thesis. This is a true copy of the thesis, including any required final revisions, as accepted by my examiners.

I understand that my thesis may be made electronically available to the public.

Abstract

Energy is one of the most important factors that continue to influence the shape of civilization in the 21st Century. The cost and availability of energy significantly impacts our quality of life, the health of national economies and the stability of our environment. In recent years there has been a significant global commitment to develop clean and alternative forms of energy resources and it is envisioned that by 2020 10% of world energy will be supplied from renewable resources, and there is an expectation that this value will grow to 50% by 2050.

Among renewable energy resources, wind generation technology has matured considerably, and wind is fairly distributed around the globe and therefore available to world communities. In the last decade, wind generation has been the fastest growing energy source globally. However more penetration of wind energy into existing power networks raises concern for power system operators and regulators. Traditionally wind energy convertors do not participate in frequency regulation or Automatic Generation Control (AGC) services, and therefore large penetration of wind power into the power systems can result in a reduction of total system inertia and robustness of the frequency response to the disturbances.

The research presented in this thesis covers some of the operational and design aspects of frequency control and AGC services in power systems with mixed generation resources. The thesis examines the operation of the Doubly Fed Induction Generator (DFIG) with a modified inertial loop control considering single-area and two-area frequency control, both primary control and AGC. The thesis presents new, small-perturbation, linear, dynamic, mathematical models for the simulation of primary regulation services and AGC services for single-area and two-area power systems with a mix of conventional and non-conventional DFIG-based wind generators. In order to improve the performance of the frequency regulation and AGC services of the above systems, a parameter optimization technique based on the minimization of the Integral of Squared Errors (ISE) is applied to determine the optimal settings for the proportional-integral (PI) controller gains of the DFIG machines.

The thesis presents analytical studies with various perturbations to demonstrate the effectiveness and participation of DFIG-based wind generators in frequency support services and draws some important conclusions. Variation in DFIG penetration levels, and wind speed levels (strong wind and weak wind) on system frequency control performance, has also been examined in the thesis.

Acknowledgements

First and foremost, I express my deepest and greatest appreciation to my supervisor, Professor Kankar Bhattacharya. Dr. Bhattacharya has consistently provided invaluable guidance and suggestions in my research project as well as over my entire course program.

I am thankful to Professor Claudio A. Cañizares and Professor El. Shatshat for reading this thesis and providing their insightful comments and suggestions, which helped to improve this work.

I am thankful to the ABB Inc Canada, Department of Protection and Substation Automation which have supported me with partial fund for my research and studies.

Dedication

This thesis is dedicated to my parents and my children Zhina and Alan.

Table of Contents

Author's Declaration ii
Abstract iii
Acknowledgements iv
Dedication v
Table of Contents vi
List of Figure vii
List of Tables ix
Nomenclature xi
Abbreviations xv
Chapter 1 Introduction 1
1.1 Motivation 1
1.2 Current State of Wind Energy Globally 2
1.2.1 Wind Power in Canada and Ontario 2
1.2.2.Wind Power in the United States: 4
1.2.3.Wind Power in the United States: 5
1.3 Objective of this Thesis 6
1.4 Organization of the Thesis: 7
Chapter 2 Wind Power overview 8
2.1 Status of wind Turbine Technology 8
2.2 Power of the Wind 11
2.3 Pitch control 13
2.4 1 Assumption and constraint in participation of DFIG in frequency regulation 19
2.4 Literature Review 17
2.4 Wind Energy Converter System Functional structure: 14
2.4.1 WECS with Fixed Speed Wind Turbines Type A 14
2.4.2 WECS with Variable speed Wind Turbines type B 15
2.4.3 WECS with Doubly-Fed Induction Generator (DFIG) Based Wind Turbine 15
2.4.4 WECS with full converter 16
2.5 Simulation: 19
2.5.1 Active Pitch Control: 19
2.6 Conclusion: 22
Chapter 3 Primary Frequency Regulation and AGC in a Single-Area System with DFIG-Based Wind Turbine 23

3.1 Introduction 23
3.2 DFIG-Based Wind Turbine Control Model 26
3.3 Dynamic Model of Primary Frequency Regulation with DFIG-Based Wind Turbines 28
3.4 Dynamic Model of AGC with DFIG-Based Wind Turbines 30
3.5 Analytical Studies 34
3.5 Optimal Tuning of DFIG-Based Wind Turbine Controller Parameters 31
3.6.1 Primary Regulation 34
3.6.2 Automatic Generation Control 38
3.7 Conclusion 44
Chapter 4 Primary and Secondary Frequency Control in Two Area Systems with DFIG- Based Wind Turbine Support: 45
4.1 Introductions: 45
4.2 Dynamic model - Primary Frequency Regulation with DFIG based Wind Turbine two area controls: 47
4.3 Dynamic model of Secondary Frequency Regulation with DFIG based Wind Turbine - two area controls: 49
4.4 Optimal Tuning of DFIG Based Wind Turbine Controller Parameters : 52
4.4.2 Secondary control analytical studies: 62
4.5 Analytical studies: 55
4.5.1 Primary control analytical studies: 55
Chapter 5 Conclusion and Future Work 71
Bibliography 73
Appendix A 76
Appendix B 77

List of Figures

Figure 2.1 Drag device based on Persian design, used in the sail boat [26] 8
Figure 2.2 Vertical Axis wind turbine [27] 9
Figure 2.3 Horizontal Axis wind turbine [28] 9
Figure 2.4 Illustration of forces around the moving blade [30] 12
Figure 2.5 WECS with fixed speed wind turbine 15
Figure 2.6 WECS with fixed speed wind turbine and variable resistor 15
Figure 2.7 WECS with DFIG based wind turbine 16
Figure 2.8 WECS with synchronous generator and convertor 17
Figure 2.9 Plots of simulation of wind speed step perturbation for induction type wind turbine .. 20
Figure 2.10 Plots of simulation of wind speed step perturbation for induction type wind turbine 21
Figure 3.1 Principle of DFIG Inertial Emulation Control [38] 25
Figure 3.2 Power system dynamic model overview with mixed generation 26
Figure 3.3 DFIG-based wind turbine control based on frequency change [35], [39] 27
Figure 3.4 Primary frequency regulation block diagram with DFIG based WT 28
Figure 3.5 Dynamic model for AGC studies with DFIG-based wind turbines 30
Figure 3.6 Optimal tuning of DFIG controller parameters for 20% wind penetration 33
Figure 3.7 Primary frequency regulations with and without DFIG 34
Figure 3.8 Primary frequency regulations with and without DFIG 35
Figure 3.9 Generator responses in primary frequency regulation with and without 36
Figure 3.10 Generator response in primary frequency regulation with and without DFIG 36
Figure 3.11 Generator response in primary frequency regulation with and without DFIG 37
Figure 3.12 DFIG generator response in primary frequency regulation 37
Figure 3.13 DFIG generator response in primary frequency regulation 38
Figure 3.14 DFIG-Based WT with AGC Simulation model in Simulink® 39
Figure 3.15 AGC with 2% load increment with and without DFIG 40
Figure 3.16 AGC with 2% load increment with and without DFIG 41
Figure 3.17 AGC with 2% load increment with and without DFIG 41
Figure 3.18 AGC with 2% load increment with and without DFIG 42
Figure 3.20 DFIG generation with AGC and 2% load increment 43
Figure 4.1 linear model of frequency control two Area Systems 45
Figure 4.2 Linear dynamic model of primary frequency control of two area systems with DIFG 47

Figure 4.3 Linear model of secondary frequency control of two area systems with DIFG-based wind turbines 51
Figure 4.4.Schematic diagram for optimal tuning of DFIG controller parameters 53
Figure 4.5.Tuning DFIG controller parameters for 50% wind penetration 54
Figure 4.6.Simulink model for frequency response studies for two-area controller with 56
Figure 4.7.Primary frequency regulation tie-line incremental power 57
Figure 4.8. Primary frequency regulation for 2% load change area 1 58
Figure 4.9.Primary frequency regulation for 2% load change area 2 58
Figure 4.10. Primary frequency regulation for 2% load change area 1 59
Figure 4.11. Primary frequency regulation for 2% load change area 2 59
Figure 4.12. Primary frequency regulation for 2% load change tie line 60
Figure 4.13. Primary frequency regulation for 2% load change area 1 60
Figure 4.14 Primary frequency regulation for 2% load change area 2 61
Figure 4.15 Primary frequency regulation for 2% load change tie line 61
Figure 4.16 Secondary frequency regulation for 2% sudden load tie line power 62
Figure 4.17 Secondary frequency regulation for 2% sudden load tie line power 63
Figure 4.22 Secondary frequency regulation for 2% sudden load change area-2 65
Figure 4.23 Secondary frequency regulation for 2% sudden load change area-1 66
Figure 4.24 Secondary frequency regulation for 2% sudden load change area-2 66
Figure 4.25 Secondary frequency regulation for 2% sudden load change area-1 67
Figure 4.26 Secondary frequency regulation for 2% sudden load change area-2 67
Figure 4.27 Area error for 2% sudden load change in area-1 68
Figure 4.28 Area error for 2% sudden load change in area-2 69
Figure 4.29 Area error for 2% sudden load change in area-2 69

List of Tables

Table 1.1 Wind farm projects and installations in Canada. [7][8] 3
Table 1.2 Installed wind capacity in Ontario [9] 4
Table 1.3 Ongoing wind development projects in Ontario [9] 4
Table 1.4 Total wind generation capacity in EU by scenario and year (GW)[3] 6
Table 2.1 Available wind turbines in the market [29] 11
Table 3.1 Optimal parameters of the controller for different wind penetration 33
Table 4.1 Optimal DFIG controller settings parameters area-1 54
Table 4.2 Optimal DFIG controller settings parameters area-2 55

Nomenclature

$\underline{A}$	State space matrix
B_1	Frequency bias factor area 1
B_2	Frequency bias factor area 2
C_p	Efficiency Coefficient
D	load damping factor
D_1	load damping factor area 1
D_2	load damping factor area 2
E_K	Kinetic Energy
E_{K0}	Initial Kinetic Energy
J	Objective function
H	Power system inertia constant
H_e	Wind generation inertia constant
H_1	Power system inertia constant area 1
H_2	Power system inertia constant area 2
K_{agc}	AGC integral control gain
K_{df}	Derivatives controller gain
K_{I1}	AGC integral control gain area 1
K_{I2}	AGC integral control gain area 2
K_p	Power system gain
K_{pf}	Proportional controller gain
K_{p1}	Power system gain
K_{p2}	Power system gain
K_{wi}	DFIG integral speed controller gain
K_{wi1}	DFIG integral speed controller gain area 1
K_{wi2}	DFIG integral speed controller gain area 2
K_{wp}	DFIG proportional speed controller gain
K_{wp1}	DFIG proportional speed controller gain area 1
K_{wp2}	DFIG proportional speed controller gain area 2
$\underline{P}$	Perturbation vector
P_{mech}	Wind turbine Mechanical Output
pu	per unit
P_{wind}	Wind power
R	Regulation droops

R_r	Rotor Radius
R_1	Regulation droop area 1
R_2	Regulation droop area 1
s	Laplace variable
T°	Tie line synchronizing Coefficient
T_a	DFIG turbine time constant
T_{a1}	DFIG turbine time constant area 1
T_{a2}	DFIG turbine time constant area 2
T_h	conventional generation governor time constant Transducer time constant
T_{h1}	conventional generation governor time constant Transducer time constant area 1
T_{h2}	conventional generation governor time constant Transducer time constant area 2
T_p	Power system time constant
T_{p1}	Power system time constant area 1
T_{p2}	Power system time constant area 2
T_r	Transducer time constant
T_{r1}	Transducer time constant area 1
T_{r2}	Transducer time constant area 2
T_t	conventional generation turbine time constant Transducer time constant
T_{t1}	conventional generation turbine time constant Transducer time constant arae1
T_{t2}	conventional generation turbine time constant Transducer time constant area 2
T_w	washout filter time constant
T_{w1}	washout filter time constant for DFIG area 1
T_{w2}	washout filter time constant for DFIG area 2
V_{rel}	Relative wind Speed
V_{tip}	Tip Speed
V_{wind}	Wind Speed
$\underline{X}$	State vector matrix
α	Angle of attack
α_W	Penetration index
β.	Blade Angle
ρ_{air}	Air density
φ	Angle of Incidence angle of incidence between the plane of the rotor and V_{rel}
ω_r	Rotor Frequency
ω	Wind Turbine speed

ω_{max}	Wind turbine cut-out speed maximum
ω_{mech}	Angular velocity of rotor rotation
ω_{min}	Wind turbine cut-out speed minimum
$\omega_{m,meas}$	wind turbine measured mechanical speed
ω_s	System Frequency
ω_{turb}	Angular velocity of the Rotor
ω_1	Wind Turbine speed area 1
ω_2	Wind Turbine speed area 2
ω_{1max}	Wind turbine cut-out speed maximum area1
ω_{2max}	Wind turbine cut-out speed maximum area2
ω_{1min}	Wind turbine cut-out speed minimum
ω_{2min}	Wind turbine cut-out speed minimum
λ	Tip Speed Ratio
$\underline{\Gamma}$	State space matrix
δ^o_1	Tie line Voltage angle area1
δ^o_2	Tie line Voltage angle area2
Δf	Incremental power frequency
Δf_1	Incremental power frequency area1 change
Δf_2	Incremental power frequency area2 change
ΔPD	Incremental active power demand
ΔPD_1	Incremental active power demand area1
ΔPD_2	Incremental active power demand area 2
ΔP_f	Incremental value of total active power mixed generation
$\Delta P^*_{f\omega}$	Incremental Wind Turbine power set point (reference) based on frequency and speed change
ΔP^*_f	Incremental Wind Turbine power set point (reference) based on frequency
ΔP_g	Incremental value of conventional generation
ΔP_{NC}	Incremental Wind Turbine active Power output (non-conventional generation)
ΔP_{NC1}	Incremental DFIG active Power output area 1
ΔP_{NC2}	Incremental DFIG active Power output area 2
$\Delta P_{NC,ref}$	Incremental Wind Turbine active Power reference (non-conventional generation)
$\Delta P_{NC1,ref}$	Incremental Wind Turbine active Power reference area1

$\Delta P_{NC2,ref}$	Incremental Wind Turbine active Power reference area2
ΔP^{*}_{ω}	Incremental Wind Turbine power set point (reference) based on speed change
ΔP_{12}	Incremental power transferred from neighboring area (area 1 to area 2)
$\Delta\ \omega$	Incremental wind turbine speed
$\Delta\ \omega_1$	Incremental wind turbine speed area 1
$\Delta\ \omega_2$	Incremental wind turbine speed area 2
ΔX_1	Measured incremental frequency change (after Transducer)
$\Delta X_{1\text{-}1}$	Measured incremental frequency change for DFIG (after Transducer) area 1
$\Delta X_{1\text{-}2}$	Measured incremental frequency change for DFIG (after Transducer) area 2
ΔX_2	Measured incremental frequency change (after wash out filter)
$\Delta X_{2\text{-}1}$	Measured incremental frequency change (after wash out filter) for DFIG area 1
$\Delta X_{2\text{-}2}$	Measured incremental frequency change (after wash out filter) for DFIG area 2
ΔX_3	Incremental DFIG active power based on mechanical speed change
$\Delta X_{3\text{-}1}$	Incremental DFIG active power based on mechanical speed change area 1
$\Delta X_{3\text{-}2}$	Incremental DFIG active power based on mechanical speed change area 2

Abbreviations

AGC	Automatic Governor Control
ACE_1	Control error area 1
ACE_2	Control error area 2
CanWEA	Canadian Wind Energy Association
DFIG	Doubly Fed Induction Machine
GHG	Green House Gas
EEA	European Environment Agency
EU	European Union
GW	Giga-watt
MW	Megawatt
MTP	Main Tracking Power
rpm	Rotation per minute
TSR	Tip Speed Ratio
WECS	Wind Energy Converter System

Chapter 1
Introduction

1.1 Motivation

The reduction of economic dependency on fossil fuel-based energy has been among the top priority goals of regulators and their governments around the world. During recent years fossil fuel resources are limited and have a significant adverse impact on the environment by raising the level of CO_2 in the atmosphere and contributing to global warming. Among renewable sources of energy, wind is one of the most promising technologies. It has already been in use for a significant period of time and, compared to other forms of alternative energy resources, has the greatest potential to reduce the conventional generation. The proportion of wind-based generation in total energy production mix has been growing continuously in many parts of the world.

It has been reported [1] that renewable energy will provide as much as 10% of the world's energy supply by 2020, and will increase to as much as 50% by 2050. Canada has outlined a future strategy for wind energy that would reach a capacity of 55,000 MW by 2025, fulfilling 20% of the country's energy needs [2]. The European Union plans to produce 22% of its electricity from renewable resources by the year 2010 [3].

Although wind-based generation is fairly well known and has been used for several years, but because of the low penetration levels of wind turbines, focus of the industry has been on turbine protection aspects. However, with the increasing amounts of wind energy into the network, new challenges with regards to the functioning of the current power grid are surfacing, especially in area of grid stability, balance, security, planning, cross-border transmission, and market design. A wind source is unpredictable. Therefore, efficient integration of large amounts of variable sources of wind turbines into the existing electrical networks can significantly impact the design, operation, and control of the network.

The work carried out and presented in this thesis is an attempt to study and examine the role of variable speed based wind turbines, in particular the Doubly Fed Induction Generators (DFIG), in frequency regulation and control with different levels of wind penetration into the system. In particular the issue of optimal tuning of the DFIG control system in single-area and two-area frequency control problems has been presented as a means to help improve the performance of the system.

1.2 Current State of Wind Energy Globally

There is an increasing commitment from global leaders and policy makers to reduce Greenhouse Gas (GHG) emissions. Efforts are being made to increase the contribution of renewable sources of energy in the energy supply mix. Several countries have already formulated policy frameworks to ensure that renewable resources play a major role in future energy scenarios.

1.2.1 Wind Power in Canada and Ontario

Early development of wind energy in Canada was primarily concentrated in Ontario, Quebec and Alberta. Throughout the late 1990s and since the beginning of the 21st Century all Canadian provinces have pursued wind power development to supplement their provincial energy grids. Alberta built the first commercial wind farm in Canada in 1993. British Columbia was the last province to add wind power to its grid with the completion of the Bear Mountain Wind Park in November 2009 [4]. With steady population growth in a country, comes growth in energy demand. Canada has seen wind power as a way to diversify its energy supply, and to help moving away from its traditional reliance on fossil fuel based thermal plants and hydroelectricity. In provinces like Nova Scotia, where only 12% of the electricity comes from renewable resources [5], the development of wind energy projects can provide a measure of electricity security that some jurisdictions are lacking. In the case of British Columbia, it is envisaged that wind energy will help close the electricity deficit gap that the province is facing in the next decade, and reduce its reliance on importing power from other jurisdictions that may not use renewable energy sources. An additional 2004 MW of wind power is scheduled to come on-line in Quebec between 2011 and 2015 [6].

In 2008, the Canadian Wind Energy Association (CanWEA), a non-profit trade association, outlined a future strategy for wind energy that envisages a capacity of 55,000 MW by 2025, fulfilling 20% of the country's energy needs. The plan, Wind Vision 2025 [1], could create over 50,000 jobs and represent around CDN $165 million annual revenue. CanWEA's target would make the country a major player in the wind power sector and would create around CDN$79 billion of investment opportunities. It would also eliminate an estimated 17 megatons of GHG missions annually [1]. Table 1.1 shows the list of wind farm projects and installations in Canada.

Table 1.1 Wind farm projects and installations in Canada. [7][8]

Province/ Territory	**Current Installed Power (MW)**	**Planned under construction (MW)**	**Expected 2015 Capacity (MW)**
Alberta	590	409	999
British Columbia	102	107.7	272.7
Manitoba	104	138	242
New Brunswick	195	114	309
Newfoundland	54.4	0	54.4
Nova Scotia	59.3	244	303.3
Ontario	1161.5	647.2	1808.7
Prince Edward	151.6	0	151.6
Quebec	659	2671.5	3330.5
Saskatchewan	171.2	24.75	195.95
Yukon	0.81	0	0.81
Total	**3,248.81**	**4,419.15**	**7,667.96**

Ontario is at the forefront of wind generation in Canada with over 1,100 MW of installed capacity on the transmission system. In Ontario, wind generation capacity has increased from 15 MW in 2003 to 1,100 MW in 2009; enough electricity to supply the needs of some 300,000 homes. Currently there are seven large-scale wind farms in operation in Ontario (Table 1.2). These facilities are dispersed across the province which helps to mitigate the impact of local weather conditions on wind energy production. There is also another 68 MW of wind generation located within distribution service areas through Ontario Power Authority contracts [9].Table 1.3 shows the planned MW power generation projects in Ontario.

Table 1.2 Installed wind capacity in Ontario [9]

Wind Farm	Capacity (MW)	Operational
Amaranth ITownship of Melancthon	67.5	Mar. 2006
Kingsbridge Norfolk and Elgin Countries	39.5	Mar 2006
Port Burwell (Erie Shores) Norfolk and Elgin Countries	99	May 2006
Prince I Sault Ste Marie District	99	Sep 2006
Prince II Sault Ste Marie District	90	Nov 2006
Ripely Township of Melancthon	76	Dec 2007
Port Alma (Kruger) Port Alma	101.2	Oct 2008
Amaranth II Township of Melancthon	132	Nov 2008
Underwood (Enbridge) Bruce County	181.5	Feb 2009
Wollfe Island Township of Frontenac Island	197.8	Jun 2009

Table 1.3 Ongoing wind development projects in Ontario [9]

Wind Farm	Capacity (MW)	Expected Operation
Byran Wind Project	64.5	2010
Gosfield Wind Project	50	2012
Greenwich Wind Farm	99	2011
Kruger Energy Chatham	101.2	2011
Raleigh Wind Center	78	2010
Talbot Wind Farm	99	2011

1.2.2 Wind Power in the United State

At the end of 2009, the installed capacity of wind power in the United States was just over 35 GW [10] [11], making it the world leader ahead of Germany. Wind power accounts for about 2% of the electricity generated in the United States [12].

Over 9,900 MW of new wind power capacity was brought online in 2009, up from 8,800 in 2008. In 2009, the added new capacity was enough to power the equivalent of 2.4 million homes or generate as much electricity as three large nuclear power plants [13]. These new installations place the US, on a trajectory to generate 20% of the nation's electricity from wind energy by 2030 [11]. Growth of MW capacity in 2008 channeled some $17 billion into the

economy, positioning wind power as one of the leading sources of new power generation in the country, along with natural gas. New wind projects completed in 2008 accounted for about 42% of the entire new power-producing capacity added in the US during the year [14] At the end of 2008, about 85,000 people were employed in the US wind industry[15], and GE Energy was the largest domestic wind turbine manufacturer [15]. Wind projects boosted local tax bases, and revitalized the economy of rural communities by providing a steady income stream to farmers with wind turbines on their land [16] Wind power in the US provides enough electricity to power the equivalent of nearly 9 million homes, avoiding the emissions of 57 million tons of carbon each year and reducing expected carbon emissions from the electricity sector by 2.5% [17]. Texas, with 9,410 MW of capacity, has the most installed wind power capacity of any US state, followed by Iowa with 3,053 MW [11]. The Roscoe Wind Farm (780 MW) in Texas is the world's largest wind farm [18].

1.2.3 Wind Power in the European Union

In 2008, according to European Wind Energy Association (EWEA), there were 5,000 wind turbines, with a total capacity of 64.93 GW in the European Union, generating 142 TWh of electricity which took an investment of 11 billion euro [19]. In 2008, the European Union produced 4.2% of its electricity from the wind [19][20]. As of 2009, the leading countries are Germany (25 GW) and Spain (16.7 GW). The European Environment Agency (EEA) report [21] states that potential of wind energy is sufficient to power Europe many times over. The report highlights Europe's wind power potential in 2020 to be three times greater than it's expected electricity demand, rising to a factor of seven by 2030 [22].

In 2008, 8.48 GW (8.1 onshore and 0.37 GW offshore) of wind energy capacity was installed in the European Union compared to 27 GW in the world [19][22]. The market for European wind power capacity grew significantly in 2006, according to statistics from the EWEA. A total of 7,588 MW of wind power capacity, worth some 9 billion Euros, was installed in the European Union (EU) in 2006, an increase of 23% compared to 2005. Currently more than 25,000 wind farms are operating throughout Europe, and capacity is expected to double by 2015. According to EWEA, the industry will be worth $109 billion Euro by 2020. Research from a wide variety of sources in various countries indicates that support for wind power is consistently between 70 and 80 per cent amongst the general public.

Wind power capacity estimates were reported for all EU twenty seven countries as well as Norway, Switzerland, Croatia and some of the Balkan states [3] as given in table 1.4.

Table 1.4 Total wind generation capacity in EU by scenario and year (GW)[3]

Year	2005	2008	2010	2015	2020	2030
Low Growth Scenario	42.2	57.2	72.3	103.3	143.9	203.3
Medium Growth Scenario	42.2	66.5	90.0	143.7	205.8	279.6
High Growth Scenario	42.2	78.1	108.2	185.0	263.4	351.1

The EU targets to meet 22 percent of its electricity from renewable energy sources by the end of 2010. Wind commercially is viable and as economically competitive renewable source, is a major player in meeting this target.

1.3 Objectives of This Thesis

In light of the above discussions, it is apparent that wind energy is one of most favorable clean energy alternatives to replace fossil fuel based energy globally. Fast growth and high penetration of wind energy in existing networks requires full integration of wind turbines from different perspectives such as operation, scheduling, control, and market aspects. Frequency control and regulation service provision from wind generation is very important and challenging compared to that from conventional sources of energy since availability of the wind energy source is not controllable. It is evident that without a through strategy, full integration of wind energy with high penetration would not be possible, and therefore studies are required. With that said, following is a summary of the objectives of this work:

- Provide mathematical models of the network with mixed generation and various penetration scenarios to examine the control strategy for primary and secondary frequency control.
- Develop a mathematical model for network with mixed generation in single area frequency control, and provide the method to improve the dynamic response of the system.
- Develop a mathematical model for network with mixed generation in two area frequency control, and provide the method to improve the dynamic response of the system.
- Compare the classical frequency control with mixed generation network, and examine and compare the responses for various penetration scenarios.

1.4 Organization of This Thesis

Chapter 2 provides the Wind power overview and WECS modeling. Chapter 3 develops mathematical model for single area control system with mixed generation, and tuning the wind machine speed controller, in order to improve frequency response of the network for small perturbation. Chapter 4 develops the mathematical model for two area control system with mixed generation, and tuning of the wind machine speed in each area, in order to improve frequency response of the network for small perturbation, and to minimize the area error and tie line disturbance for various penetration scenarios. Chapter 5 draws the important contributions of the thesis, and outlines the scope for future work.

Chapter 2

Wind Power overview

2.1 Status of wind Turbine Technology

Wind energy conversion systems can be classified into turbines that depend on aerodynamic drag and turbines that depend on aerodynamic lift. The early Persian vertical axis wind turbine shown in Figure 2.1 utilized the drag principal. The history of wind power shows a general evolution from use of simple light devices driven by aerodynamic drag forces, to heavy, material-intensive drag devices and finally to the use of light material, and efficient aerodynamic lift devices in the modern era. The earliest known use of wind power, (sail boat form ancient Persia) used this technology which had a significant impact on the pursuing wind power development.

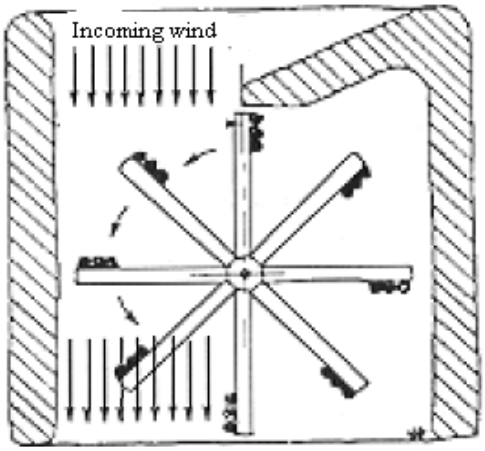

Figure 2.1 Drag device based on Persian design, used in the sail boat [26]

Modern wind turbines are predominately based on aerodynamic lift. Lift devices use blades that interact with incoming wind. The force resulting from the blade (airfoil) interaction with the air flow consists of the drag force component in the direction of the flow and a force component that is perpendicular to the drag, namely the lift. Magnitude of the lift force could be several times larger than drag force depending on the design of the airfoil blade, which provides the driving force for the rotor. Wind turbine based on aerodynamic lift can be further classified according to the orientation of spin axis, as vertical axis turbines Figure 2.2 and horizontal axis turbine Figure 2.3. In the vertical axis wind turbine, the main rotor shaft is set vertically. The advantages of this arrangement are that generators and gearboxes can be placed close to the ground and as shown in Figure 2.2, these devices do not need to be pointed into the wind direction [27].

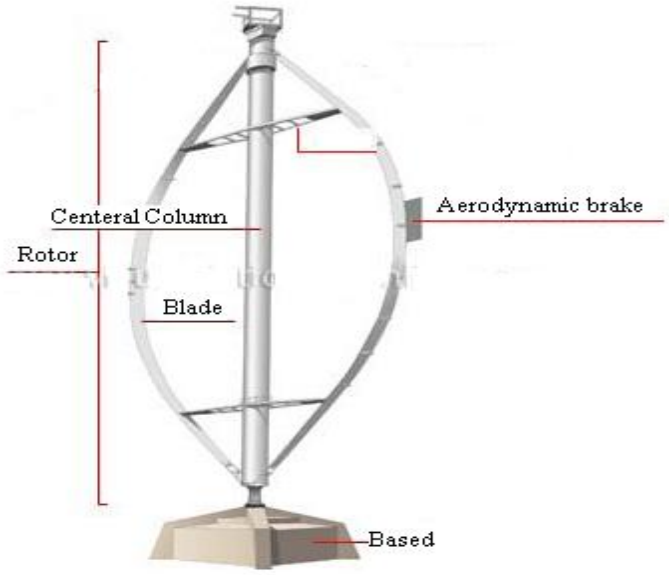

Figure 2.2 Vertical Axis wind turbine [27]

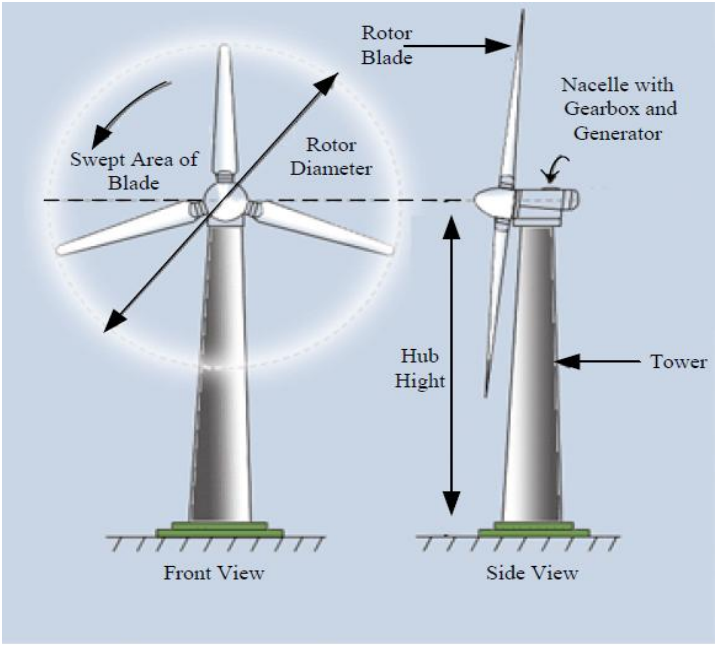

Figure 2.3 Horizontal Axis wind turbine [28]

Figure 2.3 shows a horizontal axis or propeller-type wind turbine in which the axis of the rotor's rotation is parallel to the wind stream and the ground. The wind passes over both surfaces of the airfoil shaped blade, faster over the longer (upper) side of the airfoil than the shorter side

(lower), hence creating a lower-pressure area above the airfoil with respect to the underside. The pressure differential between top and bottom surfaces results in what is called aerodynamic lift. Since the blades of a wind turbine are constrained to move in a plane with the hub as its center, the lift force causes rotation about the hub. In addition to the lift force, a drag force perpendicular to the lift force impedes rotor rotation. This approach currently dominates wind turbine applications in the industry. As shown in Figure 2.3 this type of turbine consists of a tower, a nacelle that is mounted on the top of the tower and contains a generator, gearbox and the rotor.

Different mechanisms exist for pointing the nacelle towards the wind direction, or move the nacelle out of the wind in the case of high wind speed. For small wind turbines, the rotor and the nacelle are oriented into the wind with the help of tale vanes. On the larger wind turbines, nacelle and rotor are electrically yawed into or out of the wind, in response to a control signal from wind vane. Most of horizontal axis turbines built today are with two- or three-blades, although some may have more blades. The number of blades is directly linked to the Tip Speed Ratio λ (TSR) which is the ratio of blade tip speed to wind speed, as given:

$$\lambda = \frac{\omega_{turb} R}{V_{wind}} \tag{2.1}$$

Where ω_{turb} is angular velocity or frequency of rotation, R is radius of the aerodynamic rotor and V_{wind} is wind speed. The TSR is of vital importance in the design of wind turbine generators. If the rotor of the wind turbine turns too slowly, most of the wind will pass undisturbed through the gap between the rotor blades. Alternatively, if the rotor turns too quickly, the blurring blades will appear like a solid wall to the wind. Therefore, wind turbines are designed with optimal TSR to extract as much power out of the wind as possible. When a rotor blade passes through the air it leaves turbulence in its wake. If the next blade on the spinning rotor arrives at this point while the air is still turbulent, it will not be able to efficiently extract power from the wind. However, if the rotor spans a little more slowly, the air hitting each turbine blade would no longer be turbulent. Therefore the TSR is chosen so that the blades do not pass through turbulent air.

The optimum TSR depends on the number of blades in the wind turbine rotor. The fewer the number of blades, the faster the wind turbine rotor needs to turn to extract maximum power from the wind. A two-bladed rotor has an optimum TSR of around 6, a three-bladed rotor around 5, and a four-bladed rotor around 3. A well designed typical three-bladed rotor would have a tip speed ratio of around 6 to 7. Three-bladed turbines provide lower noise, and better torque characteristics compared with two-bladed wind turbines.

In tune with growth of the industry, the wind energy technology is also changing. One apparent change is the shift towards offshore installations enabling the industry to envision large and ambitious installations to take place.

Another trend in the industry is to go for larger machines since the industry is growing from MW to multi MW scale. Bigger turbines are cheaper on per KW basis. Several manufacturers are manufacturing turbines with 5 MW size. Some of these machines have rotors with 125 m blades weighing around 9 tones. In another attempt to make offshore wind farms more profitable, Norway plans to build the world's largest turbine standing 533 feet tall with a rotor diameter of 475 feet. It will also be the single largest generating unit with capacity of 10 MW, to power over 2,000 homes, making it three times more powerful than current turbines [25].

Table 2 1 Available wind turbines in the market [29]

Application	Hub- height	Diameter	Power rating
Commercial	50-90 m	47-90 m	0.660-2.00 MW
Medium	35-50 m	13-30 m	
Residential	18-37 m	1-13 m	Below 30KW

2.2 Power from Wind

From a physical point of view, the static characteristics of a wind turbine's rotor can be described by the relationships between the total power in the wind and the mechanical power of the wind turbine. These relationships are readily described starting with the incoming wind in the rotor swept area. It can be shown that the kinetic energy of a cylinder of air of radius R travelling at wind speed V_{wind} corresponds to a total wind power P_{wind} within the rotor swept area of the wind turbine. This power, wind, can be expressed by (2.1) as given below [30],

$$P_{wind} = \frac{1}{2}\rho_{air}\pi R^2 V_{wind}^3 \qquad (2.1)$$

where ρ_{air} is the air density (1.225 kg/rn^3), R is the rotor radius and V_{wind} is the wind speed.

It is not possible to extract all the kinetic energy from the wind since this would mean that the air would stand still directly behind the wind turbine. This would not allow the air to flow away from the wind turbine, and clearly this cannot represent a physical steady-state condition. The wind speed is only reduced by the wind turbine, which thus extracts a fraction of the power in the wind. This fraction is expressed as the power efficiency coefficient, C_p, of the wind turbine. Therefore the mechanical power output of the wind turbine P_{mech} considering the definition of C_p can be stated as given by (2.2) [30],

$$P_{mech} = C_p P_{wind} \tag{2.2}$$

$$P_{mech} = \frac{1}{2} C_p \rho_{air} \pi R^2 V_{wind}^3 \tag{2.3}$$

It can be shown that the theoretical static upper limit of Cp is 16/27 (approximately 0.593); which is the maximum theoretically possible value (approximately 59%) that can be extracted from the kinetic energy of the wind. This is known as Betz's limit [31]. For comparison, a modern three bladed wind turbine has an optimal Cp value in the range of 0.52-0.55 [31] when measured at the hub of the turbine.

From a physical point of view the power, P_{mech} that is extracted from the wind will depend on rotational speed, wind speed and blade angle, β. Therefore, P_{mech} and C_p are functions of these parameters.

$$P_{mech} = f(\omega_{turb}, V_{wind}, \beta) \tag{2.4}$$

The forces of the wind on a blade section and thereby the possible energy extraction will depend on the angle of incidence φ between the plane of the moving rotor blades and the relative wind speed V_{rel} (see Figure 2.4) as seen from the moving blades. Simple geometrical considerations, which ignore the wind turbulence created by the blade tips show that the angle of incidence φ is determined by the incoming wind speed V_{wind} and the speed of the blade. The blade tip is moving at speed V_{wind}, equal to (ω_{turb}*R). This is illustrated in Figure 2.4. The highest values of C_p are typically obtained for values in the range 8 to 9 (i.e. when the tip of the blades move 8 to 9 times faster than the incoming wind). This means that the angle between the relative air speed as seen from the blade tip and the rotor plane is rather a sharp angle. Therefore, the angle of incidence φ is most conveniently calculated as:

$$\varphi = arctan(\frac{1}{\lambda}) = arctan(\frac{v_{wind}}{\omega_{turb}}) \tag{2.5}$$

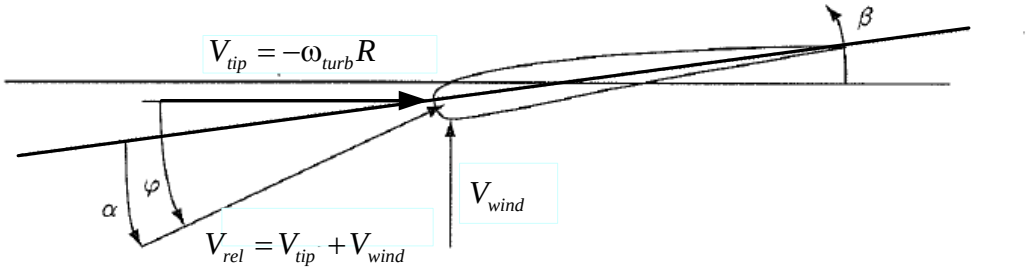

Figure 2.4 Illustration of forces around the moving blade [30]

where V_{tip} = tip speed; ω_{turb} = turbine rotational speed; R = rotor radius; V_{rel} = relative wind speed; V_{wind} = wind speed; α = angle of attack; φ = angle of incidence between the plane of the rotor and V_{rel}; β= blade angle

On modern wind turbines, it is possible to adjust the pitch angle β of the entire blade through a servo mechanism. If the blade is turned, the angle of attack α between the blade and the relative wind V_{rel} will be changed accordingly. Again, it is clear from a physical perspective that the forces of the relative wind on the blade, and thereby the energy extraction, will depend on the angle of attack α between the moving rotor blades and the relative wind speed V_{rel} as seen from the moving blades. Hence C_p can be expressed as a function of λ and β:

$$C_p = f(\lambda, \beta) \tag{2.5}$$

C_p is a characteristic of the wind turbine that can be obtained by blade element method, look-up table, or analytical approximation.

2.2.1 Pitch control [31]

Whenever the average of wind speed changes over a propeller, the propeller's pitch needs to be controlled. Commercial wind turbines are designed to produce optimum power with 15 m/s of wind speed. However, the wind speed always fluctuates up and down around this optimum. To generate the optimum power, the turbine blades have to adjust accordingly. This adjustment comes from turning the blades around their longitudinal axis (to pitch). When the wind speed decreases, the blade pitch is adjusted such that it exposes more surface area to the wind. Conversely, when wind speed picks up, the blade pitch is adjusted such that it exposes less surface area to the wind. If a blade is not designed for stall, increased wind speeds will force the rotor to turn faster without a pitch control mechanism. The pitch mechanism allows the wind to flow around the blade as smoothly as possible. To do this, air particles cannot hit the blade head on, rather they must flow almost tangent to the blade just as in an airplane's wing operating in the air.

There are two kinds of pitch control mechanism. The first is called "Active Pitch Control" where the rotor blades turn around their longitudinal axis (to pitch) by a computer controlled mechanism. This type of pitch control requires expensive equipment; however it provides good pitch control. Active pitch controls are used in one third of the large turbines currently installed. The second pitch control mechanism is called "Passive" or "Stall Pitch

Control". In this type of design the blade does not rotate around its longitudinal axis, but is designed such that it naturally creates a stall and low tip speeds. This type blade requires precise blade design and structurally strong towers.

2.3 Wind Energy Converter System Functional Structure

One of the important components in the WECS is the gearbox placed between the main shaft and the generator. Its task is to increase the rotational speed of the rotor blades to the generator's rotation speed of 1000 or 1500 revolutions per minute (rpm). Capacitor banks are used to provide the reactive power required by the induction generator power electronic converters used to facilitate the coupling of wind turbine with variable power source to the grid network with the constant frequency. Therefore from the functional point of view WECS could be classified into WECS with fixed speed wind WECS with variable-speed wind turbines.

2.3.1 WECS with Fixed Speed Wind Turbines Type A

Normally for the fixed speed wind turbine, induction generator types A [30] squirrel-cage induction generator is used as shown in Figure 2.5. The rotor of a fixed-speed wind turbine rotates at a fixed speed determined by the frequency of the grid, gear ratio, and the pole pairs of generator. A fixed-speed wind turbine is connected to the grid through a soft-starter. Since the induction generator absorbs the reactive power from the grid, a capacitor bank is necessary to provide for the reactive power compensation. A gear box is used to transform power from the turbine with lower-rotational speed to the generator rotor with high-rotational speed. The generator terminal voltage is increased with a step-up unit transformer to a medium voltage level.

Although this type of wind turbine has the advantage of being simple and relatively cost-efficient compared to other types of wind turbines, but the reactive power cannot be controlled, therefore any sever short-circuit near the wind farm may cause significant voltage dip in the weak network.

Since the rotational speed of this type is limited to a very narrow range determined by the slip of the induction generator, any fluctuations in mechanical torque due to wind speed variation will impact the network where the wind farm is connected.

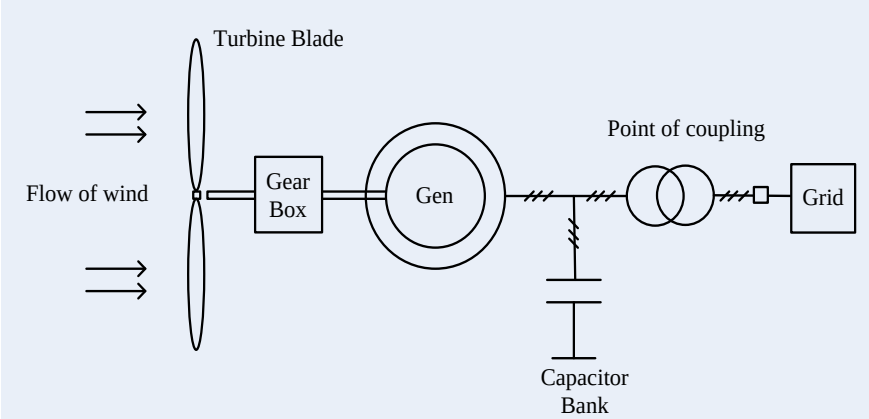

Figure 2.5 WECS with fixed speed wind turbine

Risk of loss of synchronism in case of voltage dips is high because both field and stator windings are supplied from the same bus.

2.3.2 WECS with Variable Speed Wind Turbines Type B

In the case of an induction generator with a variable rotor resistance (Type B wind turbine) Figure 2.6, it is possible to vary the speed over a somewhat wider range. However, the speed range is still rather limited and the speed cannot be controlled directly. Hence, looking at it from a control system perspective, this type of wind turbine may essentially be considered as a fixed-speed wind turbine.

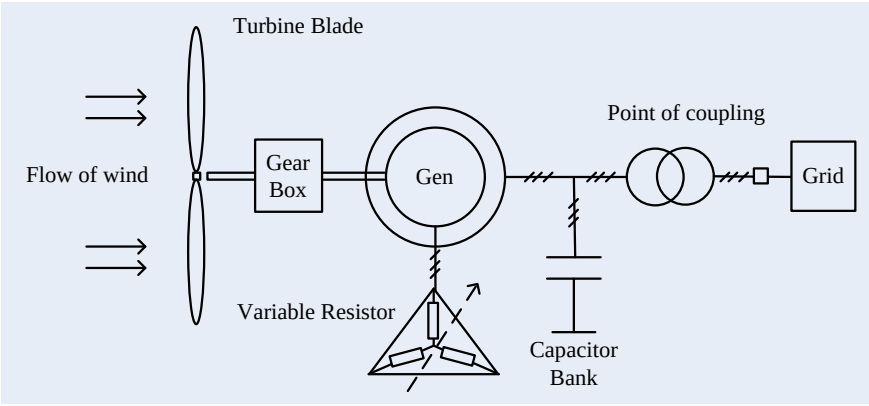

Figure 2.6 WECS with fixed speed wind turbine and variable resistor

2.3.3 WECS with DFIG Based Wind Turbine

Doubly-Fed Induction Generator (DFIG) drives Figure 2.7 and the full load converter connected generator drive are the two most frequently applied variable speed generator drive concepts.

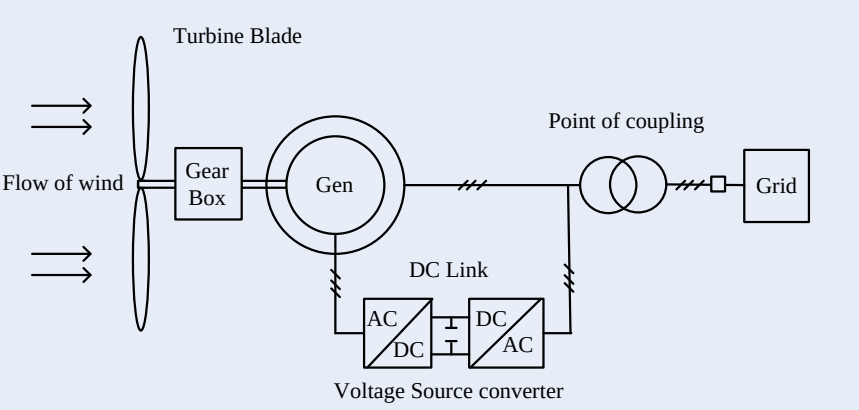

Figure 2.7 WECS with DFIG based wind turbine

Other variable-speed generator drive types are also available in the market, but currently they are not used for wind turbines. It would probably be possible to use written pole synchronous generators for instance, as a way of obtaining variable-speed capability in a generator drive. In short, theoretically all types of variable speed high-power drives electrical, mechanical or hydraulic with an electrical generator somewhere in the drive system can be used in wind turbine systems.

2.3.4 WECS with Full Converter

Variable-speed generator drives enable the wind turbine control system to adapt the rotational speed of the rotor to the instantaneous wind speed over a relatively wide range. The electrical system has a fixed frequency though. A generator drive connecting a variable-speed mechanical system to a fixed frequency electrical system must therefore contain some kind of a slip or decoupling mechanism between the two systems

In variable-speed wind turbine with full converter, Figure 2.8, the generator can be a squirrel-cage induction generator or a synchronous generator which is connected to the grid via a power electronic converter as shown in Figure 2.8. The entire power output from generator goes through the converter; therefore the converter is rated at full power. The voltage level and the reactive power can be regulated by using power electronic converters.

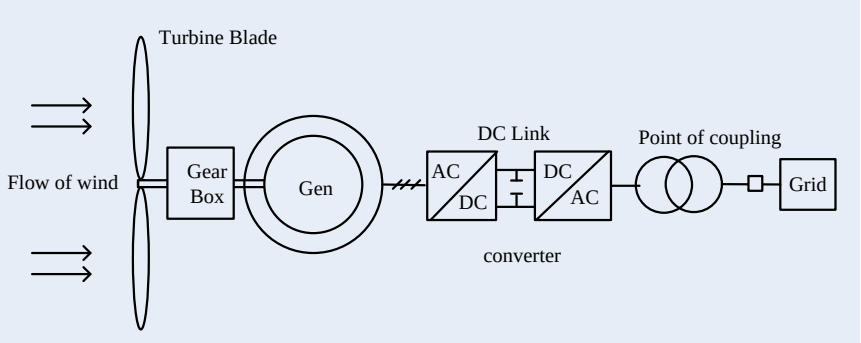

Figure 2.8 WECS with synchronous generator and convertor

2.4 Literature Review

Several researchers have carried out work on DFIG-based wind turbines to demonstrate their possibility to provide separate active and reactive power control. Therefore, DFIG-based wind turbines are the preferred choice for network operators in comparison to fixed-speed machines in which active and reactive power control is not independent.

In this section a modest attempt is made to review some of the pertinent research papers related to this study with emphasis on DFIG-based wind turbines and their role and contributions to system frequency control.

In [32], the concept of releasing the kinetic energy of a DFIG-based wind turbine when the frequency of the power system is reduced in order to prevent the reduction of system inertia is presented. The paper suggests the use of additional power set-point in the control system of the wind turbine. This additional power reference is calculated based on the rate of frequency change and inertia of the network. The additional power released by the DFIG-based wind turbine supports the primary frequency regulation and thus prevents reduction of system inertia.

In [33], the experimental results of engineering and design of a DFIG-based wind turbine, using back-to-back PWM voltage-source converters in the rotor circuit, is presented. A vector-control scheme is used for the supply-side of the PWM converter to maintain the quality of the supply source by drawing sinusoidal current from the network. The same scheme in the rotor side provides optimal speed tracking for a wide speed range of operation.

In [34], a model is developed to represent the two most important variable-speed wind turbine concepts in power system dynamic simulations. The first concept is the use of a DFIG with a back-to-back voltage source converter feeding the rotor winding. And the second concept is a direct-drive synchronous generator which is grid coupled through a diode rectifier and voltage source converter or through a back-to-back voltage source converter.

In [35], impact assessment of high penetration of wind energy to the Irish network is presented. Because of the small size of the network there could be significant impacts of small wind generation penetration. The paper studies two scenarios wherein all or none of the wind turbines provide an inertial response following a frequency transient.

In practice, the truth lies somewhere in between, and wind farms typically comprise a mix of fixed-speed turbines which can provide only limited inertial support and variable-speed machines which do not provide inertial support if they are not equipped with auxiliary 'inertial' feedback loop [2]. It has been shown in [6] that if wind turbines provide no inertia in times of low system demand, the robustness of the system is jeopardized. On the contrary, if wind turbines can participate in system inertia provisions, the frequency effect could be significantly mitigated.

In [36], a control scheme is proposed that allows DFIG-based wind turbines to participate effectively in system frequency regulation. In this approach, wind turbines operate according to a de-loaded optimum power extraction curve such that the active power provided by each wind turbine increases or decreases during system frequency changes. The control strategy defined for the wind turbine to supply primary frequency regulation capability exploits a combination of control of the static converters and pitch control, adjusting the rotor speed and the active power according to the de-loaded optimum power extraction curve. Results obtained considering a small isolated power system are presented to demonstrate the effectiveness of the approach, the drawback of this method is the loss of revenue accrued because the wind generator is not able to generate its maximum power.

In [37], the inertial response of wind turbines employing induction machine based generators is presented. A model of a Field-Oriented Controlled DFIG, based on a fifth-order induction generator model is described. The model is implemented in a reference frame that allows the factors affecting the inertial response of the DFIG to be easily examined. A comparison between the inertial response of a squirrel-cage and DFIG-based wind-turbine generator is performed using the developed models. It is found that the inertial response of a DFIG employing field-oriented controlled (FOC) strongly being influenced and effected by band width of rotor current control.

In [38], the concept of extracting the kinetic energy of DFIG machines by reducing the speed of the rotor is presented, and details of an addition power set-point in the DFIG, which is used in order to emulate the inertia of the wind turbine, is formulated. It is also observed that, as a result of supporting the frequency, the rotational speed of the DFIG decreases and therefore the power output drops considerable when the frequency control support is ended. This drop in power is undesirable, especially when all DFIG-based wind farms demonstrate this behavior. The

authors conclude that variable-speed wind turbines are able to support primary frequency control and emulate inertia by applying additional control loops. For that purpose, the kinetic energy stored in the "hidden inertia" of the turbine blades is used.

2.4.1 *Assumptions and constraint in participation of DFIG in frequency regulation*

In this study it has been assumed that the mechanical power of DFIG based wind turbine is constant (wind speed) and therefore uncertainty of wind power generation has not been considered. It is also assumed that in the power system with mixed generation, conventional generation is able to supply the additional demand during the disturbances and increase the production as needed. Maximum Power Tracking (MPT) system which tracks the optimal mechanical speed and permits temporary deviation from optimal speed is described in Chapter 3 and 4.

2.5 Simulations

2.5.1 Active Pitch Control

Figure 2.9 and 2.10 presents the behavior of induction type generator type A, being driven by a wind turbine as described in section 2.3.1. The turbine is controlled by a wind governor, during the wind speed step perturbation. Simulation is developed with PSCAD® professional program wind turbine and governor type MOD2 (generic model), which is available in the library of this program is used.

Before t=50 sec wind speed is equal to optimal wind speed 15 m/s and power output of the wind farm and mechanical torques as shown in Figure 2.10 are in the steady state condition. In t=50 sec after about 2 m/s wind speed perturbation is applied and therefore the wind speed raises to 17 m/s. thereafter pitch control system attempts to maintain the same power output by controlling the pitching angle, the output with about 20 second of perturbation returned to steady state by raising the β from about 15.6 deg to 18 deg. The active power of induction machine towards to network is shown with the negative sign.

Figure 2.10 similar to 2.9 presents the wind speed reduction steps and attempts of control system to maintain the wind farm output constant.

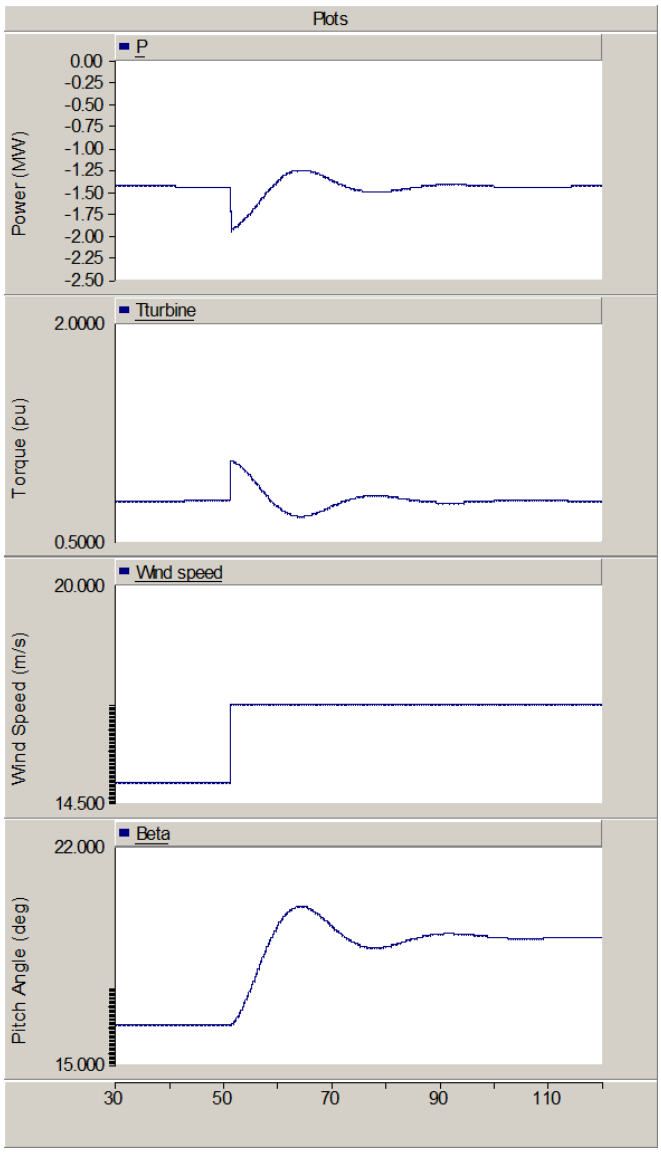

Figure 2.9 Plots of simulation of wind speed step perturbation for induction type wind turbine

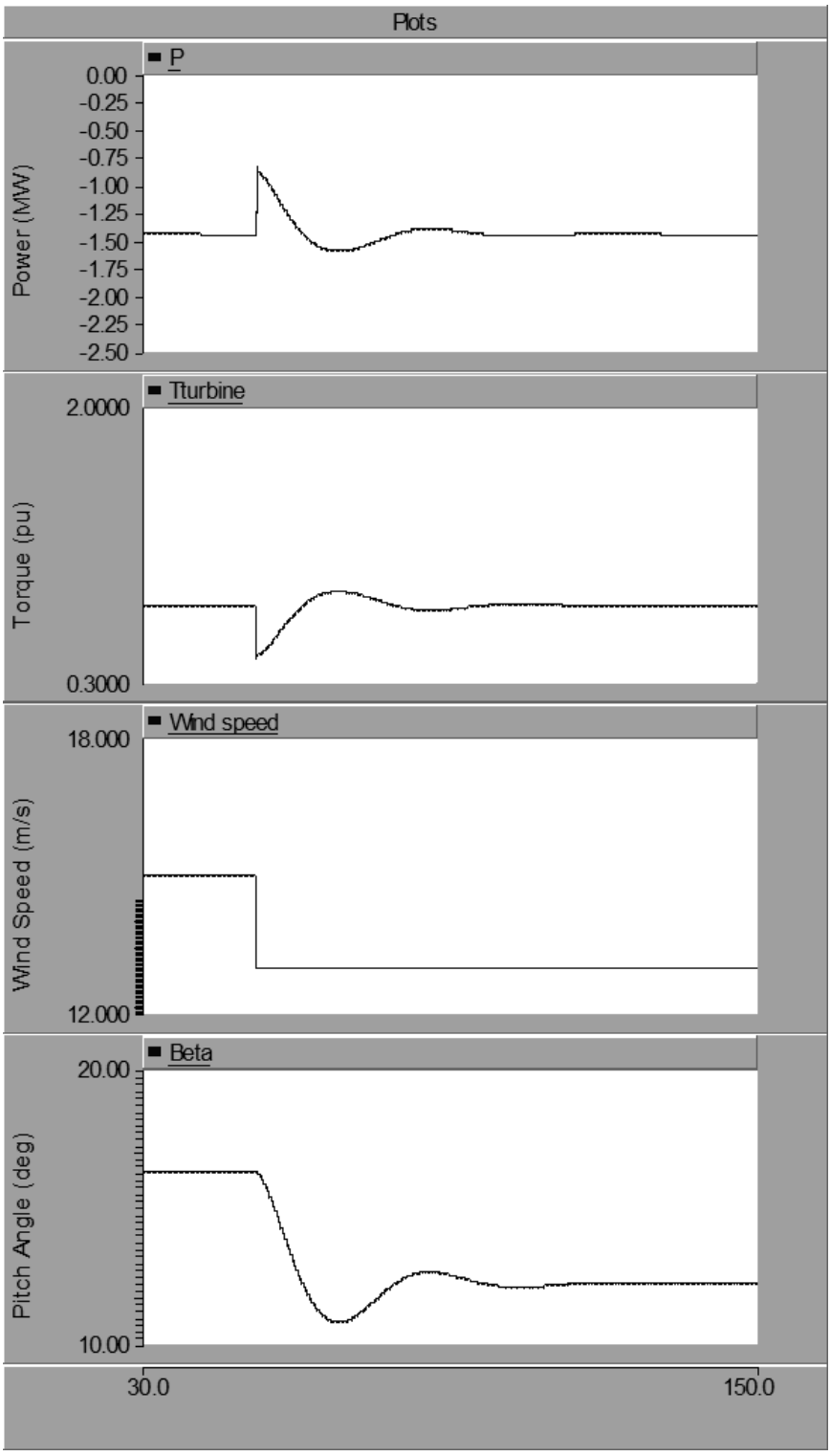

Figure 2.10 Plots of simulation of wind speed step perturbation for induction type wind turbine

2.6 Conclusion

This chapter presents a back ground review of the evolution of wind turbine technology and current status in its development. Thereafter, the mathematical relations for power from wind turbines are discussed and the importance of pitch control is highlighted. Subsequently, various classes and type of Wind Energy Converter Systems (WECS) are discussed in brief. A moderate review of literature pertaining to frequency control contribution of DFIG based wind generations is performed. Finally PSCAD simulation is performed that lay done the foundation for the research which has done in the next two chapters.

Chapter 3

Primary Frequency Regulation and AGC in a Single-Area System with DFIG-Based Wind Turbine

3.1 Introduction

In spite of the increasing penetration of wind turbines into the power grid, the frequency regulation and AGC tasks are mainly undertaken by conventional generation units. The goal of frequency regulation and AGC is to keep the frequency within specified limits through primary and secondary control of governor.

Traditionally, Wind Energy Conversion Systems (WECS) do not participate in system frequency support. Hence, wind turbines do not increase or decrease their production when the frequency falls or rises respectively, meaning that they do not contribute to the system inertia. With high rate of growth in wind generation capacity, its contribution to total generation mix is increasing but the total system inertia participating in frequency control is decreasing to inadequate levels for appropriate system frequency recovery following a power imbalance or grid disturbance. Therefore, further penetration of wind energy in the network calls for contributions from wind generators to frequency regulation and AGC in order to prevent reduction of total system inertia of the network.

Not much research has been reported on analyzing the effects of wind generator participation to frequency regulation and AGC in power systems. One of the methods discussed in several papers [32], [36], [38] with earlier types of turbines (such as fixed-speed turbines) propose preventing the wind turbines from supplying their maximum available power in normal situations so as to maintain a reserve margin that can be utilized for frequency control. More recently, extracting the kinetic energy stored in the mechanical system of wind turbines with variable-speed generators has been the subject of research [34], [35], [36]. The control system based on this concept, utilizes the ability of DFIG-based wind turbines to produce power with variable mechanical speed and extracting the kinetic energy to support the primary frequency regulation, has been based on the Wind Turbine Inertia Control model [32]. The block diagram of such a control system is shown in Figure 3.1.

Similar to conventional generators, wind turbines have a significant amount of kinetic energy stored in the rotating mass of their rotor and blades. An important feature of DFIG machines is the possibility for their active and reactive power outputs to be controlled as required by system operators. Although the steady-state active power delivered to the grid by a WECS depends on the wind speed, the power can be dynamically controlled to a certain extent by

utilizing the stored mechanical energy. This is due to the capability of these machines to work at asynchronous speeds. This way, the wind energy will transfer efficiently for a given wind speed, while the mechanical stress is relieved to some extent.

DFIG machines with slip-ring rotors are generally designed with three ac windings in the stator and rotor. The stator is normally connected directly to the grid and the rotor is supplied via a frequency converter. Thus the angular velocity of stator rotating field can be written as,

$$\frac{\omega_s}{p_s} = \omega_{mech} \pm \frac{\omega_r}{p_r} \tag{3.1}$$

In (3.1), p_s and p_r denote the number of stator and rotor poles respectively. As per (3.1), the system frequency ω_s is equal to sum of the angular velocity of mechanical rotation (ω_{mech}) and rotor current frequency (ω_r). Depending on the direction of the supply frequency, this machine can operate in over- or under- synchronous speed. The amount of kinetic energy released from the shaft of the wind turbine when the speed is reduced, given by ΔE_k, can be formulated from the relations below:

$$E_{k0} = \frac{1}{2} J \omega_{mech0}^2 \tag{3.2}$$

$$E_{k0} - E_{k1} = \frac{1}{2} J \omega_{mech0}^2 - \frac{1}{2} J \omega_{mech1}^2 \tag{3.3}$$

$$\Delta E_k = E_{k0} \left(1 - \frac{\omega_{mech1}^2}{\omega_{mech0}^2} \right) \tag{3.4}$$

E_{k0} is dependent on wind speed which varies between zero to 1.0 per unit and ω_{mech1} cannot be smaller than the minimum mechanical rotational speed of the DFIG-based wind turbine. Furthermore, the instantaneous power extracted from the wind turbine cannot exceed the maximum allowed value, as per manufacture data of the machine. These constraints, as stated in (3.5)-(3.8), have to be regarded in the control system.

$$E_{k0} = f(Wind\ Speed) \tag{3.5}$$

$$0 \le E_{k0} \le 1.0\ pu = f(Wind\ Speed) \tag{3.6}$$

$$\omega_{mech\min} \le \omega_{mech1} \tag{3.7}$$

$$E_{k0} + \Delta E_k \le E_{k\,max} \tag{3.8}$$

Figure 3.1 depicts the controllers of DFIG-based wind turbines that try to keep the turbine at its optimal speed in order to produce the maximum power. The controller provides a power set-point (P^*_{ω}) that is based on measured speed ($\omega_{m,meas}$) and measured electrical power

($P_{el,meas}$). The power set-point is an input for the converter control that realizes the torque and power by controlling the generator rotor currents. An additional control signal is added (ΔP^*_f) which adapts the power set-point as a function of the deviation and the rate of change of the grid frequency. The emulated inertia of the additional control signal is proportional to its controller parameters (K_{df} and K_{pf}). The support to primary frequency control depends on when this additional loop is activated, as the grid frequency exceeds certain limits, by adding this signal to the torque equation to set the torque demand. As the system frequency drops, the set point torque is increased and the rotor slows down and kinetic energy is released.

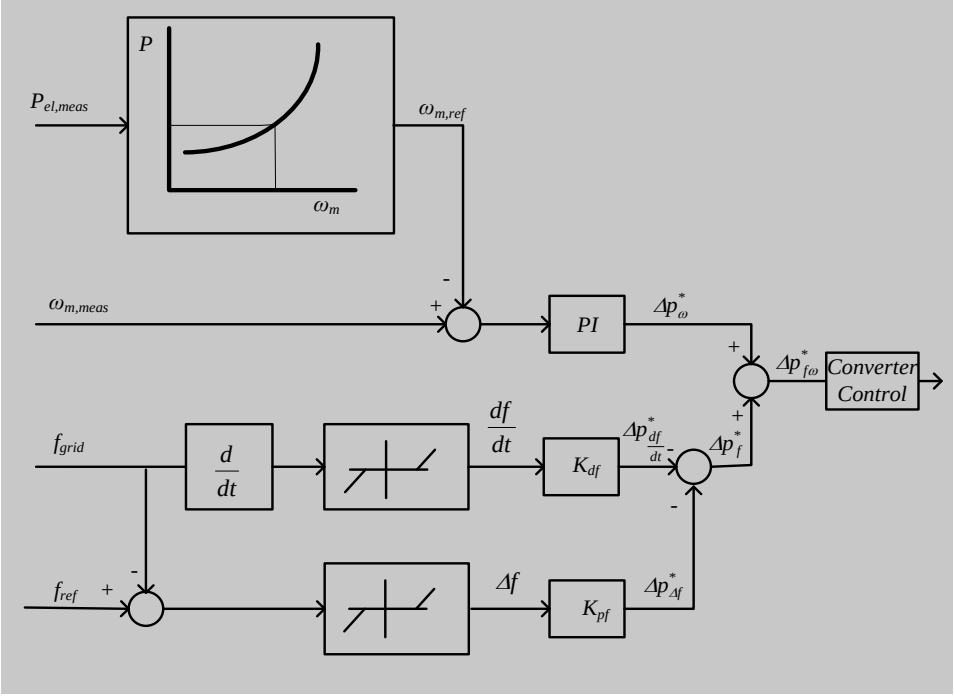

Figure 3.1 Principle of DFIG Inertial Emulation Control [38**]**

The power reference point ($\Delta P^*_{f\omega}$) has two components, ΔP^*_f the additional reference point based on frequency changes as described earlier and ΔP^*_ω which is based on optimum turbine speed as a function of wind speed, as given below [39]:

$$\Delta P_f^* = -K_{df}\frac{df}{dt} - K_{pf}\Delta f \tag{3.9}$$

$$\Delta P_\omega^* = -K_{wp}(\omega^* - \omega) + K_{wi}\int(\omega^* - \omega)\,dt \tag{3.10}$$

$$\Delta P_{f\omega}^* = \Delta P_f^* + \Delta P_\omega^* \tag{3.11}$$

K_{df} and K_{pf} are the controller gains for the derivative and proportional controllers respectively. Considering the two components of the DFIG power set-point (3.11), ΔP^*_ω changes

in relative terms, slowly, compared to the frequency derivation power set-point ΔP^*_f. Therefore, at *t=0* when disturbance occurs, we can assume ΔP^*_ω to be zero. Also, considering the instant conversion of set point to power by converter, we could assume $\Delta P_{NC} = \Delta P^*_{f\omega}$ and therefore,

$$\Delta P^*_{f\omega} = \Delta P^*_f + 0 \tag{3.12}$$

$$\Delta P_{NC} = \Delta P^*_{f\omega} = \Delta P^*_f = -K_{df}\frac{df}{dt} - K_{pf}\Delta f \tag{3.13}$$

3.2 DFIG-Based Wind Turbine Control Model

Figure 3.2 shows the overall transfer-function block diagram of a power system comprising a conventional generator providing frequency regulation as well as a non-conventional DFIG-based wind turbine generator contributing to frequency regulation. The incremental active power demand ΔPD subtracted from the incremental values of conventional generation ΔP_g and wind generation ΔP_{NC} equals the power transferred from the neighboring area, ΔP_{12} as given in (3.9).

$$\Delta P_g + \Delta P_{NC} - \Delta P_{1,2} - \Delta PD = \Delta P_f \tag{3.14}$$

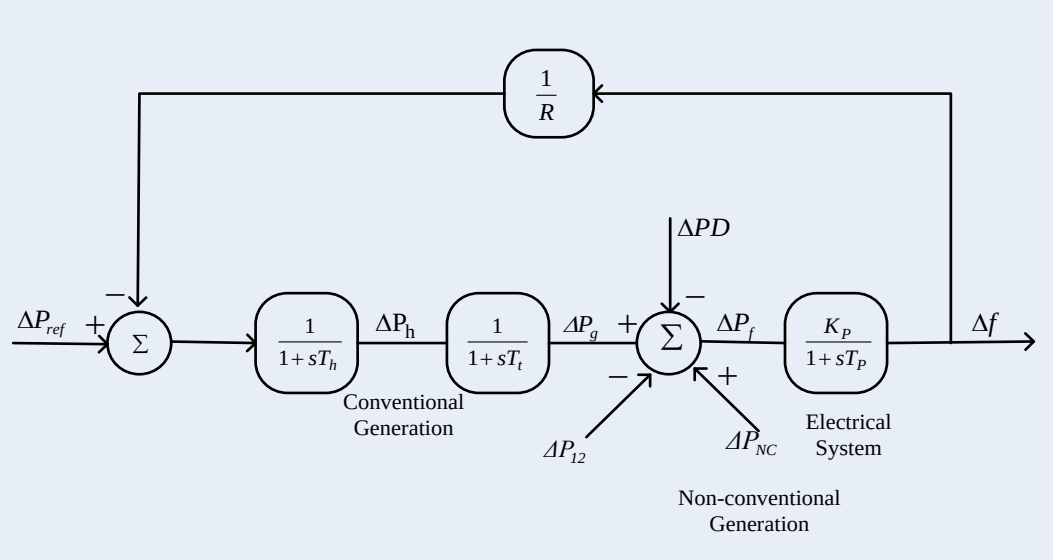

Figure 3.2 Power system dynamic model overview with mixed generation

From Figure 3.2 and (3.8), (3.9) and (3.13),

$$T_P = \frac{2H}{fD} \tag{3.15}$$

$$K_P = \frac{1}{D} \tag{3.16}$$

$$\frac{2H}{f}\frac{d\Delta f}{dt} = \Delta P_f - D\Delta f = \Delta P_g + \Delta P_{NC} - \Delta P_{12} - \Delta PD - D\Delta f \tag{3.17}$$

$$\underbrace{\left(\frac{2H}{f} + K_{df}\right)}_{2H^*}\frac{d\Delta f}{dt} = \Delta P_g - \Delta P_{12} - \Delta PD - \underbrace{(K_{pf} + D)}_{D^*}\Delta \tag{3.18}$$

Figure 3.3 shows the dynamic model adopted for the study of frequency regulation [3] with DFIG-based wind turbine generator. This model is in essence taken from the DFIG inertia emulation model presented in Figure 3.2.

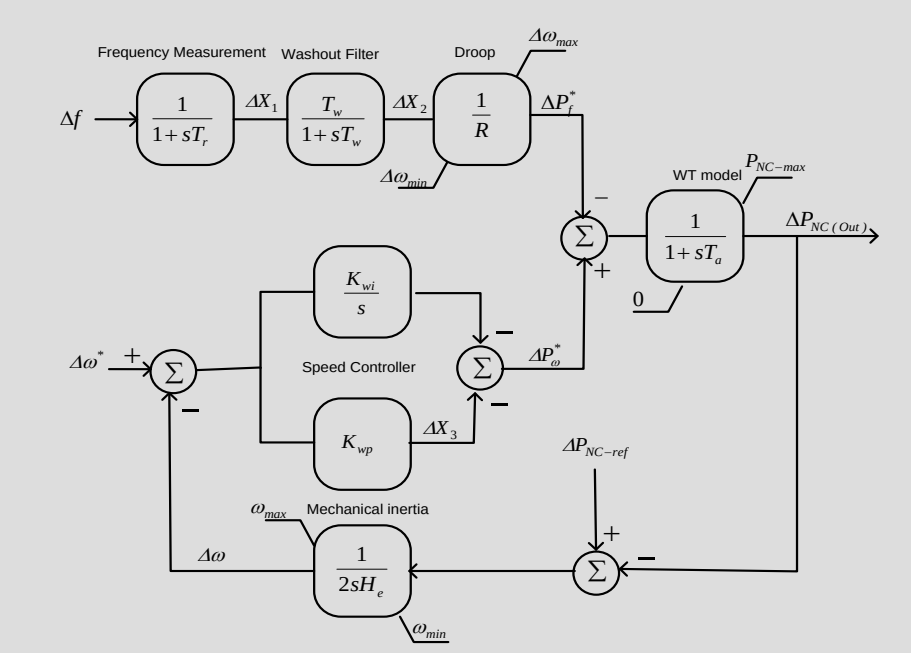

Figure 3.3 DFIG-based wind turbine control based on frequency change [35], [39]

The contribution of the DFIG towards system inertia can be seen in (3.17). The differences between the models described in Figure 3.1 and that in Figure 3.3 [3] is the additional reference power setting which is build based on the change in frequency using a washout filter with time constant T_w, which relies on a conventional primary regulation performance in a transient.

$$\Delta P_f^* = \frac{1}{R}\Delta X_2 \tag{3.19}$$

R is the droop constant as used conventionally and ΔX_2 is the frequency change measured where the wind turbine is connected to the network.

3.3 Dynamic Model of Primary Frequency Regulation with DFIG-Based Wind Turbines

The dynamic performance of a power system comprising a conventional prime-mover model, a non-reheat type turbine and a DFIG-based wind turbine is represented by the small-perturbation model shown in Figure 3.4 [3]. This model simulates the primary frequency regulation after a disturbance and includes conventional system parameters such as the load damping factor (D), the regulation droop (R), the inertia H, governor time constants T_h and T_t of the system equivalent unit (governor and turbine).

The system behavior depends on the choice of network parameters and DFIG-based wind turbine speed controllers are K_{wp} and K_{wi}. If several generators are connected to the system, the equivalent regulation droop can be determined from the (3.20) as follows:

$$\frac{1}{R} = \frac{1}{R_1} + \frac{1}{R_2} + \frac{1}{R_3} + \ldots + \frac{1}{R_n} \tag{3.20}$$

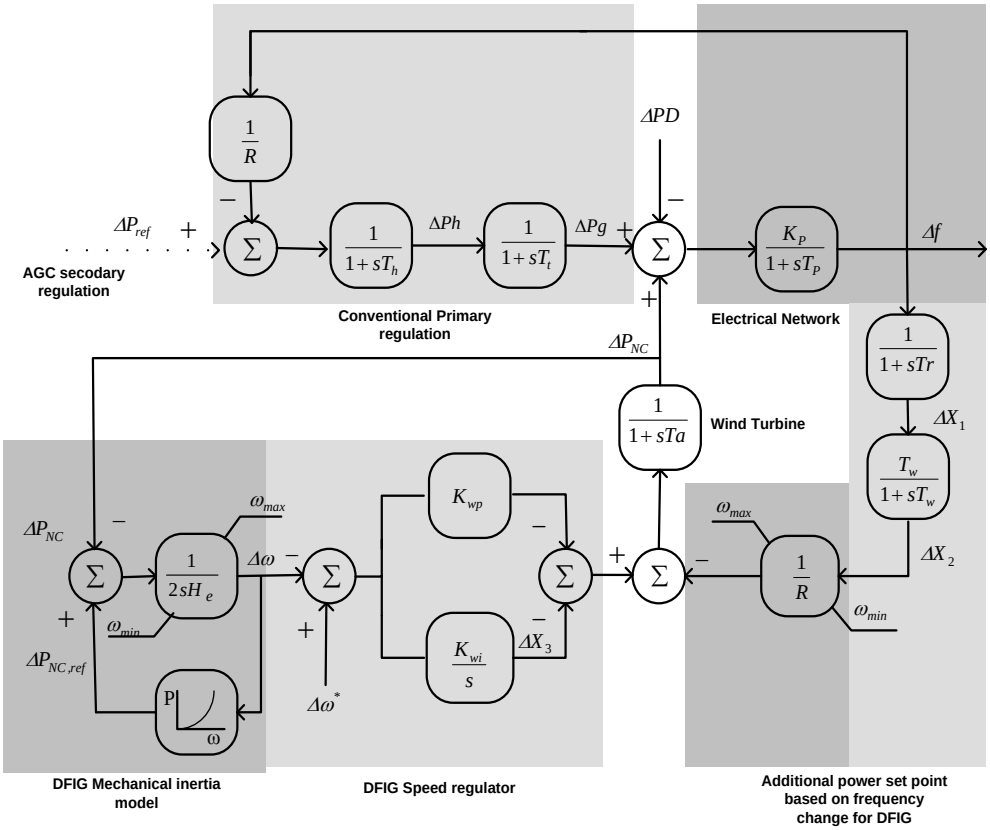

Figure 3.4 Primary frequency regulation block diagram with DFIG based WT

In Figure 3.4, ΔP_h is the incremental hydraulic governor valve position change, $\Delta\omega$ is incremental speed of the wind turbine, Δf is the incremental frequency change, ΔX_1 is frequency increment after being measured by transducer, ΔX_2 frequency change after the washout filter and ΔX_3 is the incremental change in DFIG integral speed control. The incremental model is obtained by linearizing the system around a nominal operating point. The dynamic model in state-space form can be obtained from the transfer-function model given below:

$$\frac{d\underline{X}}{dt} = A\underline{X} + \Gamma\underline{p} \tag{3.21}$$

$\underline{X}$ is the state-vector, $\underline{p}$ is the perturbation and A, Γ are state and perturbation matrices respectively. The state-equations (3.21) can be written in expanded vector-matrix form as follows:

$$\underline{X} = \begin{bmatrix} \Delta P_h & \Delta P_g & \Delta f & \Delta X_1 & \Delta X_2 & \Delta X_3 & \Delta\omega & \Delta P_{NC} \end{bmatrix}^T$$

$$A = \begin{bmatrix} \frac{-1}{T_h} & 0 & \frac{-1}{(RT_h)} & 0 & 0 & 0 & 0 & 0 \\ \frac{1}{T_t} & \frac{-1}{T_t} & 0 & 0 & 0 & 0 & 0 & 0 \\ 0 & \frac{K_p}{T_p} & \frac{-1}{T_p} & 0 & 0 & 0 & 0 & \frac{K_p}{T_p} \\ 0 & 0 & \frac{1}{Tr} & \frac{-1}{T_r} & 0 & 0 & 0 & 0 \\ 0 & 0 & \frac{1}{Tr} & \frac{-1}{T_r} & \frac{-1}{T_w} & 0 & 0 & 0 \\ 0 & 0 & 0 & 0 & \frac{-1}{(R*T_a)} & \frac{-1}{T_a} & \frac{K_{wp}}{T_a} & \frac{-1}{T_a} \\ 0 & 0 & 0 & 0 & 0 & 0 & \frac{1}{(2*H_e)} & \frac{-1}{(2*H_e)} \\ 0 & 0 & 0 & 0 & 0 & 0 & -K_{wi} & 0 \end{bmatrix}$$

$$\underline{p} = \begin{bmatrix} 0 & 0 & \Delta P_D & 0 & 0 & 0 & 0 & 0 \end{bmatrix}^T$$

$$\Gamma = \begin{bmatrix} 0 & 0 & \frac{-K_p}{T_p} & 0 & 0 & 0 & 0 & 0 \end{bmatrix}^T$$

Dynamic simulation for primary regulation with and without the DIFG-based wind turbine is carried out. The result is shown in Section 3.6.1.

3.4 Dynamic Model of AGC with DFIG-Based Wind Turbines

The small perturbation dynamic model considered for the single-area power system for AGC studies is shown in Figure 3.5. The model is similar to that described in the context of primary control except that a secondary control is added at the governor reference to regulate the set-point.

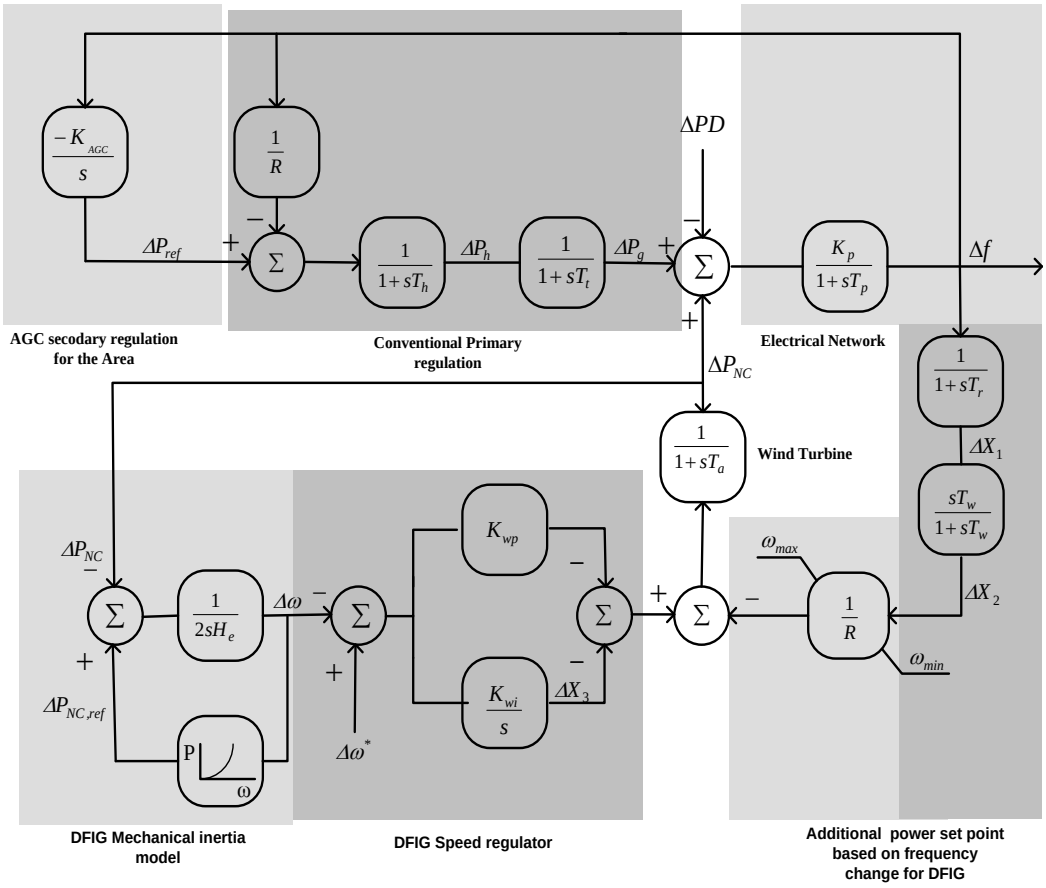

Figure 3.5 Dynamic model for AGC studies with DFIG-based wind turbines

The dynamic model in state-space form is developed from the transfer-function representation by defining the state-vector $\underline{X}$, given by:

$$\underline{X} = \begin{bmatrix} \Delta P_h & \Delta P_g & \Delta P_{ref} & \Delta f & \Delta X_1 & \Delta X_2 & \Delta X_3 & \Delta\omega & \Delta P_{NC} \end{bmatrix}^T$$

$$\frac{d\underline{X}}{dt} = A\underline{X} + \Gamma\,\underline{p} \tag{3.20}$$

$\underline{X}$ is the state-vector and $\underline{p}$ is the perturbation vector. The matrices A and Γ are state and perturbation matrixes respectively. The state-equation (3.20) can be written in expanded vector-matrix form as follows:

$$\underline{X} = \begin{bmatrix} \Delta P_h & \Delta P_g & \Delta P_{ref} & \Delta f & \Delta X_1 & \Delta X_2 & \Delta X_3 & \Delta\omega & \Delta P_{NC} \end{bmatrix}^T$$

$$A = \begin{bmatrix} \frac{-1}{T_h} & 0 & \frac{1}{T_h} & \frac{1}{(RT_h)} & 0 & 0 & 0 & 0 & 0 \\ \frac{1}{T_t} & \frac{-1}{T_t} & 0 & 0 & 0 & 0 & 0 & 0 & 0 \\ 0 & 0 & 0 & -K_{AGC} & 0 & 0 & 0 & 0 & 0 \\ 0 & \frac{K_p}{T_p} & 0 & \frac{-1}{T_p} & 0 & 0 & 0 & 0 & \frac{K_p}{T_p} \\ 0 & 0 & 0 & 0 & \frac{1}{Tr} & \frac{-1}{Tr} & 0 & 0 & 0 \\ 0 & 0 & 0 & \frac{1}{Tr} & \frac{-1}{Tr} & \frac{-1}{T_w} & 0 & 0 & 0 \\ 0 & 0 & 0 & 0 & 0 & \frac{-1}{(R*T_a)} & \frac{-1}{T_a} & \frac{K_{wp}}{T_a} & \frac{-1}{T_a} \\ 0 & 0 & 0 & 0 & 0 & 0 & 0 & \frac{1}{(2*H_e)} & \frac{-1}{(2*H_e)} \\ 0 & 0 & 0 & 0 & 0 & 0 & 0 & -K_{Wi} & 0 \end{bmatrix}$$

$$\underline{p} = \begin{bmatrix} 0 & 0 & 0 & \Delta PD & 0 & 0 & 0 & 0 & 0 \end{bmatrix}^T$$

$$\Gamma = \begin{bmatrix} 0 & 0 & 0 & \frac{-K_P}{T_P} & 0 & 0 & 0 & 0 & 0 \end{bmatrix}^T$$

Dynamic simulation is carried out with and without the DIFG-based wind turbine for sudden load increase.

3.5 Optimal Tuning of DFIG-Based Wind Turbine Controller Parameters

The objective of this section is to determine the optimal settings of the speed control parameters of the DFIG-based wind turbine so as to improve its participation in frequency control in response to system disturbances. The Integral of Squared Error (ISE) [40] technique is used for obtaining the optimum values of K_{wp} and K_{wi}. In the state-space model (3.20), a step perturbation of 0.02 per unit is considered, which remains constant during the dynamics of the process.

In order to examine the impact of the growth of wind energy in the total energy supply mix of the system, a Penetration Index (α_W) is defined as follows:

$$\alpha_w = \frac{Total\ wind\ generation}{Total\ generation\ from\ all\ sources} \times 100$$

Four cases of DFIG penetration are considered:

- $\alpha_W = 5\%$
- $\alpha_W = 10\%$
- $\alpha_W = 20\%$
- $\alpha_W = 50\%$

The initial values of the state variable, which in this study, are the incremental changes from their nominal values, will be zero since the system is stable. For $t \rightarrow \infty$, the states will approach a new steady-state and thus at any time *t*, the state-vector $\underline{X}(t)$ represents the deviations of the state variable from its steady-state value. Therefore, the dynamic performance of the system, for a given set of control parameters, can be measured using a quadratic performance index denoting the squared of the deviations of the state variables, as follows:

$$J = \int_0^\infty \left[X_1^2(t) + X_2^2(t) + X_3^2(t) + ... + X_n^2(t) \right] dt \tag{3.22}$$

In this work, the square of the frequency deviation errors is considered as the performance index for tuning the controller parameters, as stated below.

$$J = \int_0^\infty \left[\Delta f^2(t) \right] dt \tag{3.23}$$

For computational purposes, the performance index J is calculated by summing the discrete values at very small intervals, over a considerable period until the steady-state is achieved, as given below.

$$J = \sum_{k=1}^{K} \left[\Delta f^2(t_0 + k\Delta t) \right] \tag{3.24}$$

The optimal values of the DFIG speed controller parameters K_{WP} and K_{WI} are determined by searching for the minimum value of J. At first, K_{WI} is fixed at a certain value and K_{WP} is varied over a wide range. It is observed that J decreases as K_{wp} is increased, attains a minimum, J_{Min}, and then increases again. The values of K_{wp} and K_{wi} that yields the minimum of J_{Min} (J^*_{Min}), are the optimal controller parameters. Figure 3.6 shows the plot of J versus K_{WP} for several values of K_{WI}

considering ,20% wind turbine penetrations in the system respectively following a 0.02 per unit step load perturbation.

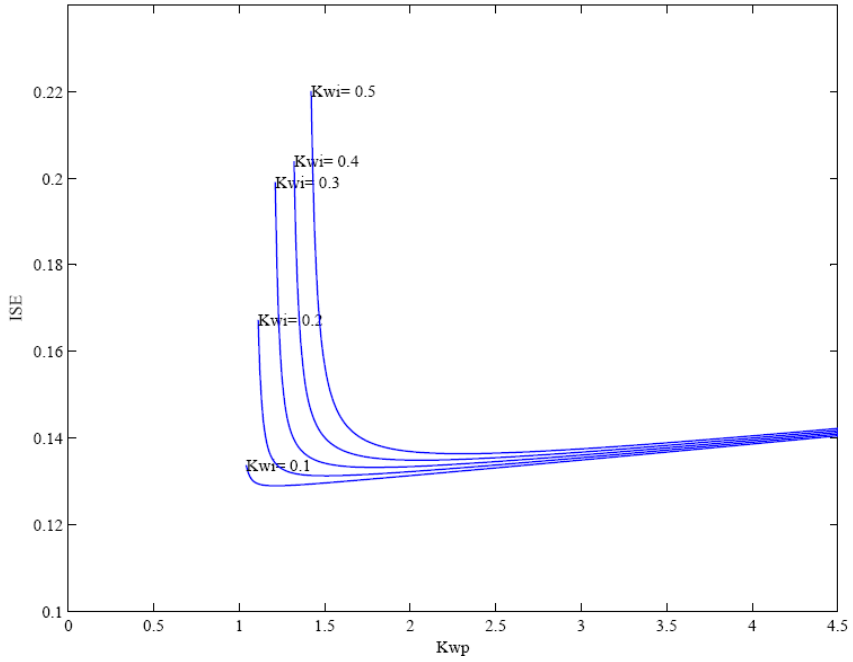

Figure 3.6 Optimal tuning of DFIG controller parameters for 20% wind penetration

It can be observed from Table-3.1 that the optimal settings of the controller gains are slightly affected by the wind penetration levels and the performance is expected to worsen with a higher penetration of wind generation, since J^*_{Min} is higher for 50% penetration than that with 20% penetration.

Table 3.1 Optimal parameters of the controller for different wind penetration

Wind Penetration	**K_{wi}**	**K_{wp}**	**J^*_{Min}**
5%	0.05	1.00	0.0151
10%	0.05	1.00	0.0161
20%	0.1	1.23	0.1209
50%	0.1	1.98	0.1235

3.6 Analytical Studies

3.6.1 Primary Regulation

Simulations are carried out considering the dynamic model presented in Figure 3.4 for a 0.02 per unit load perturbation with and without DFIG wind turbine to examine its contribution in primary frequency regulation, different plots for theses simulations are presented in Figure 3.7 to 3.11. During the simulations it has been assumed that DFIG-based wind turbines are in their optimal mechanical speed with the maximum power obtainable form the wind, and wind speed remain constant during the simulation.

Figure 3.7 to 3.8 presents the frequency plots following a 0.02 per unit step load perturbation with and without the DFIG. It is observed that the frequency response following the disturbance is improved, by way of lower frequency peak excursion when DFIG participation is considered. It is also observed that when the wind penetration level increases from 5% to 50%, although the lower frequency peak excursion is improved by higher penetration but the frequency response deteriorates by way of increased settling time and higher steady-state frequency error,. It can be generally concluded that with lower penetrations 5 % there is no significant improvement compare to no-DFIG case.

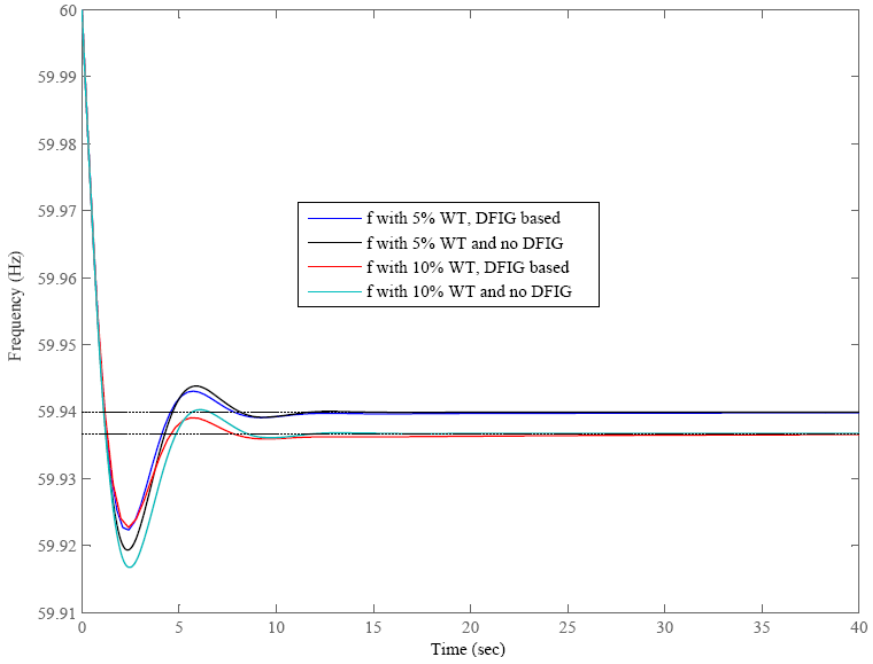

Figure 3.7 Primary frequency regulations with and without DFIG

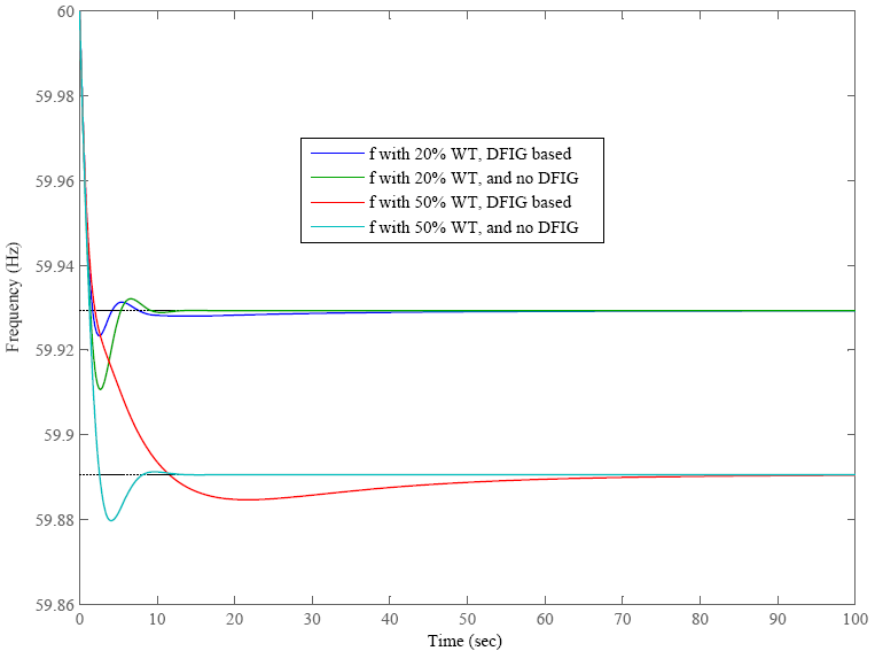

Figure 3.8 Primary frequency regulations with and without DFIG

Figure 3.9 and 3.11 shows the responses of the conventional generator and the DFIG providing primary regulation services. It can be seen that when the load increases at t=0, the DFIG instantly releases its kinetic energy by reducing the mechanical speed instantly therefore can increases its output to participate in primary frequency regulation. Thereafter DFIG output decreases since the speed is no longer at the optimal and power extracted from the wind is reduced. As the DFIG speed controller acts and the optimal speed is recovered, the DFIG power output returns to its nominal.

It is also observed that the DFIG does not contribute to the frequency support after steady-state is reached, and only provides frequency regulation during the transient phase. The conventional generator, on the other hand, regulates its output and attains a new steady-state operation level while providing primary regulation service.

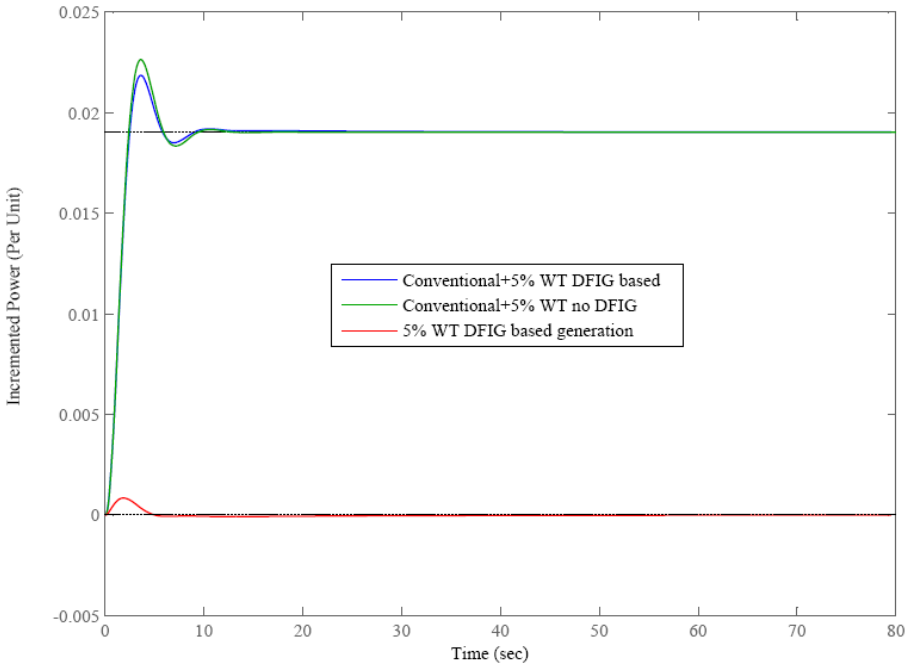

Figure 3.9 Generator responses in primary frequency regulation with and without

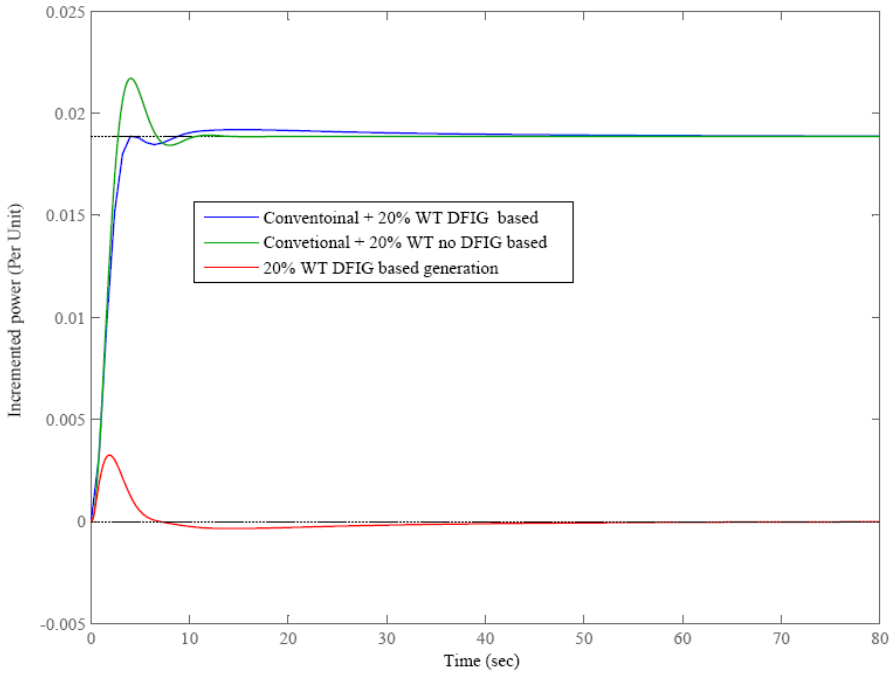

Figure 3.7 Generator response in primary frequency regulation with and without DFIG

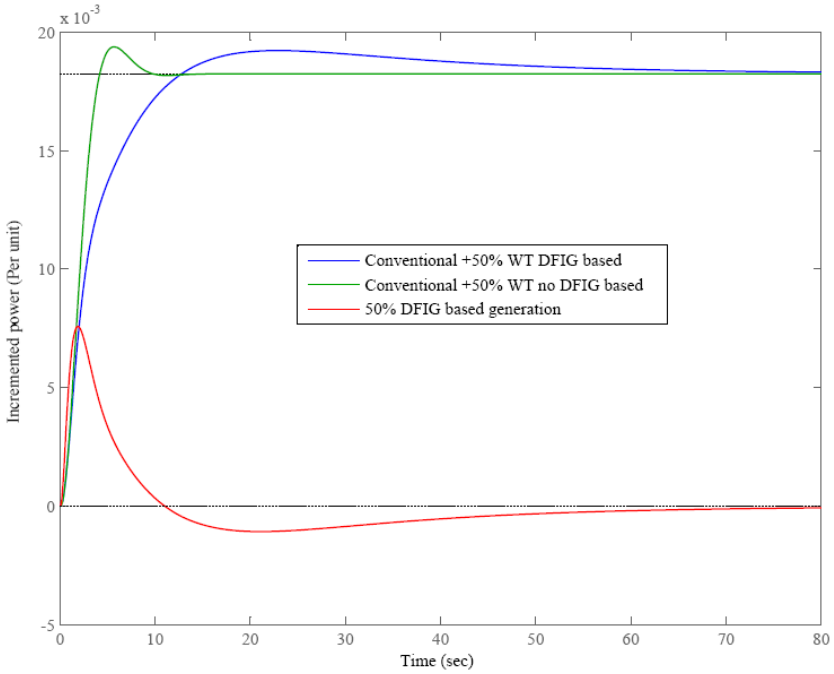

Figure 3.8 Generator response in primary frequency regulation with and without DFIG

Figure-3.12 and 3.13 shows the relation of the DFIG-based wind turbine incremental power output and mechanical speed change, during the participation of the DFIG in primary frequency regulation services. It can be seen that the additional power output of DFIG after load perturbation is obtained by reduction of mechanical speed.

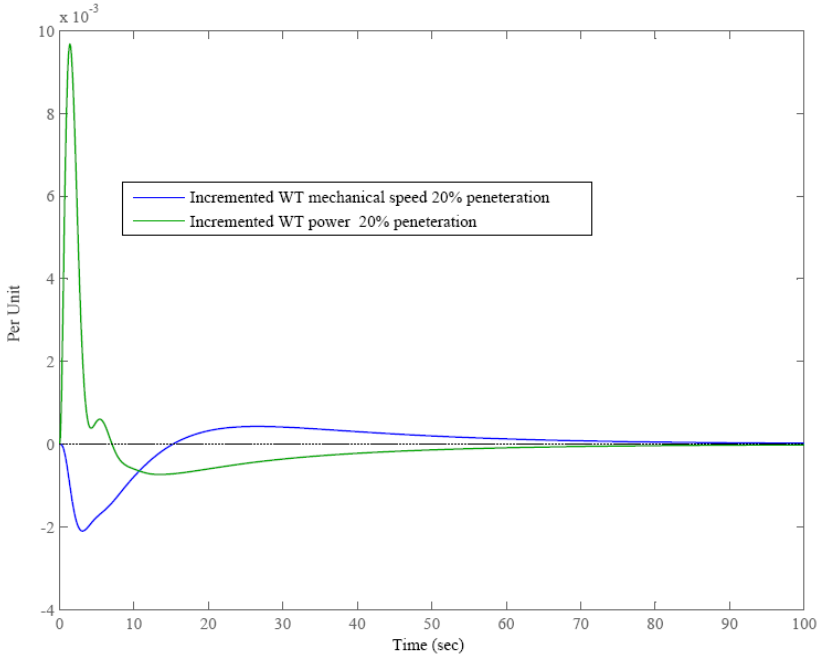

Figure 3.9 DFIG generator response in primary frequency regulation

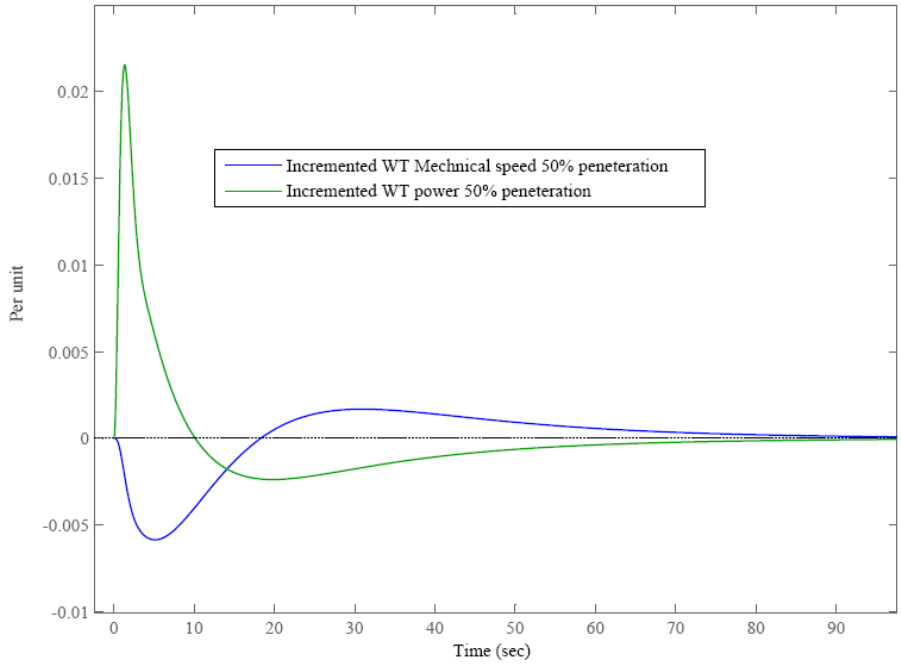

Figure 3.10 DFIG generator response in primary frequency regulation

3.6.2 Automatic Generation Control

Figure 3.14 shows the MATLAB Simulink® model for examining the secondary frequency control or AGC effects of the DFIG-based wind turbine generator. In this model wind turbine mechanical speed limit during week wind or very strong wind is defined. DFIG maximum power output constraint is implemented, and finally both strong and weak wind mechanical source has been considered. Wind turbine speeds has to be within the threshold of cut out speed is been implemented.

The energy extraction from DFIG machine is permitted only when the ultimately the mechanical speeds lay within cut out speeds, and speed controller will not permit the speed to be lower than minimum speed.

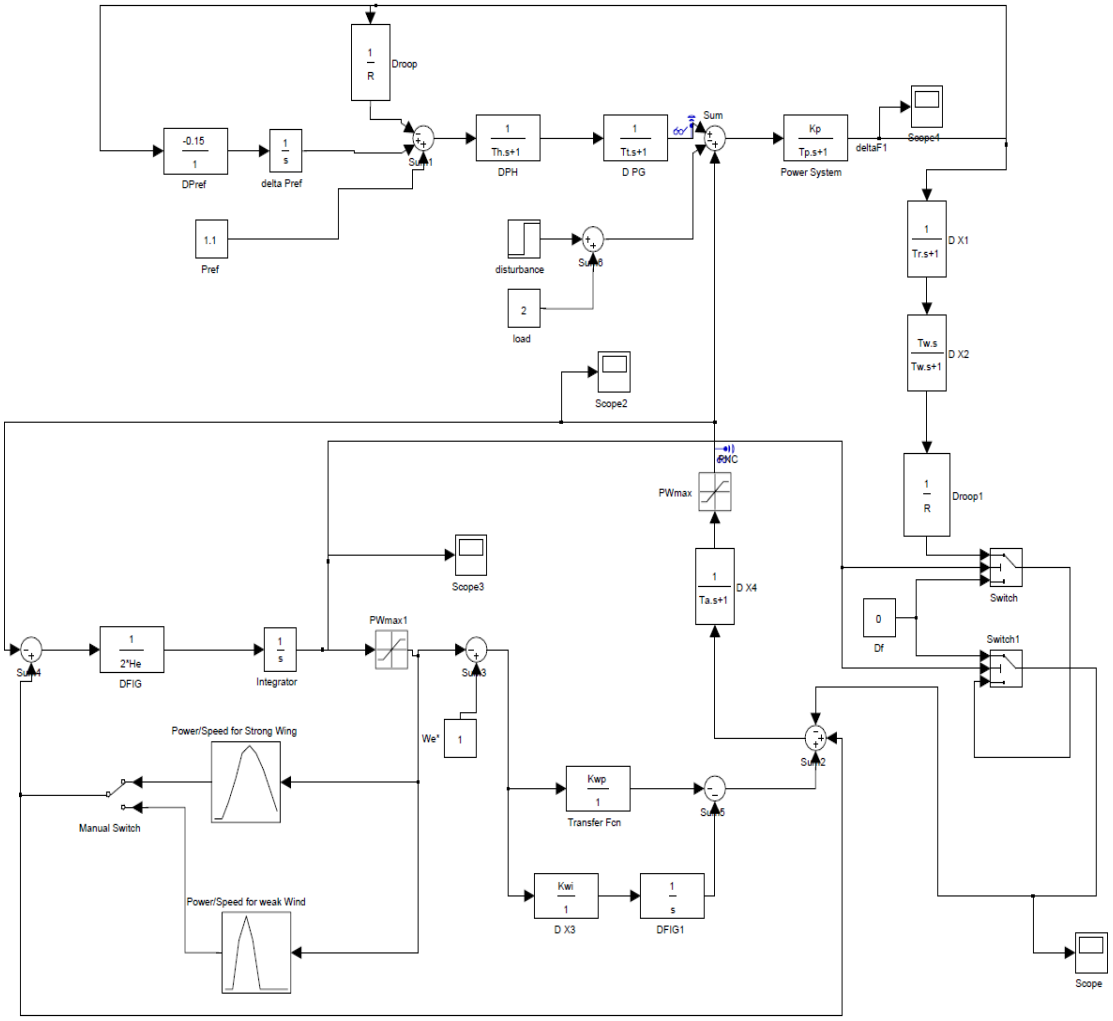

Figure 3.11 DFIG-Based WT with AGC Simulation model in Simulink®

Simulations are carried out considering the dynamic model presented in Figure- 3.5 for a 0.02 per unit load perturbation with and without DFIG wind turbine to examine its contribution in AGC service, The simulations are carried out for two levels of wind penetration, 20% and 50% and the corresponding optimally tuned parameters for the DFIG controller, obtained in Section-3.5, are used. As mentioned earlier, it has been assumed that DFIG-based wind turbines are in their optimal mechanical speed with the output corresponding to the maximum power obtainable form the wind, and wind speed remain constant during the simulation and the conventional generator is able to supply the additional load after settlement of the transient.

Different plots for theses simulations are presented in Figure 3.15 to 3.18. Figure 3.15 shows the frequency responses with AGC for 5% wind power penetration with and without DFIG. It is observed that the frequency responses for the case with and without DFIG very close,

and it is improved, by way of lower frequency peak excursion when DFIG participation is considered. It is also observed that by using the DFIG tuned speed controller parameters the settling time for cases 5%, 10%, 20% and 50% wind penetration are improved. It can be generally expected that with the higher wind penetration the settling time will be longer.

Figure 3.15 to 3.18 shows low penetration of wind energy will not have negative impact on frequency transient settling time between 5% to 20 %, while with further wind power penetration 50% wind power frequency transient settling time will deteriorates, therefore it generally can be concluded that the performance of AGC following a small load perturbation can be improved with participation of DFIG. Peak frequency excursion will be reduced in direct relation to the level of DFIG penetration while frequency settling time compare to no DFIG-based wind turbine is not improved.

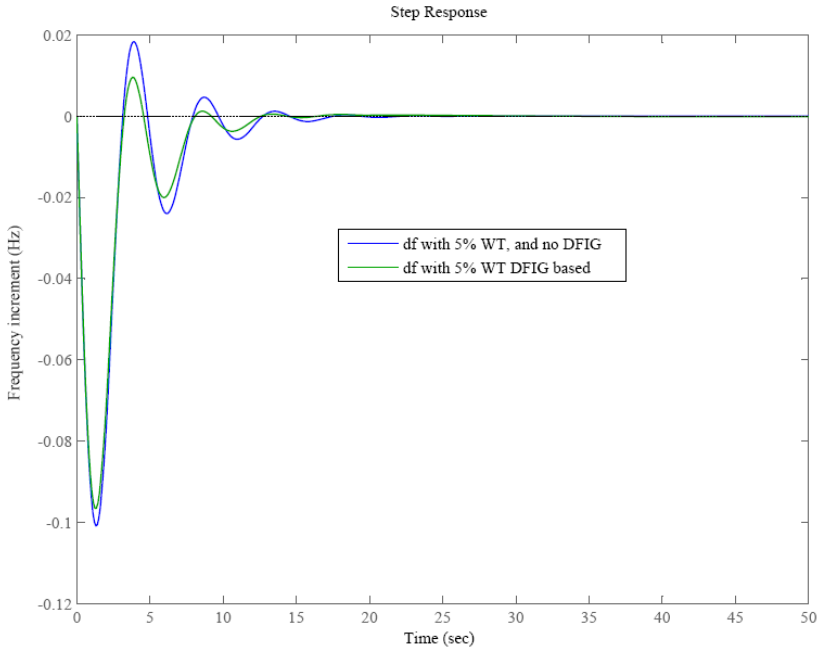

Figure 3.12 AGC with 2% load increment with and without DFIG

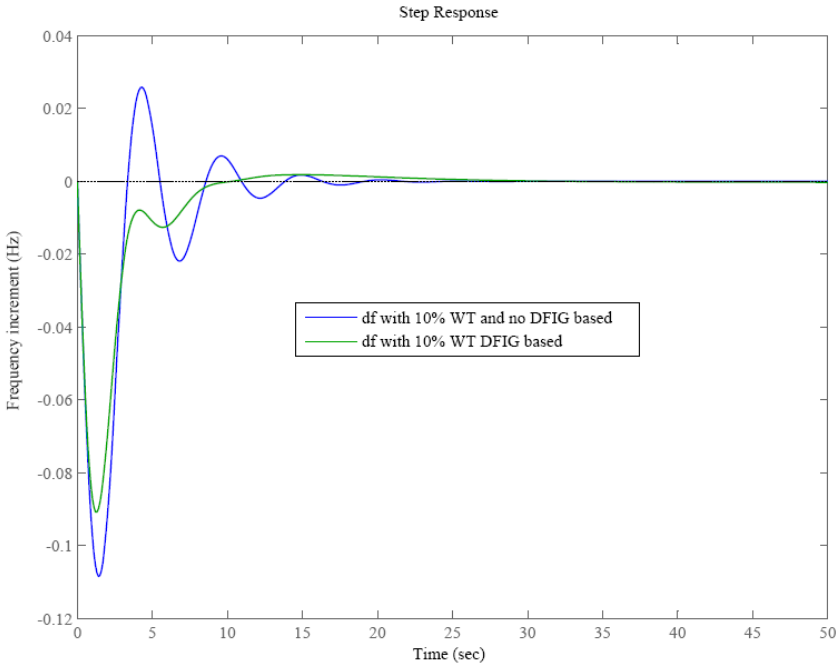

Figure 3.13 AGC with 2% load increment with and without DFIG

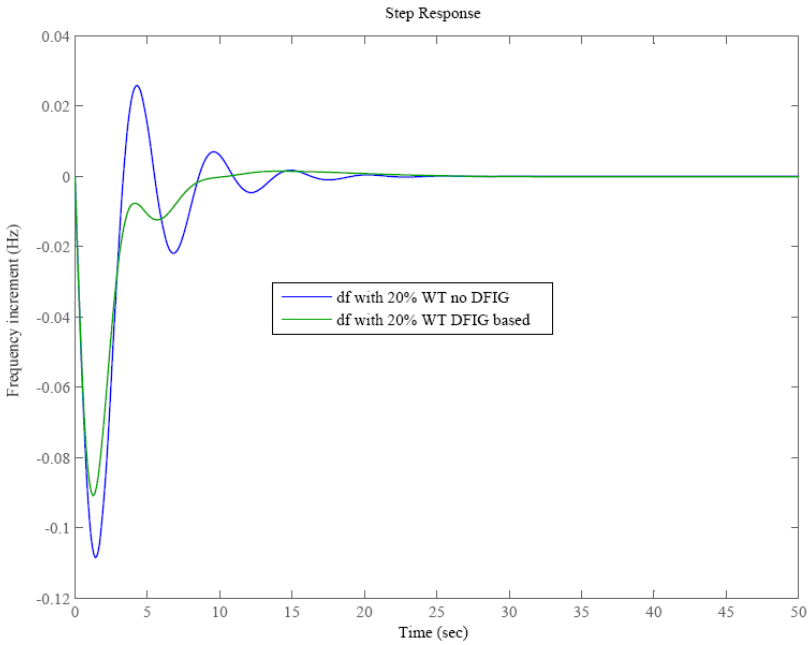

Figure 3.14 AGC with 2% load increment with and without DFIG

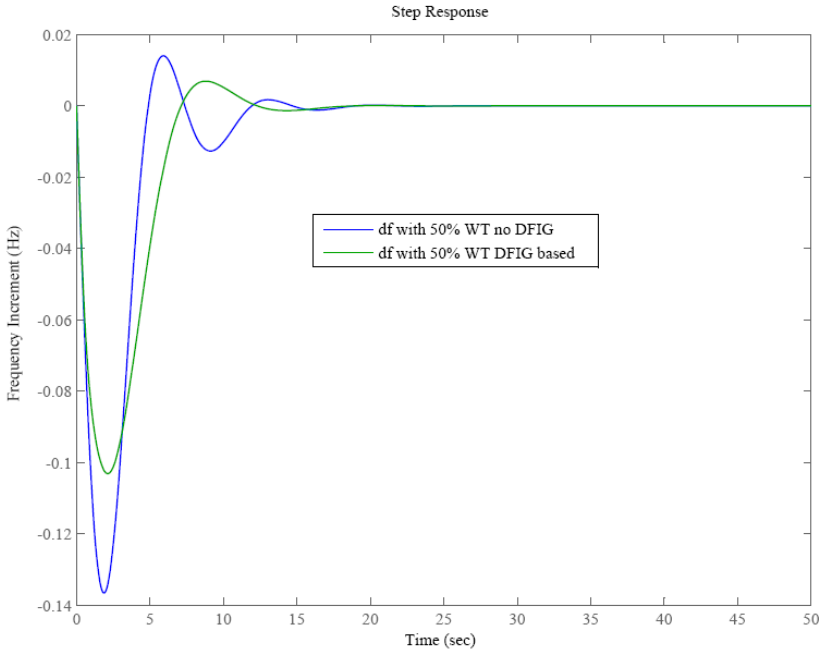

Figure 3.15 AGC with 2% load increment with and without DFIG

Figure 3.19 and 3.20 shows the responses of the DFIG supporting AGC services. It can be seen that when the load increases at t=0, the DFIG instantly releases its kinetic energy by reducing the mechanical speed instantly therefore can increases its output to participate and support AGC. Thereafter as has been indicated in the earlier section DFIG output decreases since the speed is no longer at the optimal and power extracted from the wind is reduced. As the DFIG speed controller acts and the optimal speed is recovered, the DFIG power output returns to its nominal.

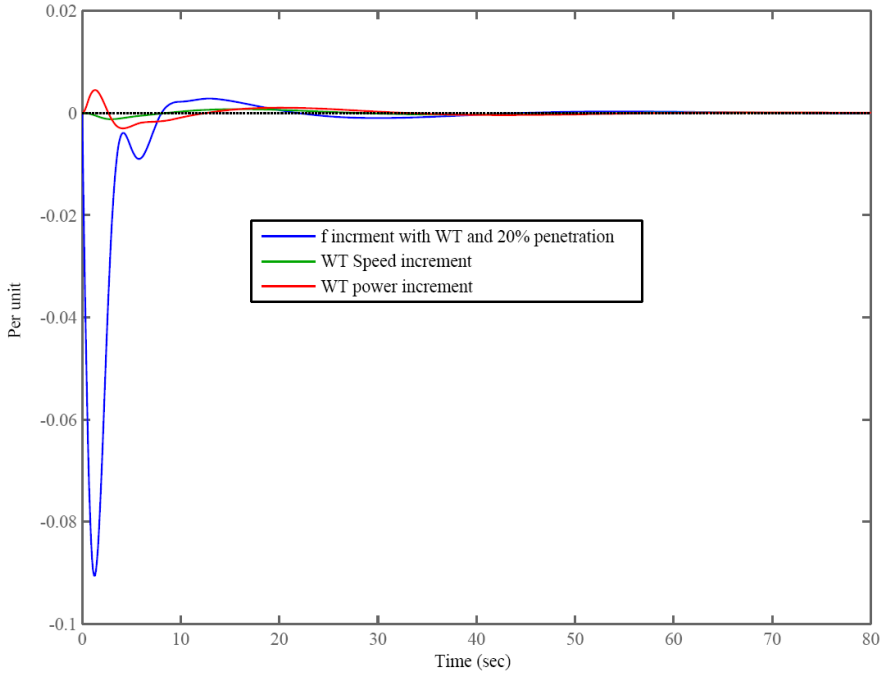

Figure 3.19 DFIG generation with AGC and 2% load increment

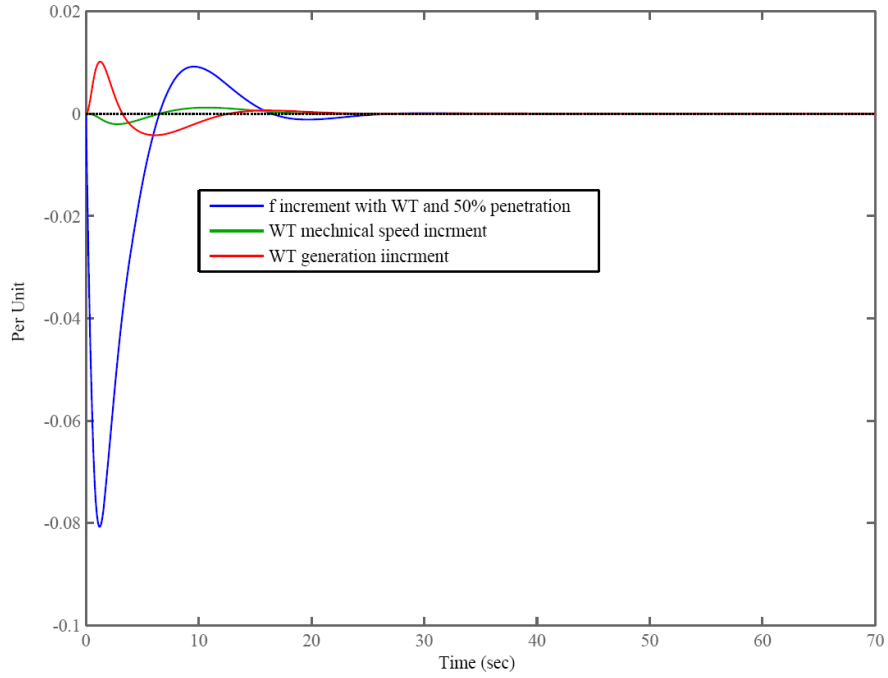

Figure 3.16 DFIG generation with AGC and 2% load increment

3.7 Conclusion

Traditionally, wind turbine is not participating in the frequency regulation. With further growth of wind energy, operators are demanding more and more participation of wind turbine in the ancillary services especially frequency regulation. Doubly fed induction generators with the ability of delivering power with different mechanical speed in one side, and the ability to instantly reduce the speed, release the stored mechanical energy is able to support the conventional generator in regulating frequency. This will reduce the frequency dip even more efficiently whenever DFIG, PI controller is tuned. The extraction of energy from DFIG will be coordinated with AGC of conventional generators which as result, damping of overshoot and frequency excursion can be improved significantly. With further penetration of wind energy in the electrical network with a target of growing to 20% of installed based power in North America and most of the European countries, PI controller and AGC characteristics should be tuned, in order to optimize the use of DFIG machine and their performance in participation of frequency regulation.

Chapter 4

Primary and Secondary Frequency Control in Two Area Systems with DFIG- Based Wind Turbine Support

4.1 Introduction

Multiple-area frequency control issues for an interconnected power system are far more significant and complicated than those associated with isolated networks. In isolated networks (single area) it is assumed that the frequency is uniform across the network resulting in single-area control. Certainly this is not the case in large interconnected system where numerous control areas can be identified. These control areas are traditionally associated with vertically integrated utilities in charge of well defined geographical areas, and with their own secondary frequency controls.

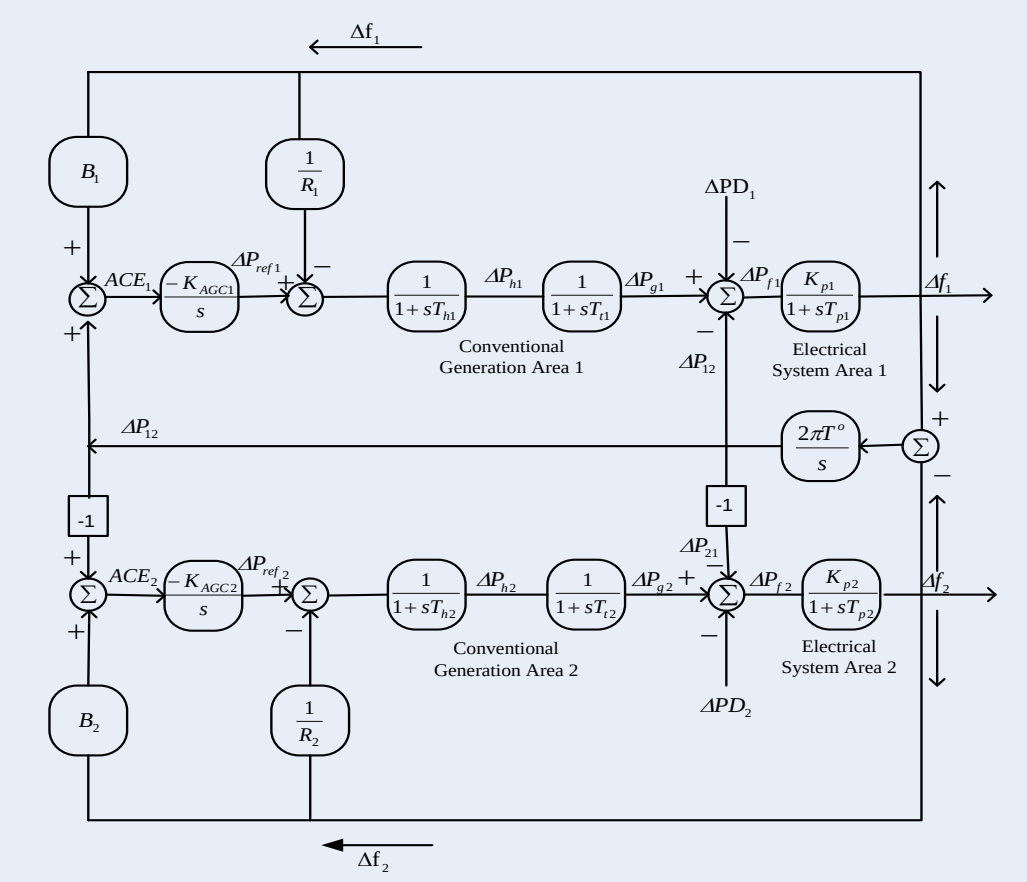

Figure 4.1 linear model of frequency control two Area Systems

The dynamic performance of a two-area interconnected system can be analyzed using a small-perturbation transfer-function model (Figure 4.1). This model includes both the primary and secondary frequency regulation controls after a disturbance. The system performance largely depends on the integral control gains (K_{AGC1} and K_{AGC2}) and the frequency bias factors (B_1 and B_2), in addition to system parameters and operating conditions.

Under normal operating conditions each area strives to carry its own load, and a portion of the neighboring area's load through the tie-line if agreed upon and scheduled in advance. Similar to a single-area each system frequency control area is characterized by the same frequency, therefore incremental frequency changes are represented by Δf_1 and Δf_2 respectively.

During normal operation, tie-line power flow obtained (4-1):

$$P_{12}^{o} = \frac{\left|V_1^{o}\right|\left|V_2^{o}\right|}{X} Sin(\delta_1^{o} - \delta_2^{o}) \tag{4-1}$$

Where δ°_1 and δ°_2 are the angles of the tie end voltages V°_1 and V°_2 respectively, and P°_{12} is the power in the tie line. For small value of δ_1 and δ_2 the tie line power incremental can be written as follows:

$$\Delta P_{12} \approx T_{12}(\Delta\delta_1 - \Delta\delta_2) \tag{4-2}$$

$$T_{12} \overset{\Delta}{=} \frac{\left|V_1^{o}\right|\left|V_2^{o}\right|}{X} Cos(\delta_1^{o} - \delta_2^{o}) \tag{4-3}$$

Analogous to electric stiffness concept of synchronizing machines, (4-3) is considered as the synchronizing torque coefficient.

For two area-control system, the Area Control Error (ACE) for each area consists of linear combination of frequency and tie line error, as given below:

$$ACE_1 = \Delta P_{12} + B_1 \Delta f_1 \tag{4-4}$$

$$ACE_2 = \Delta P_{21} + B_2 \Delta f_2 \tag{4-5}$$

4.2 Dynamic Model of Primary Frequency Regulation with DFIG-Based Wind Turbines

The small perturbation model in the form of transfer-function block diagram for a two-area frequency control system comprising a simple conventional prime-mover model, with a non-reheat type turbine and DFIG-based wind turbine in each area is shown in Figure 4.2.

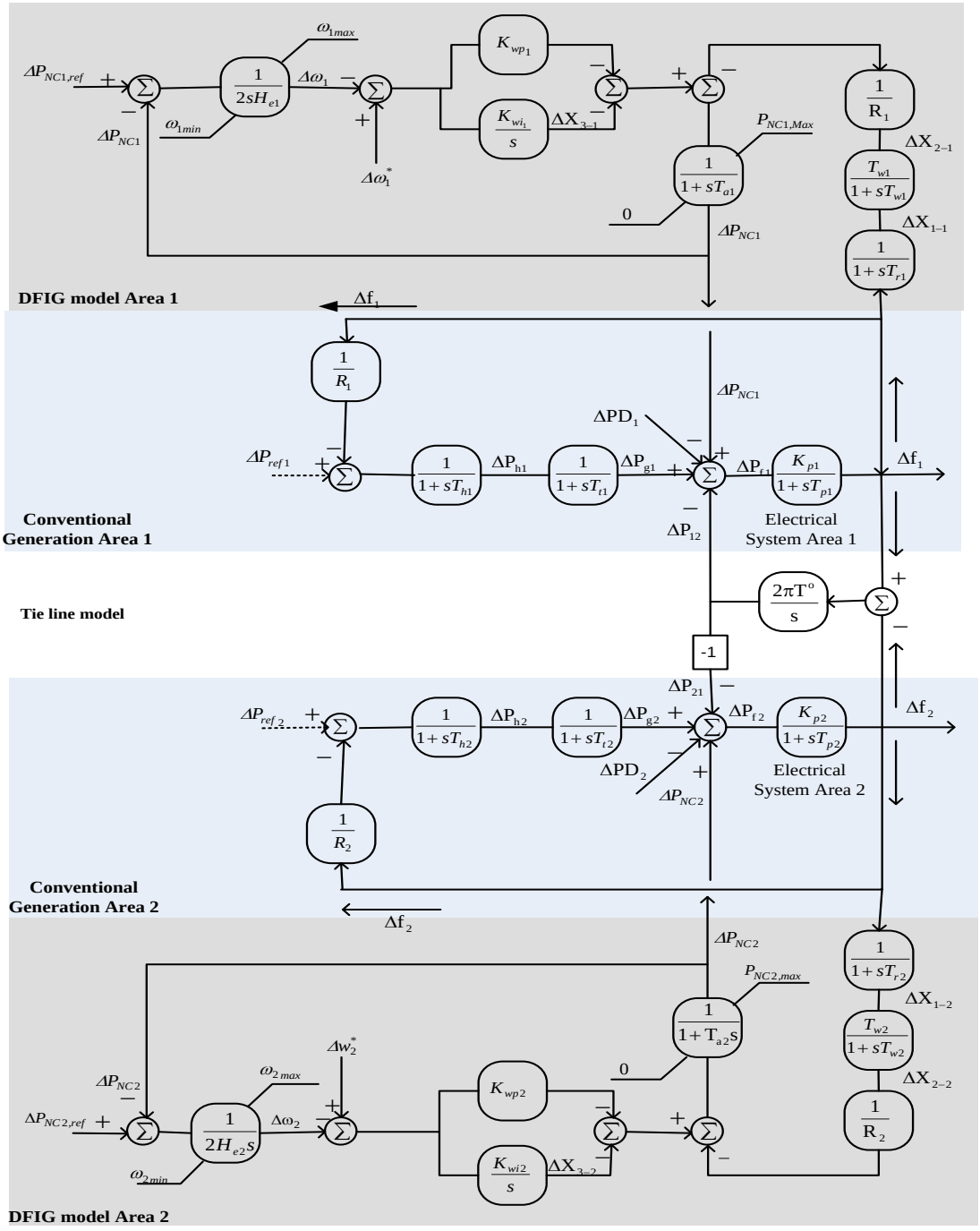

Figure 4.2 Linear dynamic model of primary frequency control of two area systems with DIFG

The dynamic model in state-space form can be obtained from the transfer-function model as given below:

$$\frac{d\underline{X}}{dt} = A\underline{X} + \Gamma\,\underline{p} \tag{4.6}$$

$\underline{X}$ is the state-vector and $\underline{p}$ is the perturbation vector. The matrices A and Γ are state and perturbation matrixes respectively. The state-equation (4.6) can be written in expanded vector-matrix form as given below:

$$\underline{X} = \begin{bmatrix} \Delta P_{h1} & \Delta P_{g1} & \Delta f_1 & \Delta P_{12} & \Delta X_{1-1} & \Delta X_{2-1} & \Delta X_{3-1} & \Delta P_{NC1} & \Delta\omega_1 & & & & & & & & \\ & & & & & & & & & \Delta P_{h2} & \Delta P_{g2} & \Delta f_2 & \Delta X_{1-2} & X_{2-2} & \Delta X_{3-2} & \Delta P_{NC2} & \Delta\omega_2 \end{bmatrix}^T$$

$$A = \begin{bmatrix}
\frac{-1}{T_{h1}} & 0 & \frac{-1}{T_{h1} * R1} & 0 & 0 & 0 & 0 & 0 & 0 & 0 & 0 & 0 & 0 & 0 & 0 & 0 & 0 \\
\frac{1}{T_{t1}} & \frac{-1}{T_{t1}} & 0 & 0 & 0 & 0 & 0 & 0 & 0 & 0 & 0 & 0 & 0 & 0 & 0 & 0 & 0 \\
0 & \frac{K_{p1}}{T_{P1}} & \frac{-1}{T_{P1}} & \frac{-K_{p1}}{T_{P1}} & 0 & 0 & 0 & \frac{K_{p1}}{T_{P1}} & 0 & 0 & 0 & 0 & 0 & 0 & 0 & 0 & 0 \\
0 & 0 & 2\pi T^o & 0 & 0 & 0 & 0 & \frac{K_{p1}}{T_{P1}} & 0 & 0 & 0 & -2\pi T^o & 0 & 0 & 0 & 0 & 0 \\
0 & 0 & \frac{1}{T_{r1}} & \frac{-1}{T_{r1}} & 0 & 0 & 0 & 0 & 0 & 0 & 0 & 0 & 0 & 0 & 0 & 0 & 0 \\
0 & 0 & \frac{1}{T_{r1}} & \frac{-1}{T_{r1}} & \frac{-1}{Tw1} & 0 & 0 & 0 & 0 & 0 & 0 & 0 & 0 & 0 & 0 & 0 & 0 \\
0 & 0 & 0 & 0 & 0 & 0 & 0 & -K_{wi1} & 0 & 0 & 0 & 0 & 0 & 0 & 0 & 0 & 0 \\
0 & 0 & 0 & 0 & \frac{-1}{Ta_1 * R_1} & \frac{-1}{T_{a1}} & \frac{-1}{T_{a1}} & \frac{K_{wp_1}}{T_{a1}} & 0 & 0 & 0 & 0 & 0 & 0 & 0 & 0 & 0 \\
0 & 0 & 0 & 0 & 0 & 0 & \frac{-1}{2 * He_1} & \frac{-1}{2 * He_1} & 0 & 0 & 0 & 0 & 0 & 0 & 0 & 0 & 0 \\
0 & 0 & 0 & 0 & 0 & 0 & 0 & 0 & 0 & \frac{-1}{T_{h2}} & 0 & \frac{-1}{T_{h2} * R_2} & 0 & 0 & 0 & 0 & 0 \\
0 & 0 & 0 & 0 & 0 & 0 & 0 & 0 & 0 & \frac{1}{T_{t2}} & \frac{-1}{T_{t2}} & 0 & 0 & 0 & 0 & 0 & 0 \\
0 & 0 & 0 & \frac{K_{p2}}{T_{p2}} & 0 & 0 & 0 & 0 & 0 & 0 & \frac{K_{p2}}{T_{p2}} & \frac{-1}{T_{p2}} & 0 & 0 & 0 & \frac{K_{p2}}{T_{p2}} & 0 \\
0 & 0 & 0 & 0 & 0 & 0 & 0 & 0 & 0 & 0 & 0 & \frac{1}{T_{r2}} & \frac{-1}{T_{r2}} & 0 & 0 & 0 & 0 \\
0 & 0 & 0 & 0 & 0 & 0 & 0 & 0 & 0 & 0 & 0 & \frac{1}{T_{r2}} & \frac{-1}{T_{r2}} & \frac{-1}{T_{w2}} & 0 & 0 & 0 \\
0 & 0 & 0 & 0 & 0 & 0 & 0 & 0 & 0 & 0 & 0 & 0 & 0 & 0 & 0 & 0 & -K_{wi2} \\
0 & 0 & 0 & 0 & 0 & 0 & 0 & 0 & 0 & 0 & 0 & 0 & 0 & \frac{-1}{T_{a2} * R_2} & \frac{-1}{T_{a2}} & \frac{-1}{T_{a2}} & \frac{K_{wp_2}}{T_{a2}} \\
0 & 0 & 0 & 0 & 0 & 0 & 0 & 0 & 0 & 0 & 0 & 0 & 0 & 0 & 0 & \frac{-1}{2 * H_{e2}} & \frac{-1}{2 * H_{e2}}
\end{bmatrix}$$

$$\Gamma = \begin{bmatrix} 0 & 0 & -\frac{K_{p1}}{T_{p1}} & 0 & 0 & 0 & 0 & 0 & 0 & 0 & 0 & -\frac{K_{p2}}{T_{p2}} & 0 & 0 & 0 & 0 & 0 \end{bmatrix}^T$$

$$\underline{p} = \begin{bmatrix} 0 & 0 & \Delta PD_1 & 0 & 0 & 0 & 0 & 0 & 0 & 0 & 0 & \Delta PD_2 & 0 & 0 & 0 & 0 & 0 \end{bmatrix}^T$$

The system behavior depends on the network parameters, tie line, conventional system parameters such as damping factor of the load (D_1 and D_2) , the regulation droop (R_1 and R_2), the inertia (H_1 and H_2), governor and turbine time constants T_h & T_t respectively. The constants K_P and T_P are evaluated as $K_P = 1/D$ and $T_P = 2H/fD$. DFIG based turbine speed controllers are K_{wp} and K_{wi}.

4.3 Dynamic model of Secondary Frequency Regulation with DFIG –based Wind Turbine - Two Area Controls

The small-perturbation transfer-function block diagram of the two area power system for secondary frequency regulation is Figure- 4.3.

The dynamic model in state-space form is developed from the transfer-function representation as follows:

$$\frac{d\underline{X}}{dt} = A\underline{X} + \Gamma\underline{p} \tag{4.6}$$

Where,

$$\underline{X} = \begin{bmatrix} \Delta P_{h1} & \Delta P_{g1} & \Delta f_1 & \Delta P_{12} & \Delta X_{1-1} & \Delta X_{2-1} & \Delta X_{3-1} & \Delta P_{NC1} & \Delta\omega_1 & & & & \\ & & & & \Delta P_{ref2} & \Delta P_{h2} & \Delta P_{g2} & \Delta f_2 & \Delta X_{1-2} & X_{2-2} & \Delta X_{3-2} & \Delta P_{NC2} & \Delta\omega_2 \end{bmatrix}^T$$

$$\Gamma = \begin{bmatrix} 0 & 0 & 0 & -\frac{K_{p1}}{T_{p1}} & 0 & 0 & 0 & 0 & 0 & 0 & 0 & 0 & -\frac{K_{p2}}{T_{p2}} & 0 & 0 & 0 & 0 & 0 \end{bmatrix}^T$$

$$\underline{p} = \begin{bmatrix} 0 & 0 & 0 & \Delta PD_1 & 0 & 0 & 0 & 0 & 0 & 0 & 0 & 0 & 0 & \Delta PD_2 & 0 & 0 & 0 & 0 & 0 \end{bmatrix}^T$$

Similar to previous section, $\underline{X}$ is the state-vector and $\underline{p}$ is the perturbation vector. The matrices A and Γ are state and perturbation matrixes respectively. The state-equation (4.11) can be written in expanded vector-matrix form as follows:

$$A=\begin{bmatrix}
0 & 0 & 0 & K_{AGC1}B_1 & -K_{AGC1} & 0 & 0 & 0 & 0 & 0 & 0 & 0 & 0 & 0 & 0 & 0 & 0 & 0 & 0 \\
\frac{1}{T_{h1}} & \frac{-1}{T_{h1}} & 0 & \frac{-1}{T_{h1}R_1} & 0 & 0 & 0 & 0 & 0 & 0 & 0 & 0 & 0 & 0 & 0 & 0 & 0 & 0 & 0 \\
0 & \frac{1}{T_{t1}} & \frac{-1}{T_{h1}} & 0 & 0 & 0 & 0 & 0 & 0 & 0 & 0 & 0 & 0 & 0 & 0 & 0 & 0 & 0 & 0 \\
0 & 0 & \frac{K_{p1}}{T_{p1}} & \frac{1}{T_{p1}} & \frac{-K_{p1}}{T_{p1}} & 0 & 0 & 0 & \frac{K_{p1}}{T_{p1}} & 0 & 0 & 0 & 0 & 0 & 0 & 0 & 0 & 0 & 0 \\
0 & 0 & 0 & 2\pi T^{\circ} & 0 & 0 & 0 & 0 & \frac{K_{p1}}{T_{p1}} & 0 & 0 & 0 & 0 & -2\pi T^{\circ} & 0 & 0 & 0 & 0 & 0 \\
0 & 0 & 0 & \frac{1}{T_{r1}} & \frac{-1}{T_{r1}} & 0 & 0 & 0 & 0 & 0 & 0 & 0 & 0 & 0 & 0 & 0 & 0 & 0 & 0 \\
0 & 0 & 0 & \frac{1}{T_{r1}} & \frac{-1}{T_{r1}} & \frac{1}{T_{w1}} & 0 & 0 & 0 & 0 & 0 & 0 & 0 & 0 & 0 & 0 & 0 & 0 & 0 \\
0 & 0 & 0 & 0 & 0 & 0 & 0 & 0 & -K_{wi1} & 0 & 0 & 0 & 0 & 0 & 0 & 0 & 0 & 0 & 0 \\
0 & 0 & 0 & 0 & 0 & \frac{-1}{T_{a1}R_1} & \frac{-1}{T_{a1}} & \frac{-1}{T_{a1}} & \frac{-K_{wp1}}{T_{a1}} & 0 & 0 & 0 & 0 & 0 & 0 & 0 & 0 & 0 & 0 \\
0 & 0 & 0 & 0 & 0 & 0 & 0 & \frac{-1}{2H_{e1}} & \frac{-1}{2H_{e1}} & 0 & 0 & 0 & 0 & 0 & 0 & 0 & 0 & 0 & 0 \\
0 & 0 & 0 & 0 & K_{AGC2} & 0 & 0 & 0 & 0 & 0 & 0 & 0 & 0 & -K_{AGC2}B_2 & 0 & 0 & 0 & 0 & 0 \\
0 & 0 & 0 & 0 & 0 & 0 & 0 & 0 & 0 & 0 & \frac{1}{T_{h2}} & \frac{-1}{T_{h2}} & 0 & \frac{1}{T_{h2}R_2} & 0 & 0 & 0 & 0 & 0 \\
0 & 0 & 0 & 0 & 0 & 0 & 0 & 0 & 0 & 0 & 0 & \frac{1}{T_{t2}} & \frac{-1}{T_{t2}} & 0 & 0 & 0 & 0 & 0 & 0 \\
0 & 0 & 0 & 0 & \frac{K_{p2}}{T_{p2}} & 0 & 0 & 0 & 0 & 0 & 0 & 0 & \frac{K_{p2}}{T_{p2}} & \frac{-1}{T_{p2}} & 0 & 0 & 0 & \frac{K_{p2}}{T_{p2}} & 0 \\
0 & 0 & 0 & 0 & 0 & 0 & 0 & 0 & 0 & 0 & 0 & 0 & 0 & \frac{1}{T_{r2}} & \frac{-1}{T_{r2}} & 0 & 0 & 0 & 0 \\
0 & 0 & 0 & 0 & 0 & 0 & 0 & 0 & 0 & 0 & 0 & 0 & 0 & \frac{1}{T_{r2}} & \frac{-1}{T_{r2}} & \frac{-1}{T_{w2}} & 0 & 0 & 0 \\
0 & 0 & 0 & 0 & 0 & 0 & 0 & 0 & 0 & 0 & 0 & 0 & 0 & 0 & 0 & 0 & 0 & 0 & -K_{wi2} \\
0 & 0 & 0 & 0 & 0 & 0 & 0 & 0 & 0 & 0 & 0 & 0 & 0 & 0 & 0 & \frac{-1}{T_{a2}R_2} & \frac{-1}{T_{a2}} & \frac{-1}{T_{a2}} & \frac{K_{wp2}}{T_{a2}} \\
0 & 0 & 0 & 0 & 0 & 0 & 0 & 0 & 0 & 0 & 0 & 0 & 0 & 0 & 0 & 0 & 0 & \frac{-1}{2H_{e1}} & \frac{-1}{2H_{e1}}
\end{bmatrix}$$

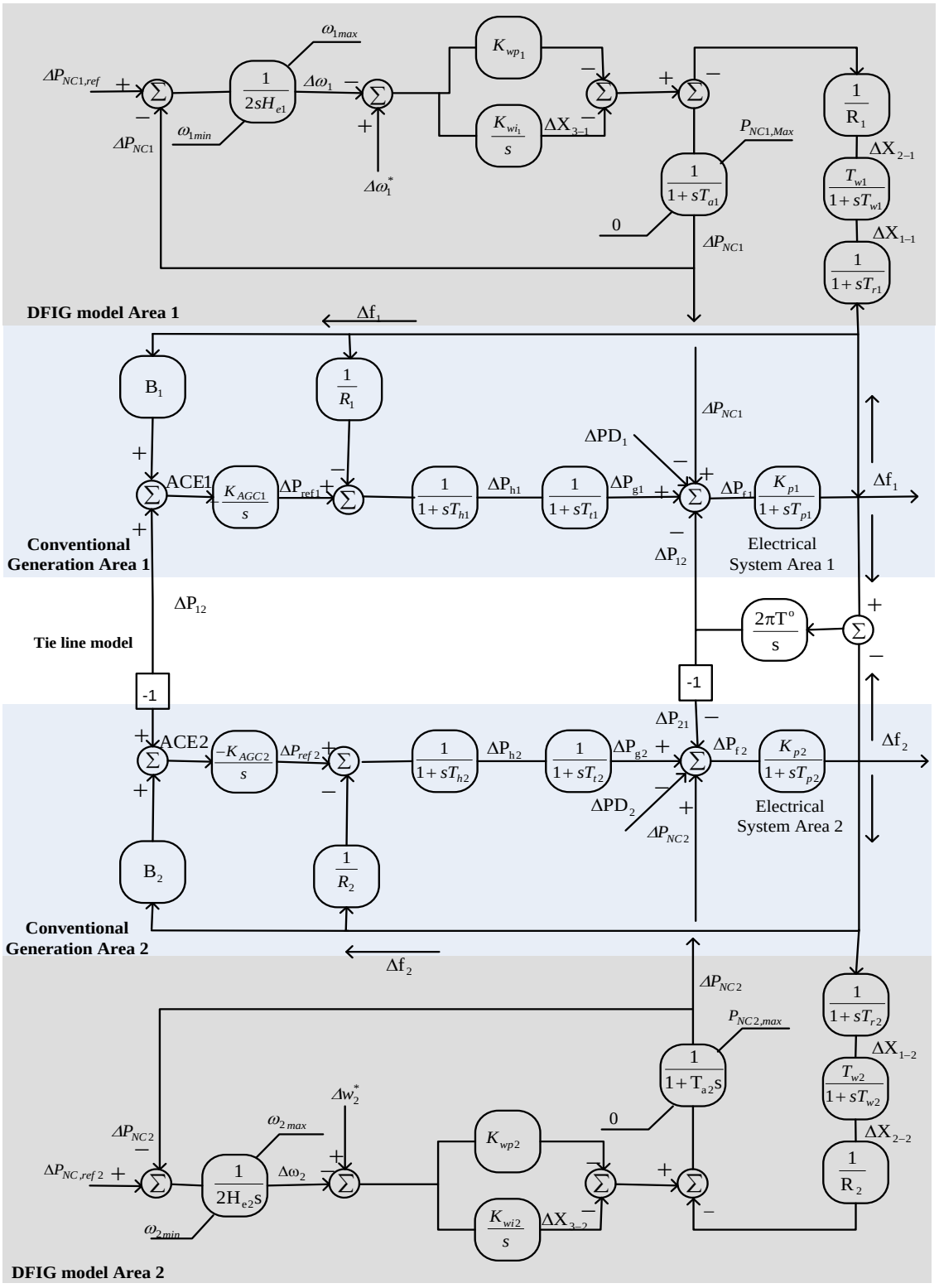

Figure 4.3 Linear model of secondary frequency control of two area systems with DIFG-based wind turbines

4.4 Optimal Tuning of DFIG Based Wind Turbine Controller Parameters

The objective of this section is to determine the optimal set of parameters of the Proportional-Integral controller of the DFIGs in the two-area power system. The ISE technique discussed in Chapter-3 is used for obtaining the optimum settings for K_{wp} and K_{wi} parameters of DFIG in each area. A quadratic performance index denoting the squared of the deviations of the state variables, is considered as follows:

$$J = \int_0^\infty \left[X_1^2(t) + X_2^2(t) + X_3^2(t) + ... + X_n^2(t) \right] dt \tag{4.12}$$

In this chapter, the square of the ACE is considered as the performance index for tuning the controller parameters in each area, as stated below.

$$J_1 = \int_0^\infty (ACE_1)^2 \, dt \tag{4.13}$$

$$J_2 = \int_0^\infty (ACE_2)^2 \, dt \tag{4.14}$$

For computational purposes, the performance index J is calculated by summing the discrete values at very small intervals, over a considerable period until the steady-state is achieved, as given below.

$$J_1 = \sum_{k=1}^{K} \left[\Delta ACE_1^{\,2}(t_0 + k\Delta t) \right] \tag{4.14}$$

$$J_2 = \sum_{k=1}^{K} \left[\Delta ACE_2^{\,2}(t_0 + k\Delta t) \right] \tag{4.15}$$

The optimal settings of the DFIG controller parameters in the two areas are obtained by using a heuristic iterative scheme that seeks to minimize the integral squared error of the ACE in each area. The schematic step-wise flow diagram of the optimal tuning process is shown in Fig.4.4 and the optimal values of the DFIG speed controller parameters $K_{wp1,}$ K_{wi1} and $K_{wp2,}$ K_{wi2} are determined. As per the flow diagram, first we arbitrarily chose the DFIG controller parameters of both areas, and then sequentially determine the optimal settings for Area-1 and Area-2 controllers using ISE technique. A check for convergence of the optimal parameters is carried out to ensure the program arrives at the optimal settings for the two DFIG controllers.

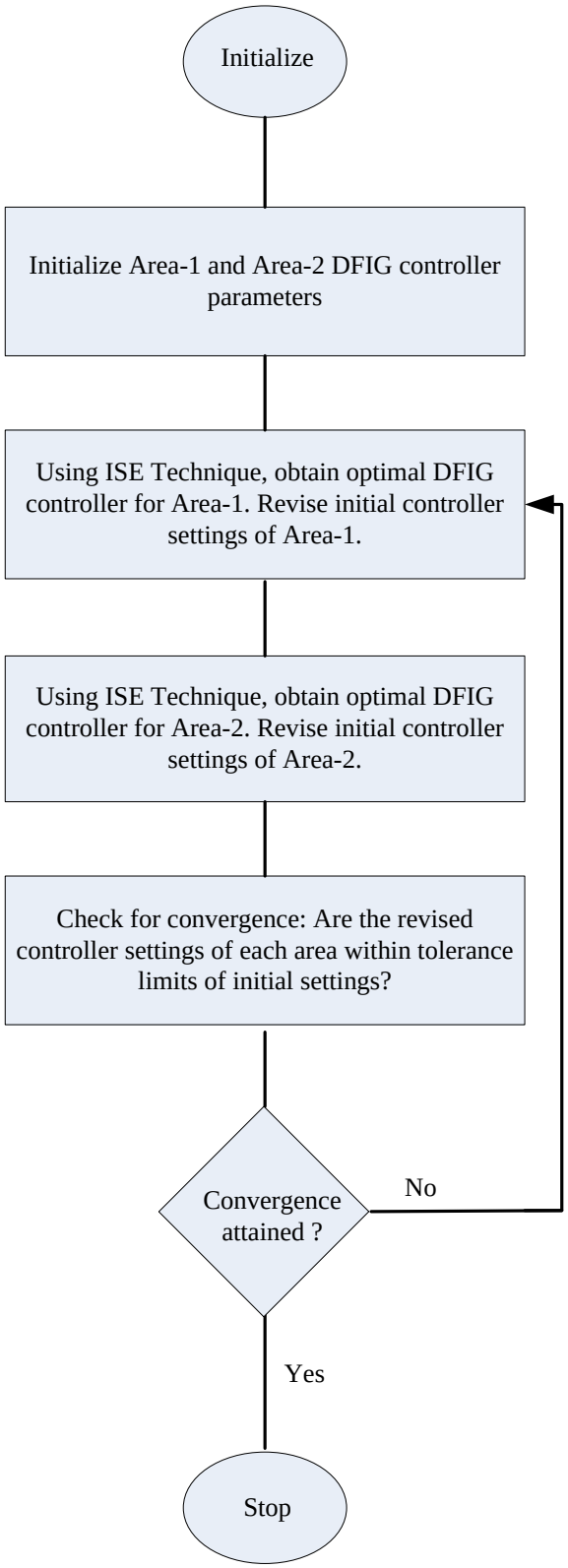

Figure 4.4.Schematic diagram for optimal tuning of DFIG controller parameters

Figure 4.5 shows a typical working result of the optimization procedure for a 50% wind penetration case, how the DFIG controller parameters converge to their optimal settings, while the objective of minimization of ACE is achieved. Tables 4-1 and 4-2 present the results of the optimal parameter tuning for 20% to 50% penetration of wind generation in area-1 and area-2 respectively.

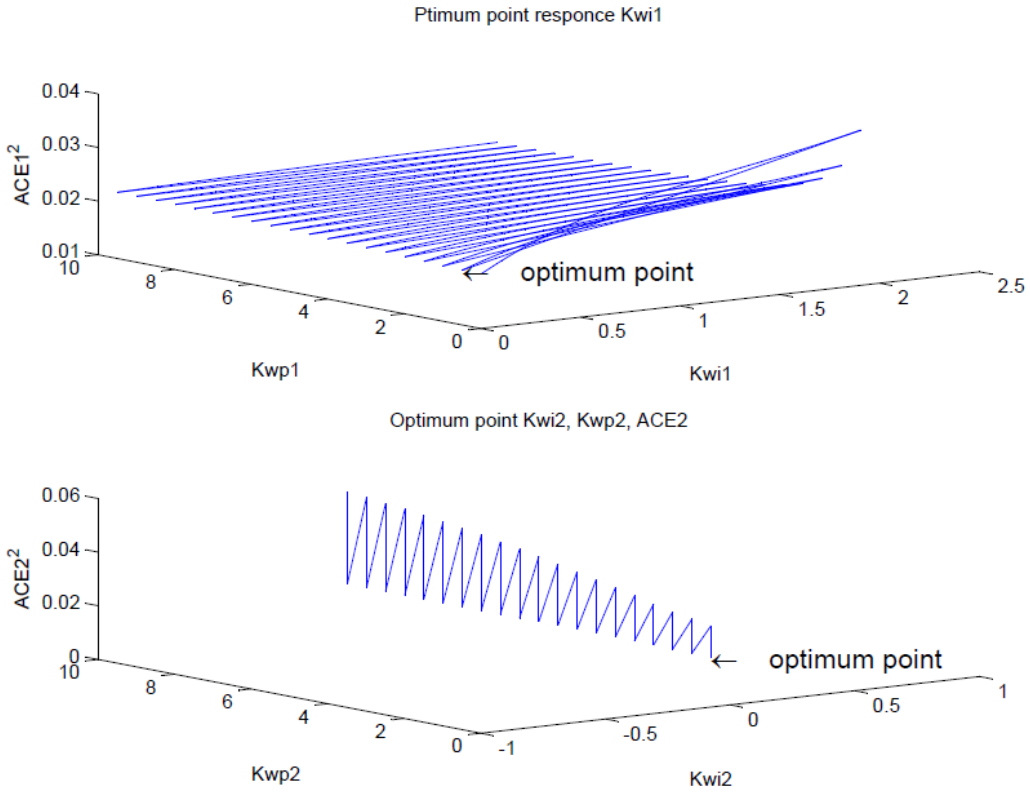

Figure 4.5.Tuning DFIG controller parameters for 50% wind penetration

Table 4.1 Optimal DFIG controller settings parameters area-1

Penetration	K_{wi1}	K_{wp1}	J_1
20%	0.2	1.2	0.0507
50%	0.2	1.7	0.0797

Table 4.2 Optimal DFIG controller settings parameters area-2

Penetration	K_{wi2}	K_{wp2}	J_2
20%	0.1	1.0	0.0499
50%	0.1	1.0	0.0765

4.5 Analytical Studies

4.5.1 Primary Frequency Control

Simulations were carried out based on the dynamic model shown in Figure- 4.2 for 0.02 per unit step load perturbation in both areas, with and without DFIG wind generation to examine the impact of wind generator participation in primary frequency regulation. The corresponding MATLAB SIMULINK model is given in Figure 4.6.

During the simulations in both area, it has been assumed that DFIG-based wind turbines are in their optimal mechanical speed with the maximum power obtainable form the wind, and wind speed remain constant during the simulation. Different plots for theses simulations are presented in Figure 4.7 to 4.9. The parameters used for this simulation has been shown in appendix B.

Figure 4.7 presents power increment change for tie-line power for 20%, 50% wind power penetration and also without wind power generation, It is observed that tile-line generation increment response following the disturbance is improved with participation of DFIG, by way of lower tie-line power increment. It is also observed that when the wind penetration level increases from 20% to 50% the response is deteriorates by way of increased settling time. It can be generally concluded that with 20% DFIG-based wind power penetration, primary frequency regulation and the settling time is improved, compare to no-WT case, which the steady state errors are very close.

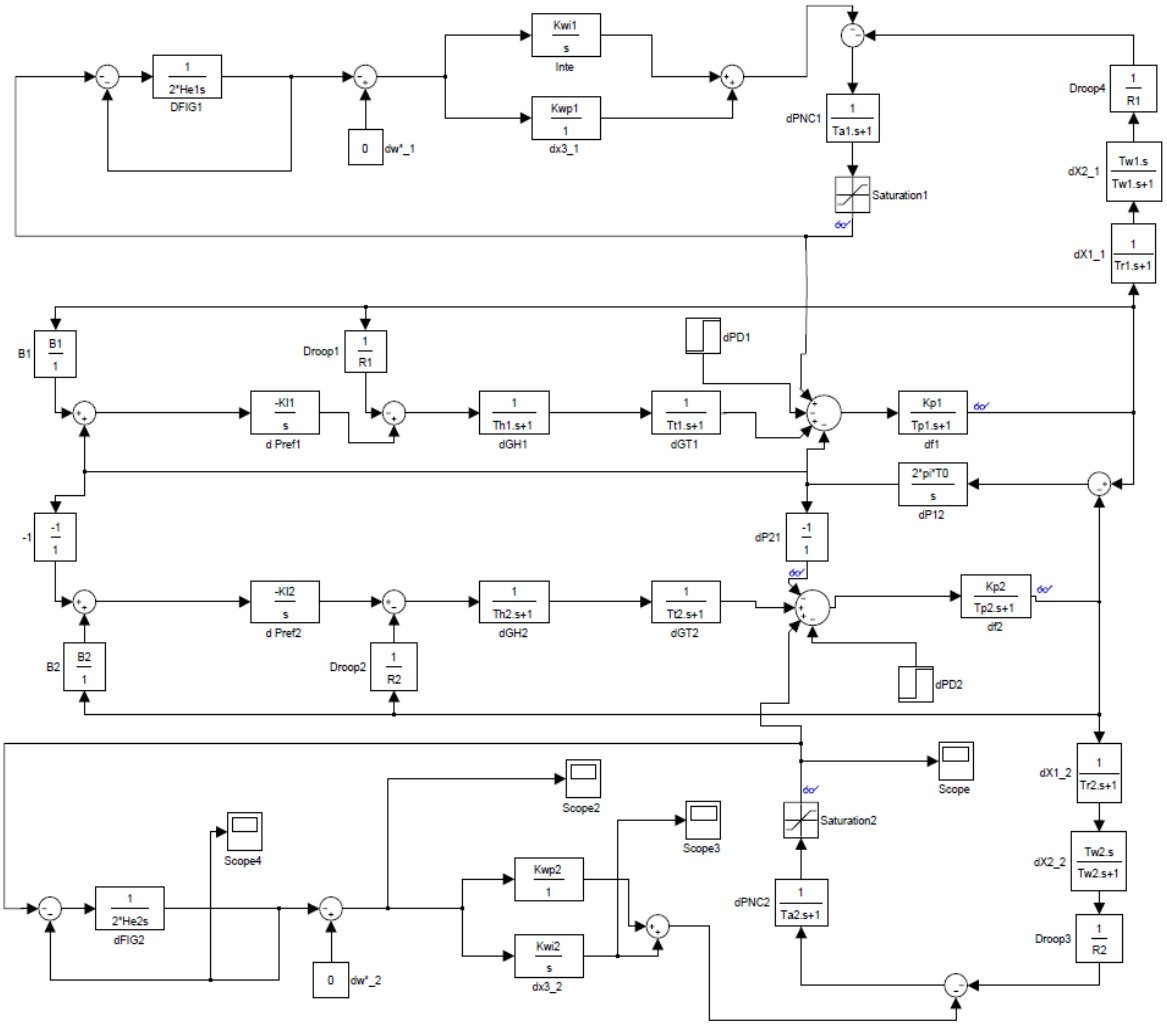

Figure 4.6.Simulink model for frequency response studies for two-area controller with DFIG-based wind Turbine

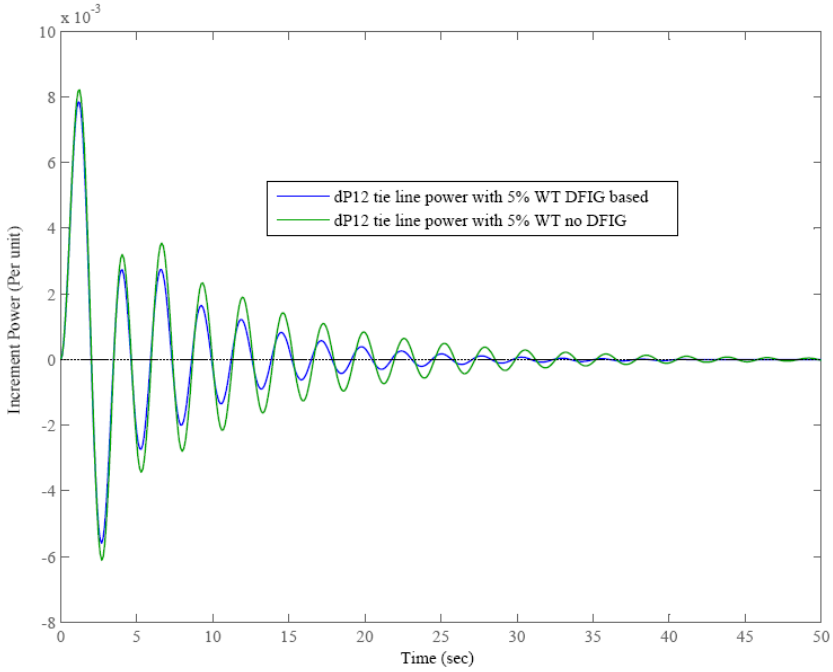

Figure 4.7.Primary frequency regulation tie-line incremental power

Figure-4.8 to 4.15 presents the frequency plots following a 0.02 per unit step load perturbation in both areas for 5%, 10%, 20% and 50% penetration of DFIG based WT in comparison with non-DFIG based WT which is not participating in frequency regulation. It is observed that the frequency response following the disturbance is improved, by way of lower frequency peak excursion when DFIG participation is considered. It is also observed that when the wind penetration level increases from 5% to 50%, although the lower frequency peak excursion is improved by higher penetration but the frequency response deteriorates by way of increased settling time and higher steady-state frequency error. It can be generally concluded that with lower penetration, the settling time is improved, compare to no-DFIG case, which the steady state errors are close for both of the areas.

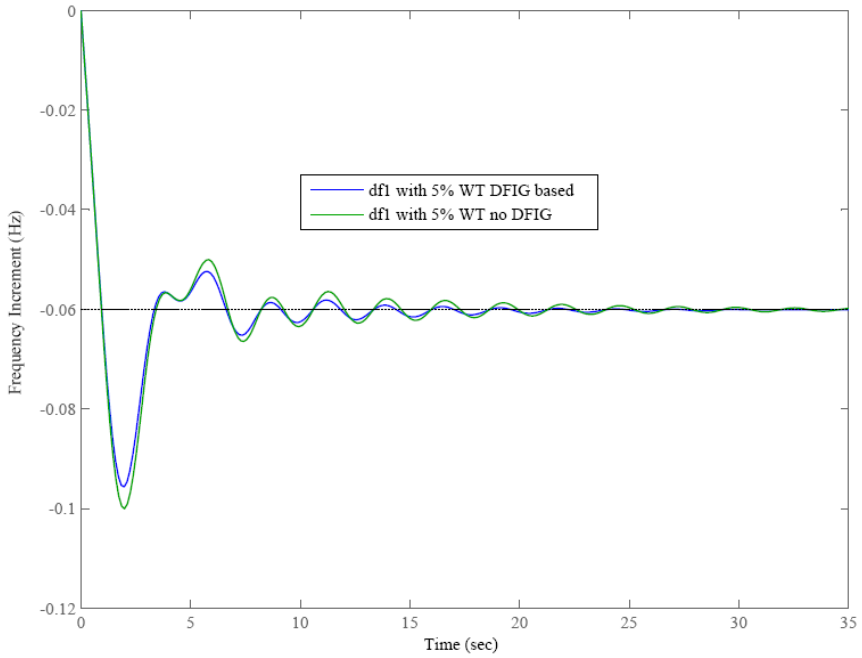

Figure 4.8. Primary frequency regulation for 2% load change area 1

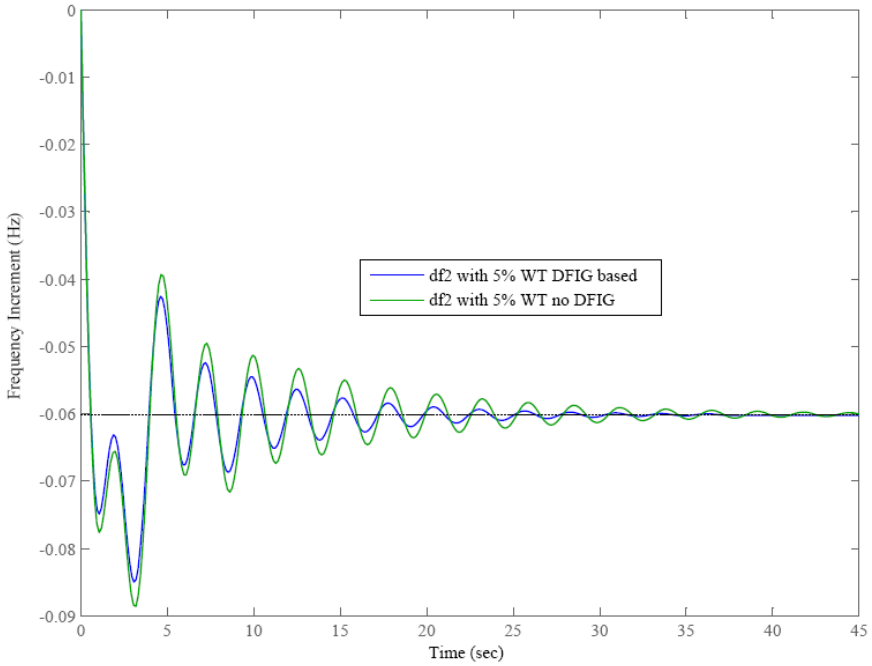

Figure 4.9.Primary frequency regulation for 2% load change area 2

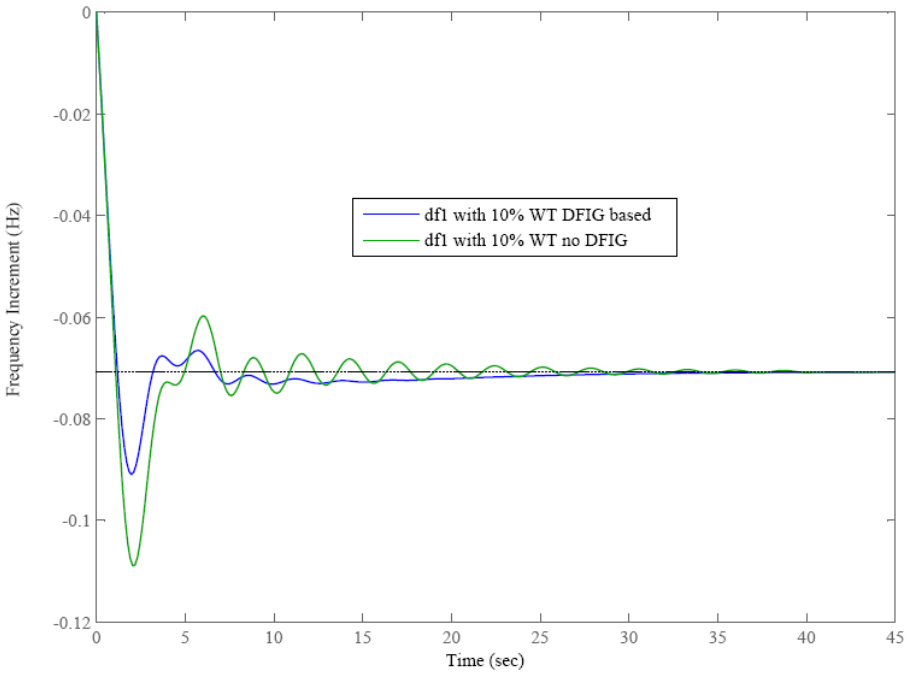

Figure 4.10. Primary frequency regulation for 2% load change area 1

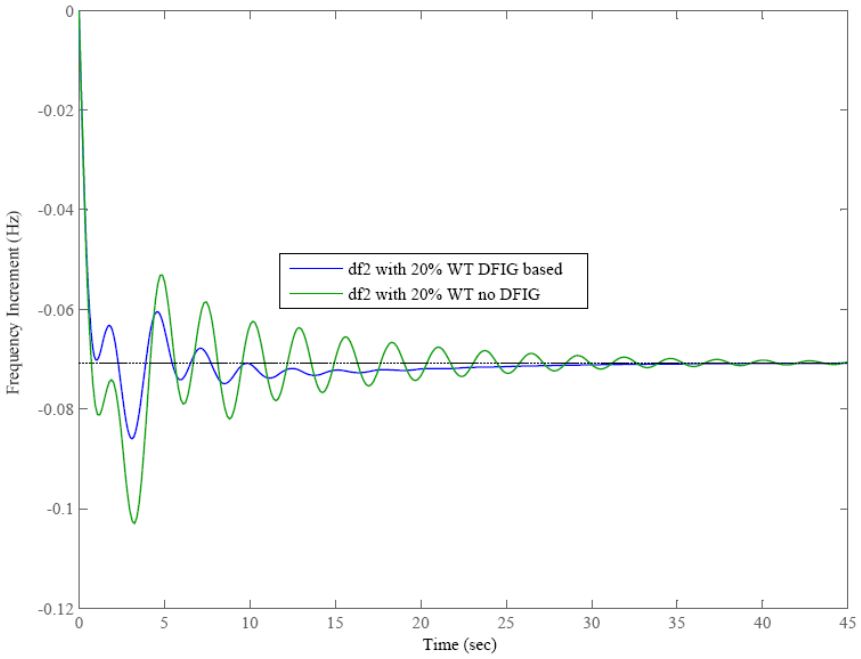

Figure 4.11. Primary frequency regulation for 2% load change area 2

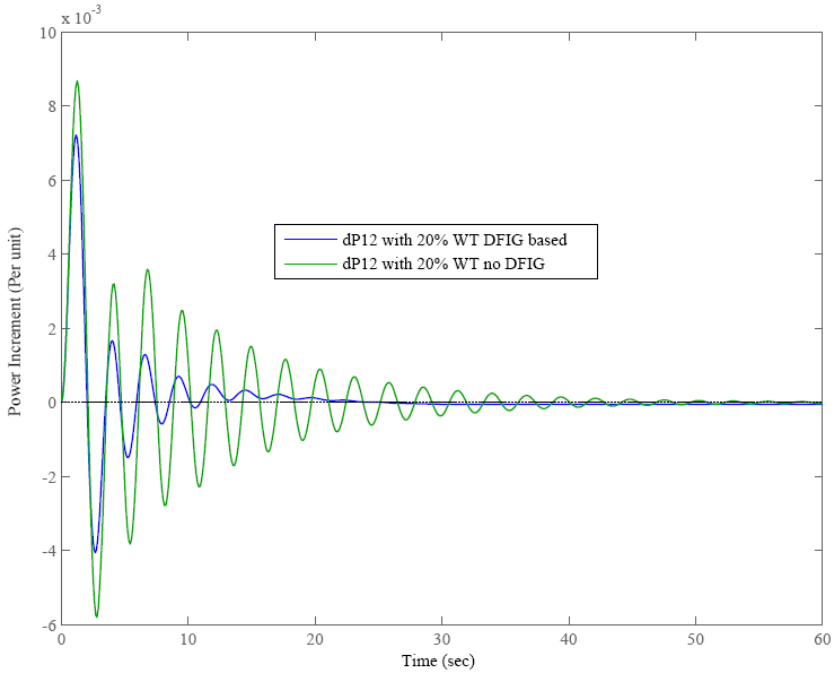

Figure 4.12. Primary frequency regulation for 2% load change tie line

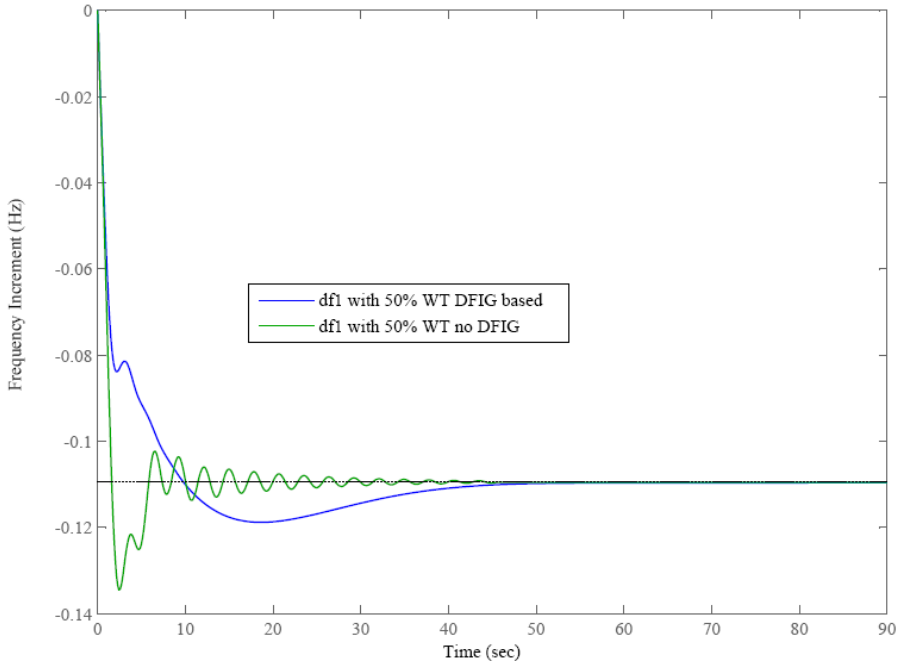

Figure 4.13. Primary frequency regulation for 2% load change area 1

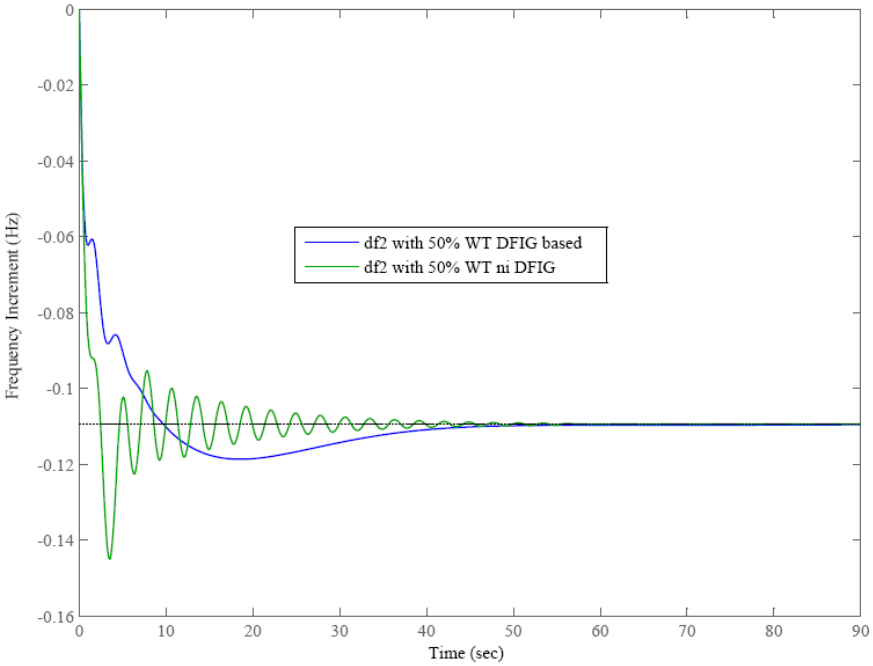

Figure 4.14 Primary frequency regulation for 2% load change area 2

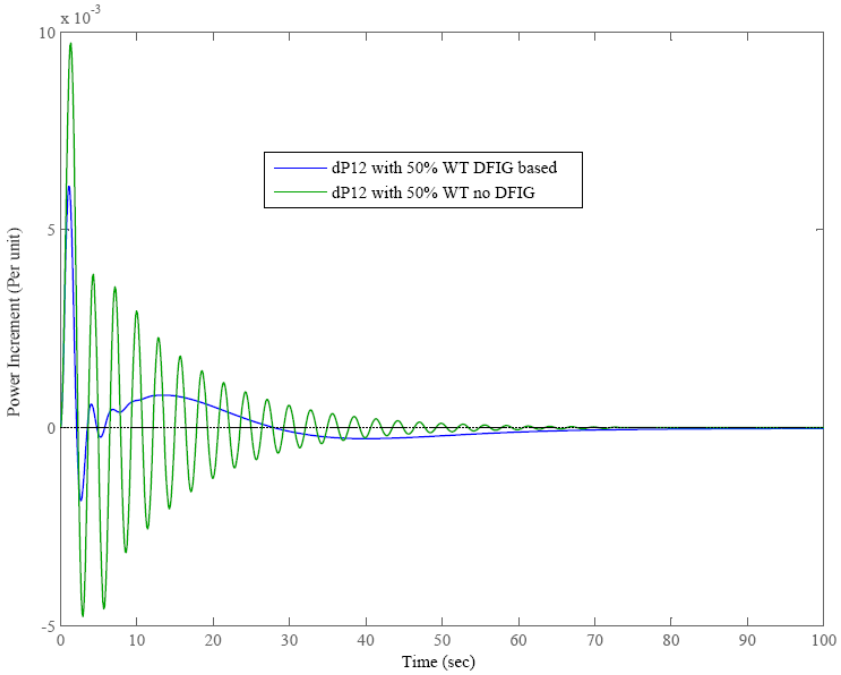

Figure 4.15 Primary frequency regulation for 2% load change tie line

4.4.2 Secondary Frequency Control

Simulations are carried out considering the dynamic model shown in Figure 4.3 for a 0.02 per unit step load perturbation in both areas considering the optimally tuned DFIG controllers, to examine their impact on secondary frequency control.

The simulations are carried out for four levels of wind penetration, 5%, 10%, 20% and 50% and the corresponding optimally tuned parameters for the DFIG controller, obtained in Section-4.3, are used. As mentioned earlier, it has been assumed that DFIG-based wind turbines are in their optimal mechanical speed with the output corresponding to the maximum power obtainable form the wind, and wind speed remain constant during the simulation and the conventional generator is able to supply the additional load after settlement of the transient.

Different plots for theses simulations are presented in Figure 4.16 to 4.26. Figure4.16 to 4.19 shows the tie-line incremental power change for four cases of 5%, 10%, 20% and 50% of wind power penetration with and without DFIG based WT. It is observed that response of AGC with support of DFIG compare to no DFIG based WT to minimize the tie-line power incremental change is improved, by way of shorter transient time settlement and lower transient power excursion peak.

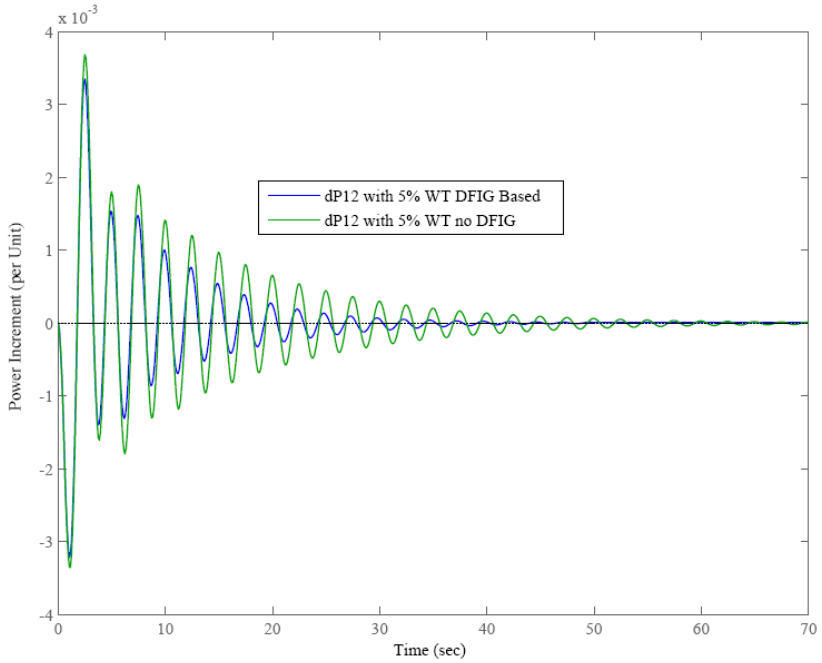

Figure 4.166 Secondary frequency regulation for 2% sudden load tie line power

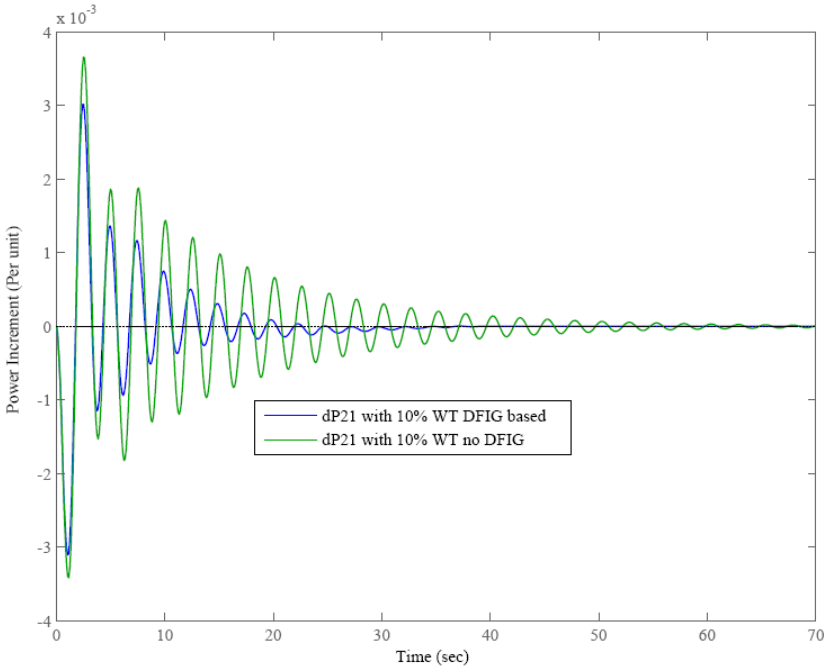

Figure 4.17 Secondary frequency regulation for 2% sudden load tie line power

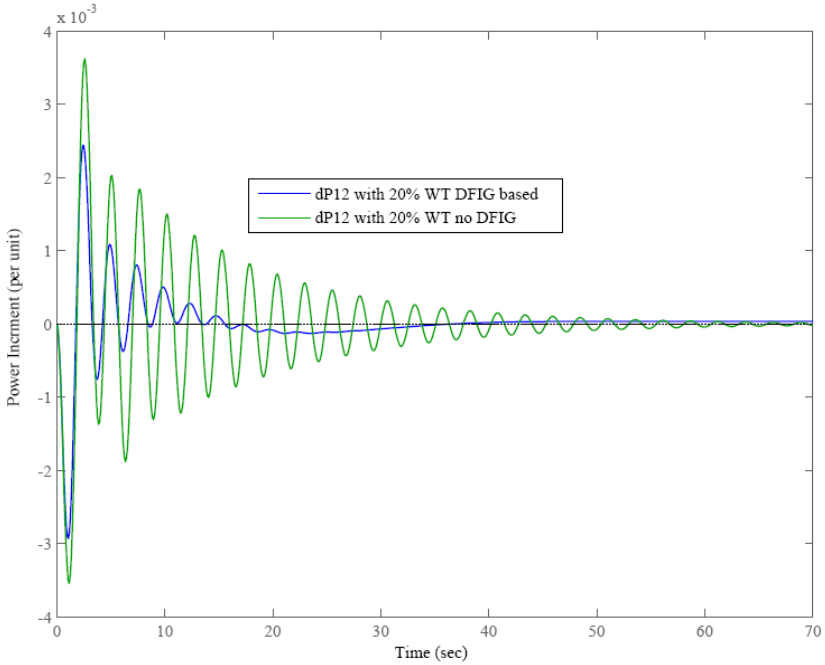

Figure 4.18 Secondary frequency regulation for 2% sudden load change tie line power

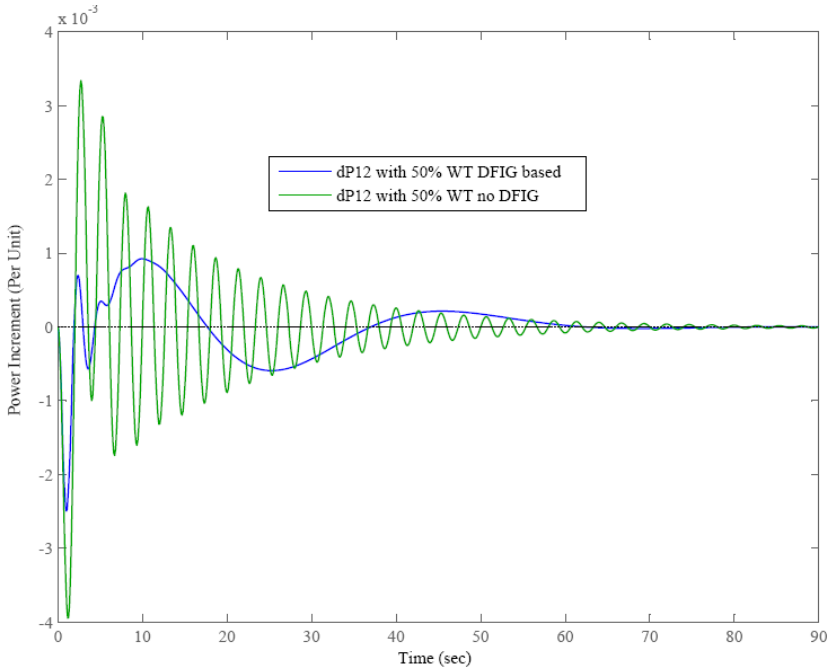

Figure 4.19 Secondary frequency regulation for 2% sudden load change tie line power

Figure-4.20 to 4.26 shows frequency response of area-1 and area-2 following the same step load perturbation. It is observed that frequency peak excursion has been improved in all cases with DFIG based WT for 5%, 10%, 20% and 50% wind power penetration while with higher penetration frequency transient settling time is increased compare to no DFIG WT power case.

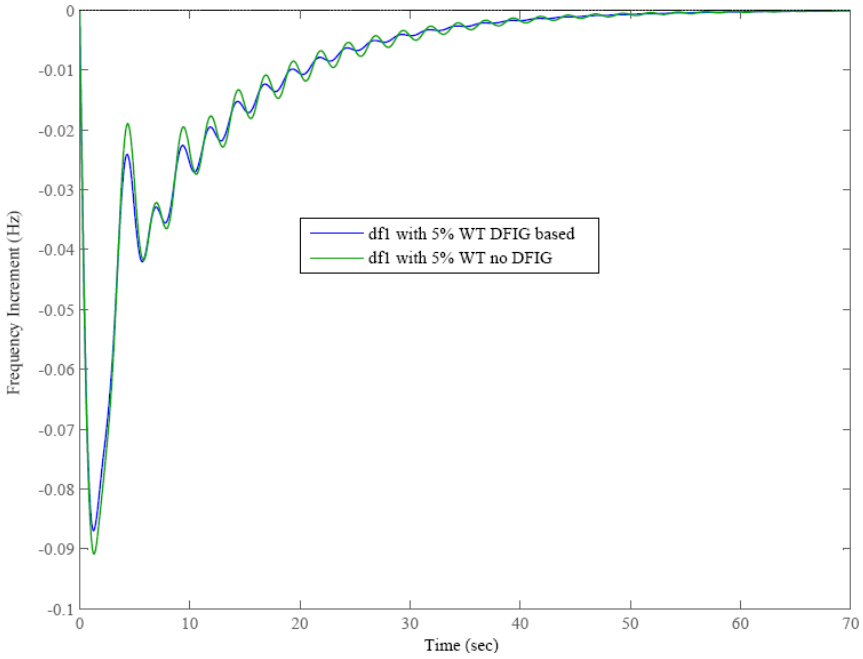

Figure 4.20 Secondary frequency regulation for 2% sudden load change area-1

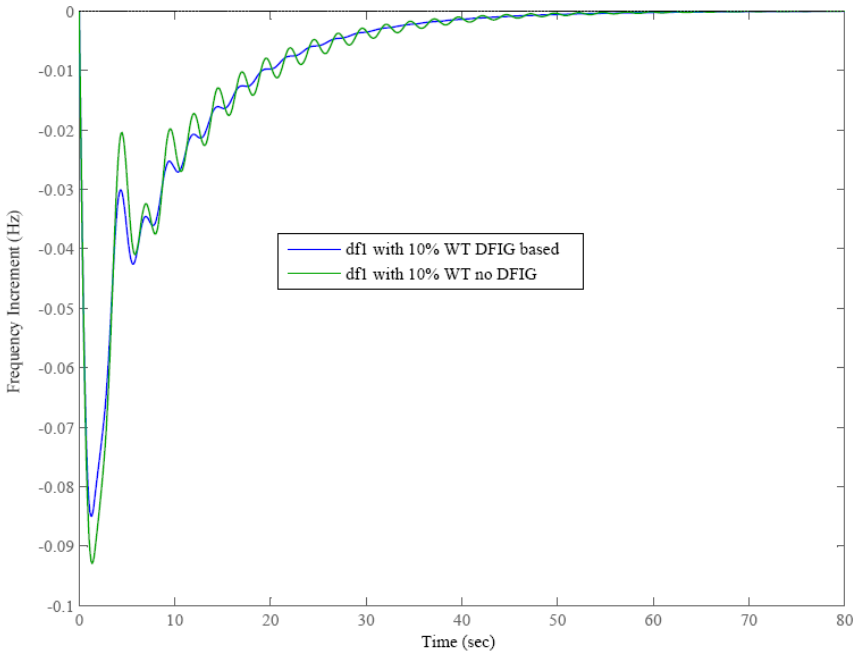

Figure 4.21 Secondary frequency regulations for 2% sudden load change area-1

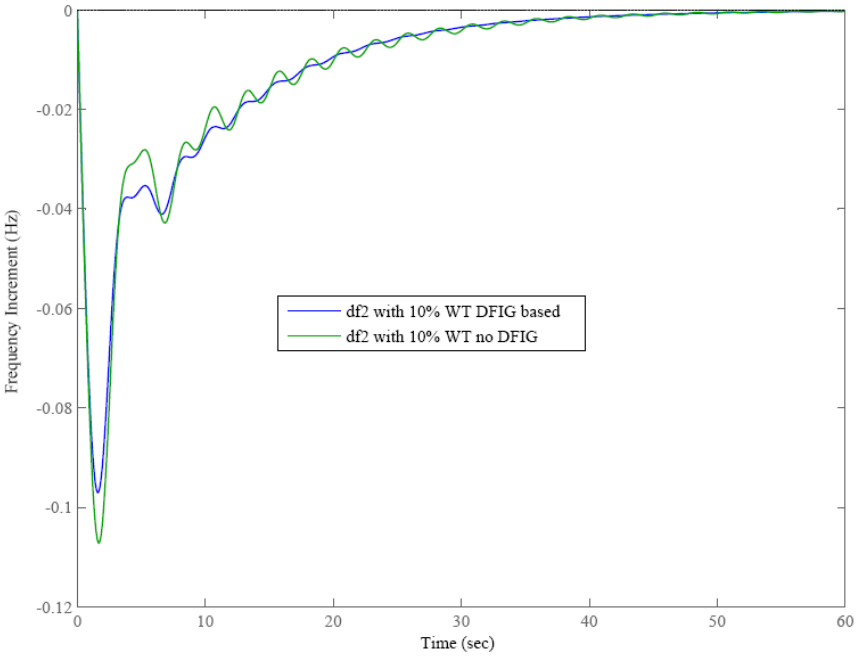

Figure 4.18 Secondary frequency regulation for 2% sudden load change area-2

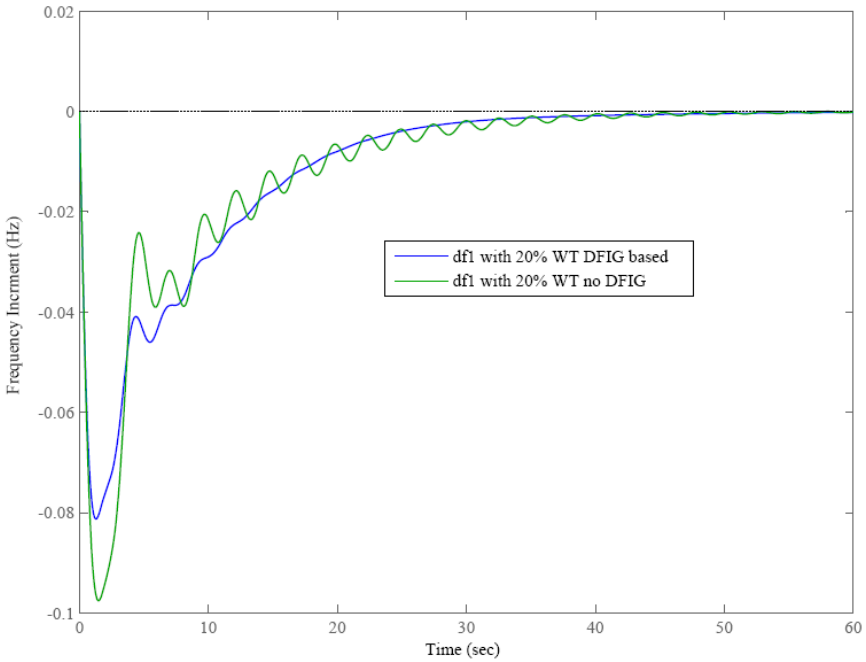

Figure 4.19 Secondary frequency regulation for 2% sudden load change area-1

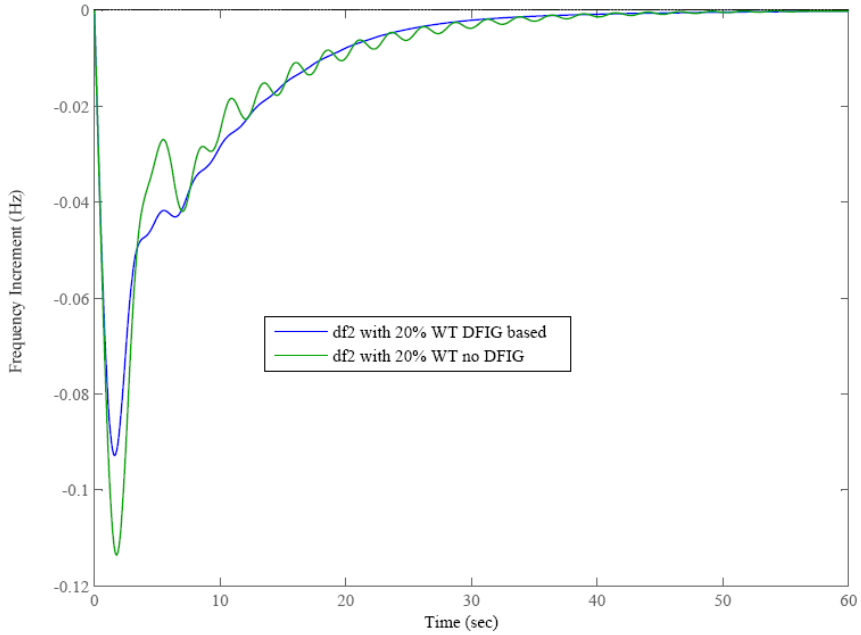

Figure 4.20 Secondary frequency regulation for 2% sudden load change area-2

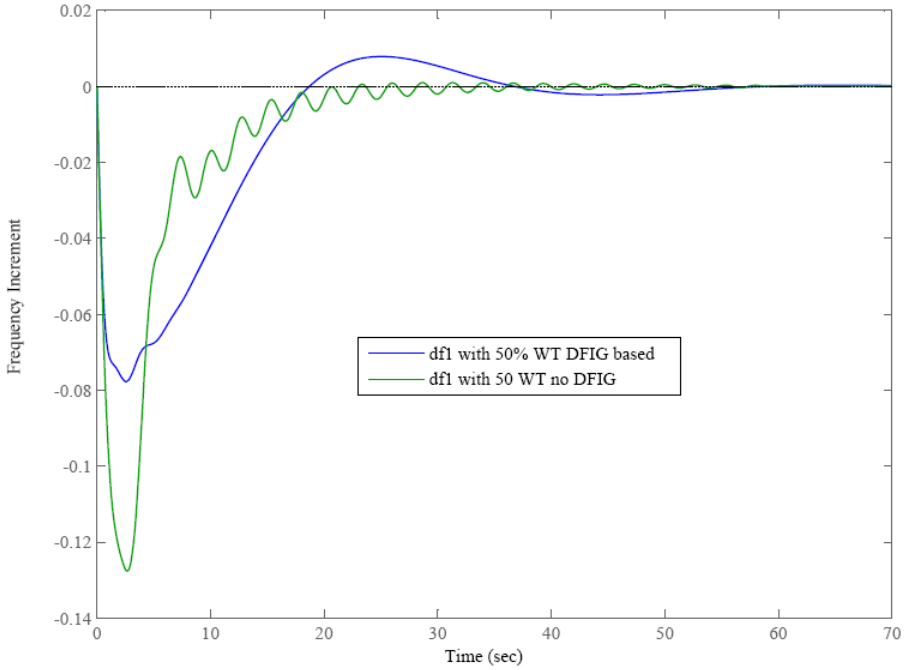

Figure 4.21 Secondary frequency regulation for 2% sudden load change area-1

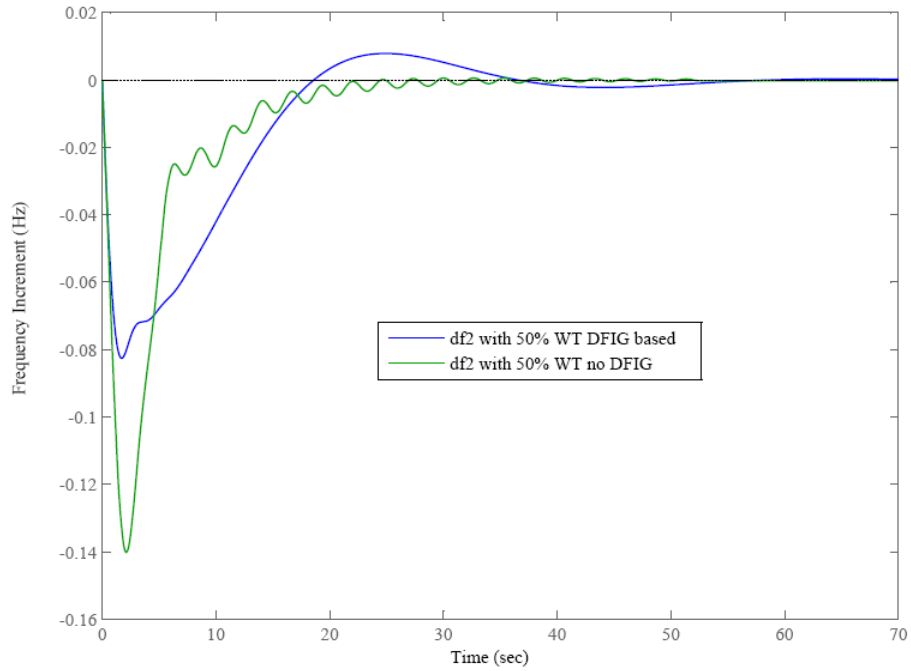

Figure 4.22 Secondary frequency regulation for 2% sudden load change area-2

It can be generally concluded with higher penetration of wind power energy the performance of AGC, initially compare to lower penetration and ultimately compare to no DFIG wind power

case, due to the fact that after release of kinetic energy by DFIG, its mechanical speed is reduced, and therefore as described earlier in the chapter 3, the power output of DFIG is reduced, compare to steady condition. Therefore for larger penetration of DFIG, this reduction of the power output will be additional burden in AGC and conventional generation to control the load- frequency balance.

Figures 4.27 to 4.29 presents the ACE_1 and ACE_2 plots following a step load perturbation. It is observed that ACE is deteriorated with high wind energy penetration. Deviation of DFIG from optimal mechanical speed in case of high wind energy penetration has a more negative impact on ACE as it increases the total settling time. In the case of low wind energy penetration, a 5% contribution of DFIG in reduction of ACE after applying 2% step load perturbation is not significant.

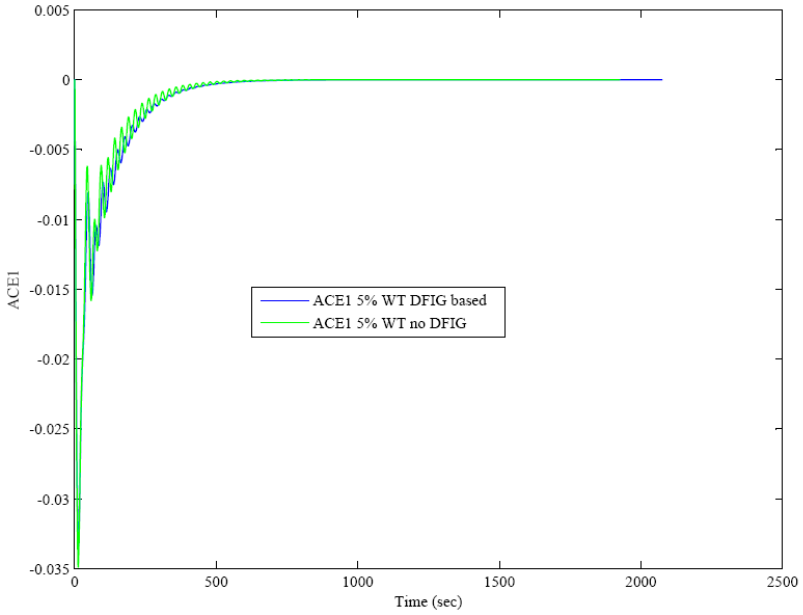

Figure 4.23 Area error for 2% sudden load change in area-1

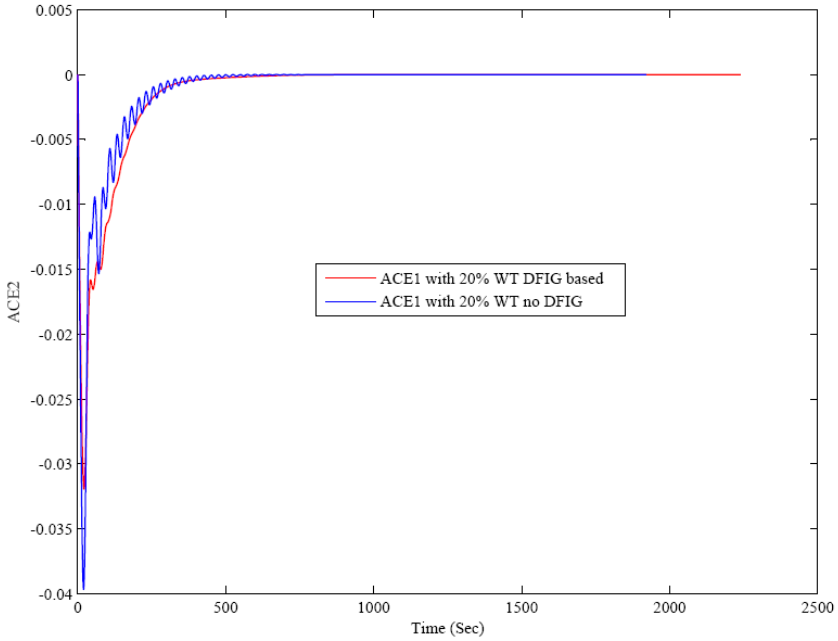

Figure 4.24 Area error for 2% sudden load change in area-2

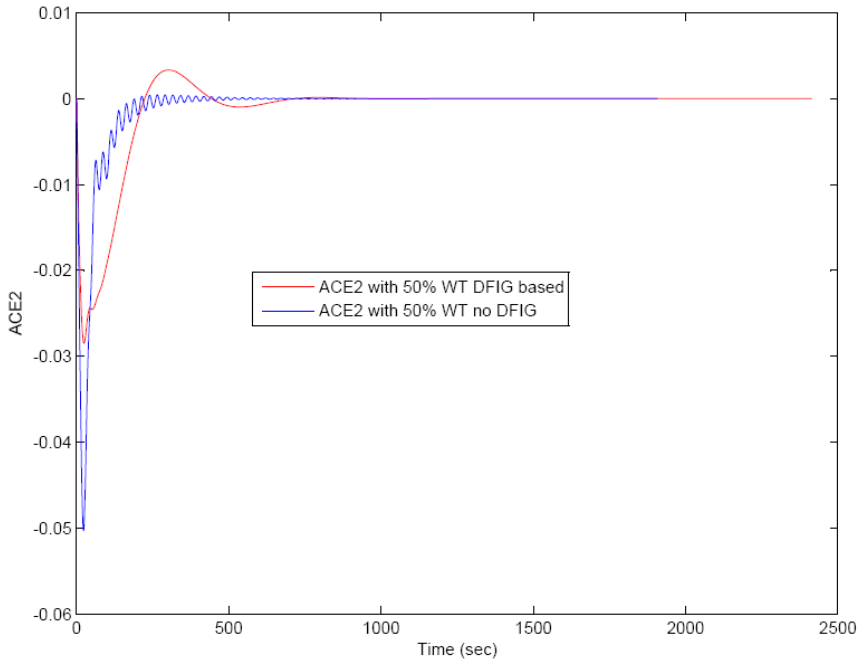

Figure 4.25 Area error for 2% sudden load change in area-2

4.6 Conclusion

Participation of DFIG based wind generators in frequency regulation and automatic generation control (AGC) services in multi-area control systems is a complex problem. The DFIG contrary to fixed speed WT could participate and improve the frequency performance and support conventional generation in frequency regulation services by reduction in ACE in each area.

This chapter presents a small-perturbation transfer function model for a two-area power system, each area equipped with DFIG based wind generators. As in the previous chapter, integral squared error based optimal tuning of the DFIG controllers is carried out. However, the optimal tuning process becomes more complex because of the presence of more parameters to be tuned simultaneously. Therefore, a heuristic iterative optimal tuning scheme is proposed, that helps determine the optimal parameters successfully.

Detailed simulation studies have been presented to compare the performance of the optimally tuned DFIG controllers and their contribution to frequency regulation and AGC in the two-area power system. Also, studies have been presented to compare the system impact of a 5%, 10%, 20% and 50% penetration of wind generation.

Chapter 5

Conclusion and Future Work

5.1 Conclusion

This thesis attempts to address some of the important issues associated with the integration of wind generation with conventional generation sources in the total energy supply mix of the power system. The thesis is particularly focused on examining the frequency regulation and Automatic Generation Control (AGC) effects of DFIG based wind generators. The main contributions and findings from this research are as follows:

- Small perturbation, transfer function models in state-space form are developed for the first time, for both single-area and two-area power systems with a mix of conventional generation and wind generation sources. The state-space models are developed to examine both primary regulation and AGC effects in the two classes of models. DFIG based wind generation is considered for the model development of the wind generation sources.
- A simple parameter optimization technique based on the ISE criterion is applied to optimally tune the DFIG controller parameters. In the case of the two-area power system, with DFIGs in both areas, the number of parameters to be optimally tuned is larger, and hence a sequential application of ISE criterion is presented.
- Dynamic performance analysis is carried out considering the optimally tuned DFIG controllers to examine their contribution to system frequency support services, both primary regulation and AGC.
- A wind generation penetration index is defined and the effect of variation in penetration is studied for the cases of 5%, 10%, 20% and 50 % wind energy penetration in line with global world wind energy penetration targets of 2020 and 2050, respectively

5.2 Scope for Future Work

With respect to future research directions, the following problems can be examined, based on the research presented in this thesis:

a. The state-space model of the system developed, considering the DFIG based wind generator can be further extended to include pitch control effects of the wind generator. Considering the result of simulation presented in chapter 2 for wind speed changes and overall response of pitch control system to this disturbance, in one side and secondary frequency regulation settling time presented in chapter 3 and 4 are about the same and

close, therefore further study could be conducted to examine use of DFIG based wind turbine with de-loaded operation (operation with less than maximum power) to full participation of DGFIG in frequency regulation in transient and with increasing the generation by pitch control.

b. This work considers the traditional proportional-integral controllers for the DFIG machines. There is scope for research into examining other controller structures, in particular design of adaptive DFIG controllers for frequency control contributions, which can provide improved dynamics performances because of the intermittent nature of wind generation.

c. There is scope for examining how wind generators can participate in frequency regulation and AGC services based on market mechanisms and developing appropriate incentives for DFIGs to participate in frequency regulation support.

Bibliography

[1] "Wind Vision for Canada", Recommendations for Achieving Canada's Wind Energy Potential, Report by the Canadian Wind Energy Association (CanWEA).

[2] Quick Facts about Wind Energy, Canadian Wind Energy Association (CanWEA), http://www.canwea.ca.2001, http://www.canwea.ca/pdfs/CanWEA-WindVision.pdf.

[3] European of Wind Energy in the European Power Supply: Analysis, Issues and Recommendations, 2005. Available online: http://www.ewea.org/.

[4] Canadian Wind Energy Association (CanWEA) Wind farm over view http://www.canwea.ca/featuredWindFarm_e.php?farmId=104

[5] "Nova Scotia Power is generating cleaner, greener energy". From Nova Scotia Power web site. http://www.nspower.ca/en/ Retrieved 2007-12-16.

[6] Qazette Montreal May 5 2008, Article "Quebec picks 15 wind-power projects"

[7] Project reference from CanWEA, http://www.canwea.ca/farms/index_e.php

[8] Project reference from Can WEA http://www.canwea.ca/pdf/Proposed%20projects.pdf

[9] Installed wind capacity in Ontario Reference from IESO, http://www.ieso.ca/imoweb/marketdata/windpower.asp

[10] American Wind Energy Association (2009). Annual Wind Industry Report, Year Ending 2008 pp. 9-10.

[11] Reference from American Wind Energy Association 2009 report http://www.awea.org/publications/reports/4Q09.pdf

[12] Peter Behr. Predicting Wind Power's Growth -- an Art That Needs More Science New York Times, April 28, 2010.

[13] US Wind Resource Even Larger Than Previously Estimated: Government Assessment AWEA February 18, 2010

[14] American Wind Energy Association FOR EMBARGOED RELEASE: October 20, 2009, 3:00 PM ET

[15] American Wind Energy Association (2009). Annual Wind Industry Report, Year Ending 2008 p. 17.

[16] Office of Energy Efficiency and Renewable Energy (2010-02-04). "Installed Wind Capacity by State". United States Department of Energy. http://www.windpoweringamerica.gov/docs/installed_wind_capacity_by_state.xls

[17] Office of Energy Efficiency and Renewable Energy (2010-03-05). "US Installed Wind Capacity and Wind Project Locations". United States Department of Energy. http://www.windpoweringamerica.gov/wind_installed_capacity.asp

[18] Investment US b 9 of the World's Most Amazing Wind Farms 'http://www.investmentu.com/latest-research/testimonials.php?code=X300L118 "Wind 2010 report

[19] Count on Wind Energy by EWEA 2008 report http://www.ewea.org/fileadmin/ewea_documents/documents/press/campaigns/Count_on_Wind_Energy_Briefing.pdf

[20] Wining with European Wind by EWEA public report 2008 http://www.ewea.org/fileadmin/ewea_documents/documents/publications/ Annual_Report_2008.pdf

[21] Europe's onshore and offshore wind energy potential An assessment of environmental and economic constraints by EEA No6/2009 http://www.eea.europa.eu/publications/europes-onshore-and-offshore-wind-energy-potential

[22] "Ocean of Opportunity" by European Wind Energy Association http://www.ewea.org/fileadmin/ewea_documents/documents/publications/reports/Offshore_Repo rt_2009.pdf

[23] Reference from "EWEA wind is power", European Market for Wind Turbines Grows 23% in 2006

[24] Bloombeg Business week, Scott is a reporter in BusinessWeek's London bureau http:/www.busineesweek.com/globalbiz/content/aug2007/gb2007083_852915_page_2.htm

[25] Science and Technology Solar. by Jerry James Stone, San Francisco, CA on 02.15.10 www.treehugger.com

[26] Illustrated history of wind power generation by Darrell M. Dodge, Littleton, Colorado

[27] Reference from Visual Dictionary Online http://www.visualdictionaryonline.com/energy/wind-energy/wind-turbines

[28] Reference from encyclopedia of alternative energy www.daviddarling.info

[29] Community Wind Power fact sheet # 4 by Renewable Energy Research Laboratory, University of Massachusetts at Amherst.

[30] Introduction to the modeling of wind turbine, Wind Power system 2005 John Wiley and Sons Ltd ISBN 0-470-85508-8 (HB)

[31] Wind energy Converter System by Siegfried Heier Kassel University of Germany Published by John Wiley and Sons Ltd

[32] Janaka Ekanayake and Nick Jenkins, Comparison of the Response of Doubly Fed and Fixed-Speed Induction Generator Wind Turbines to Changes in Network Frequency IEEE Transaction on Energy Conversion, Vol. 19, NO. 4, December 2004

[33] R. Pena J.C.Clare, Doubly fed induction generator using back-to-back PWM converters and its application to variable speed wind-energy generation, Power Appl., Vol. 143, No 3, May 1996

[34] J. G. Slootweg, S. W. H. de Haan, H. Polinder, and W. L. Kling, General Model for Representing Variable Speed Wind Turbines in Power System Dynamics Simulations, IEEE Transaction on Power Systems, Vol. 18, NO. 1, February 2003

[35] Gillian Lalor, Julia Ritchie, Shane Rourke, Damian Flynn and Mark J. O'Malley Dynamic Frequency Control with Increasing Wind Generation

[36] Rogério G. de Almeida and J. A. Peças Lopes, IEEE Transaction on Power Systems, Participation of Doubly Fed Induction Wind Generators in System Frequency Regulation Vol. 22, NO. 3, August 2007

[37] Alan Mullane, and Mark O'Malley, The Inertial Response of Induction-Machine-Based Wind Turbines, IEEE Transaction on Power Systems, VOL. 20, NO. 3, August 2005

[38] Johan Morren, Sjoerd W. H. de Haan, Wil L. Kling, and J. A. Ferreira, Wind Turbines Emulating Inertia and Supporting Primary Frequency Control , IEEE Transaction on Power Systems, Vol. 21, NO. 1, February 2006

[39] Juan Manuel Mauricio, Alejandro Marano, Antonio Gómez-Expósito, and José Luis Martínez Ramos, Frequency Regulation Contribution Through Variable-Speed Wind Energy Conversion Systems, IEEE Transaction on Power Systems,, VOL. 24, NO. 1, February 2009

[40] Andreoiu and K. Bhattacharya, Robust tuning of power system stabilizers using Layapunove method based generic algorithm, IEEE Proc.Gener Transaction Vol 149,No 5 Sep 2002

Appendix A

System Parameters Single Area

H_e=3	PU. MW.sec
$K_{agc=}$0.1	
K_p=62	HZ/PU
K_{wi}=0.1	
K_{wp}=1.58	
R=3	Hz/PU.MW
T_a=0.2	Sec
T_h=0.1	Sec
T_p=10	sec
T_r=0.1	Sec
T_t=1	Sec
T_w=6	Sec

Appendix B

System Parameters Two Area

H_{e1}=3.5	PU. MW.sec
H_{e2}=3.5	PU. MW.sec
K_{agc1}=0.05	
K_{agc2}=0.05	
K_{p1}=62	HZ/PU
K_{wi1}=0.1	
K_{wp1}=1.58	
K_{p2}=62	HZ/PU
K_{wi2}=0.1	
K_{wp2}=1.61	
R_1=3	Hz/PU.MW
R_2=3	Hz/PU.MW
T°=0.07	PU.MW/Hz
T_{a1}=0.2	Sec
T_{a2}=0.2	Sec
T_{h1}=0.1	Sec
T_{h2}=0.1	Sec
T_{p1}=10	sec
T_{p2}=15	sec
T_{r1}=0.1	Sec
T_{r2}=0.1	Sec
T_{t1}=1	Sec
T_{t2}=1	Sec
T_{w1}=6	Sec
T_{w2}=6	Sec